

2015-09-29

# Quantification of HIV-1 Proviral DNA Forms in Gut Tissues Using Real-Time PCR

Bahafzallah, Laila

---

Bahafzallah, L. (2015). Quantification of HIV-1 Proviral DNA Forms in Gut Tissues Using Real-Time PCR (Master's thesis, University of Calgary, Calgary, Canada). Retrieved from <https://prism.ucalgary.ca>. doi:10.11575/PRISM/27495

<http://hdl.handle.net/11023/2542>

*Downloaded from PRISM Repository, University of Calgary*

UNIVERSITY OF CALGARY

Quantification of HIV-1 Proviral DNA Forms in Gut Tissues Using Real-Time PCR

by

Laila Bahafzallah

A THESIS

SUBMITTED TO THE FACULTY OF GRADUATE STUDIES  
IN PARTIAL FULFILMENT OF THE REQUIREMENTS FOR THE  
DEGREE OF MASTER OF SCIENCE

GRADUATE PROGRAM IN MICROBIOLOGY AND INFECTIOUS DISEASES

CALGARY, ALBERTA

SEPTEMBER, 2015

© Laila Bahafzallah 2015

## **Abstract**

Previous studies have shown that infection of gut tissues (esophagus-stomach-duodenum-colon) by HIV is compartmentalized with increased HIV-1 diversity and selection for drug resistance in the colon. We looked at the kinetics of HIV-1 in the gut tissues obtained from infected patients receiving ART (i.e AZT or ddI). We established real-time PCR protocols to detect HIV-1 proviral DNA forms. The total HIV-1 proviral DNA was the most frequent form found in the gut tissues. 2-LTR proviral DNA was also detected but in low levels which might indicate low viral replication. HIV-1 latent infection was also detected in the gut tissues as represented by the integrated proviral DNA levels. The levels detected of the proviral DNA forms varied between gut tissues, visits and patients, and no difference or correlation were found for patients receiving AZT or ddI.

## **Acknowledgments**

My journey to get this degree was faced with many challenges, however, I met amazing people who did not give up on me and always encouraged me to thrive for excellent. I could not have completed this degree without them. First, I would like to thank Allah for blessing me everyday. I also would like to thank my mentor and my supervisor Dr. Guido van Marle for giving the opportunity to be in his lab and for his constant support throughout my degree. I would never be at this point in my journey without his help and guidance. I am also grateful for my committee members for their advice and suggestions for my research. Dr. Glen Armstrong it was honor to have a great scientist like you in my committee and I am truly thankful for everything you have done for me. Dr. Carla Coffin thank you for the continuous support and encouragement. Dr. Markus Czub thank you for all your advice and insights. Dr. Careem thank you for your time and help.

I would like to give a special thanks to Dr. Michael Eschbaumer for his generous sharing of his real time PCR expertise. I also would like to thank our lab technician Sandi Nishikawa for saving the day and make things right. I also thank Dr. Wendy Hutchins for her continuous support and generous advice. She has been a great teacher that I always look up to.

I would like to acknowledge the department of Microbiology and Infectious Diseases Graduate program, Snyder Institute for Chronic Diseases and the ministry of higher education in Saudi Arabia for the funding. A special thanks goes to our late King Abdulla may he rest in peace. I also acknowledge Dr. Ali Al-Beshri for his help. I give my great appreciation to my academic advisor Dr. Ahmad Ismail who always been generous with his time and advice through my entire journey.

I would like to thank our Virology group with all the students and investigators as I am so grateful to be a part of that joyful group.

Finally, I want to thank my family and friends who put up with all my drama and draw a smile on my face. I am grateful for your love and support.

I dedicate this thesis to my all my family, especially my Mom, Dad, my sisters Lamis and Lama, my brother Louay, Aunt Lolly and uncle Mohammed-Ali, uncle Mohammed-Noor and last but not least for my beautiful daughter Sara.

## Table of Contents

Abstract.....	ii
Acknowledgments.....	iii
Dedication.....	v
Table of Contents.....	vi
List of Tables.....	viii
List of Figures and Illustration.....	x
List of Symbols and Abbreviations and Nomenclature.....	xii
CHAPTER ONE: INTRODUCTION.....	1
1.1 HIV/AIDS.....	1
1.2 HIV Genome and Life Cycle.....	2
1.3 1-LTR and 2-LTR Circles Formation.....	3
1.4 HIV-1 Therapy and Drug Resistant.....	7
1.4.1 Anti HIV-1 Therapy.....	7
1.4.2 HIV-1 Treatment in Africa.....	9
1.4.3 HIV-1 Vaccines.....	12
1.4.4 Drug Resistance Mechanisms.....	13
1.5 HIV-1 Reservoirs.....	15
1.6 The Immune System in the Gastrointestinal Tract and Blood.....	16
1.7 HIV in the Gut.....	18
1.8 Rationale.....	20
1.9 The Hypothesis of the Study.....	21
CHAPTER TWO: PATIENTS, METHODS AND METERAIALS.....	23
2.1 Patient Samples.....	23

2.2 Nucleic Acid Extraction from PBL and Biopsies.....	28
2.3 Construction of Positive Controls for the Quantification of Total HIV-1 proviral DNA, 2-LTR and integrated proviral DNA Forms.....	28
2.4 <i>E.coli</i> Heat Shock Transformation with (pNL4-3, Integrated HIV-DNA and 2- LTR Plasmids).....	29
2.5 PCR Primers and Probes.....	30
2.6 Conventional Polymerase Chain Reaction (PCR).....	32
2.7 Real- Time PCR.....	34
2.8 Optimized Polymerase Chain Reaction (PCR) primers and Probes.....	35
2.8.1 Optimized Conventional PCR.....	36
2.8.2 Optimized Quantitative Real-Time Polymerase Chain Reaction.....	38
2.9 Approaches to Overcome Quantitative Real- Time PCR Inhibition.....	40
CHAPTER THREE: RESULTS.....	41
3.1 Conventional PCR Optimization.....	41
3.2 Quantification of Real- Time PCR Optimization.....	41
3.3 Bovine Albumin Serum to Neutralize the Inhibitory Factors in Patients Sample.....	42
3.4 HIV-1 Proviral Quantification in PBMC's .....	43
3.5 The Presence of Various Types of HIV-1 Proviral DNA Levels in Different Gut Tissues.....	44
3.6 Quantification of Total HIV-1 proviral DNA Levels in Different Gut Tissues.....	45
3.7 Quantification of 2-LTR Proviral DNA Levels in Different Gut Tissues.....	46
3.8 Quantification of Integrated Proviral DNA Levels in Different Gut Tissues.....	47
CHAPTER FOUR: DISCUSSION AND CONCLUSIONS.....	49
REFERENCES.....	97



## List of Tables

Table 1: Types of samples on each visit.....	24
Table 2A: Summary of the Clinical Information of Patients #1 to #3.....	24
Table 2B: Summary of the Clinical Information of Patients #5 to #14.....	25
Table 2C: Summary of the Clinical Information of Patients #16 to #20.....	26
Table 2D: Summary of the Clinical Information of Patients #22 to #39.....	27
Table 2E: Summary of the Clinical Information of Patients #57 and #60.....	28
Table 3: The Primers and Probes Sequences.....	31
Table 4: Standard PCR cycling and reaction conditions.....	33
Table 5: Standard Cycling and Reaction Conditions for Integrated Proviral DNA PCR.....	33
Table 6: Total HIV-1 and 2-LTR Proviral DNA Quantification PCR Conditions.....	34
Table 7: The Integrated HIV-1 Proviral DNA Quantification PCR (First Round) Conditions.....	35
Table 8: The Integrated HIV-1 Proviral DNA Quantification PCR (Second Round) Conditions.....	35
Table 9: Optimized PCR Cycling and Reaction Conditions.....	37
Table 10: Total HIV-1 and 2-LTR Proviral DNA Optimized Quantification PCR Conditions.....	39
Table 11: The Integrated HIV-1 Proviral DNA Optimized Quantification (First Round) PCR Conditions.....	39
Table 12: The Integrated HIV-1 Proviral DNA Optimized Quantification (Second Round) PCR Conditions.....	39
Table 13: Quantification real time PCR with BSA conditions.....	40
Table 14: Positive Gut Tissue Samples for Total HIV-1 Proviral DNA from AZT Group Various Visits.....	86

Table 15: Positive Gut Tissue Samples for Total HIV-1 Proviral DNA from ddI Group	
Various Visits.....	87
Table 16: Positive Gut Tissue Samples for Total HIV-1 Proviral DNA from Switched Treatment	
Group Various Visits .....	88
Table 17: Positive Gut Tissue Samples for 2-LTR Proviral DNA from AZT Group	
Various Visits.....	89
Table 18: Positive Gut Tissue Samples for 2-LTR Proviral DNA from ddI Group	
Various Visits.....	90
Table 19: Positive Gut Tissue Samples for the Integrated Proviral DNA from ddI	
Group Various Visits.....	91
Table 20: Positive Gut Tissue Samples for Total HIV-1 Proviral DNA from Switched Treatment	
Group Various Visits.....	92

## List of Figures and Illustrations

Figure 1: A Schematic Representation of the HIV-1 Genome.....	59
Figure 2: A Schematic Representation of the HIV-1 Life Cycle.....	60
Figure 3: A Schematic Representation of pNL4-3 Plasmid Map.....	61
Figure 4: A Schematic Representation of 2-LTR Plasmid Map.....	62
Figure 5: A Schematic Representation of the Integrated DNA Plasmid Map.....	63
Figure 6: A Schematic Representation of the Locations of the PCR Primers in the HIV DNA..	64
Figure 7: Detection of Amplified Total HIV-1 proviral DNA by conventional PCR.....	65
Figure 8: Detection of Amplified 2-LTR Proviral DNA by Conventional PCR.....	66
Figure 9: Detection of Amplified Integrated DNA by Conventional PCR.....	67
Figure 10: Total HIV Proviral DNA Syber Green Real-Time PCR Standard Curve.....	68
Figure 11: 2-LTR Proviral DNA Syber Green Real-Time PCR Standard Curve.....	69
Figure 12: The Integrated Proviral DNA Syber Green Real-Time PCR Standard Curve.....	70
Figure 13: Optimization of Total HIV Proviral DNA Detection by Real- Time PCR Standard Curve.....	71
Figure 14: Optimization of 2-LTR Proviral DNA Detection by Real- Time PCR Standard Curve.....	72
Figure 15: Optimization of the Integrated Proviral DNA by Real- Time PCR Standard Curve.....	73
Figure 16: Optimization of Total HIV Proviral DNA by Real- Time PCR Standard Curve Mixed with Chromosomal DNA.....	74
Figure 17: Optimization of 2-LTR Proviral DNA by Real- Time PCR Standard Curve Mixed with Chromosomal DNA.....	75

Figure 18: Optimization of the Integrated Proviral DNA by Real- Time PCR Standard Curve Mixed with Chromosomal DNA.....	76
Figure 19: Samples Dilutions from Various Gut Tissues to Test for the Optimal DNA Concentration.....	77
Figure 20: Total HIV-1 Proviral DNA Detection by Real- Time PCR without/with the Presence of BSA.....	78
Figure 21: 2-LTR and Integrated Proviral DNA Detection Real- Time PCR without/with the Presence of BSA.....	79
Figure 22: HIV-1 Proviral DNA Forms Detection from PBMC's of HIV-1 Infected Patients.....	80
Figure 23: Total HIV-1 Proviral DNA Quantification from PMBC's of HIV-1 Infected Patietsns.....	81
Figure 24: 2-LTR Proviral DNA Quantification from PBMC's of HIV-1 Infected Patients.....	82
Figure 25: The Integrated Proviral DNA Quantification from PBMC's of HIV-1 Infected Patients.....	83
Figure 26: HIV-1 Proviral DNA forms Detection in the Gut Different Tissues of HIV-1 Infected Patients.....	84
Figure 27: HIV-1 DNA Distribution in Gut Tissues of HIV-1 Infected Patients.....	85
Figure 28: All Positive Gut Tissue Samples for the Total HIV-1 Proviral DNA from Various Visits.....	93
Figure 29: Comparison of Total HIV-1 Proviral DNA Levels from HIV-1 Infected Patients.....	94
Figure30: 2-LTR Proviral DNA Levels in the Gut Tissues from HIV-1 Infected Patients.....	95
Figure 31: The Integrated Proviral DNA Levels in the Gut Tissues from HIV-1 Infected Patients.....	96

## List of Symbols and Abbreviations and Nomenclature

<u>Symbol</u>	<u>Definition</u>
ADCC	Antibody-dependant cell mediated cytotoxic
AIDS	Acquired immunodeficiency syndrome
ART	Antiretroviral therapy
APOBEC3G	Apolioprotein B mRNA editing enzyme catalytic polypeptide like 3G
APOBEC3F	Apolioprotein B mRNA editing enzyme catalytic polypeptide like 3F
AZT	Azidothymidine/ Zidovudine
BSA	Bovine albumin serum
CA	Capsid
cART	Combined antiretroviral therapy
CCR5	C-C chemokine receptor type 5
cDNA	Complementary deoxyribonucleic acid
CHREB	Conjoint Health research Ethics Board
CNS	Central nervous system
CSF	Cerebrospinal fluid
CTL	Cytotoxic T lymphocytes
CXCR4	C-X chemokine receptor type 4
DC	Dendritic cell
ddC	Dideoxycytidine/ Zalcitabine
ddI	Didanosine
DNA	Deoxyribonucleic acid

dNTP	Deoxyribonucleic triphosphate
Env	Viral Envelope
EFV	Efavirenz
FDA	Food and Drugs Administration
Gag	Group specific antigen
GALT	Gut associated lymphoid tissue
HAART	Highly active antiretroviral therapy
HBV	Hepatitis B virus
HIV	Human immunodeficiency virus type 1
HR	Homologous recombination
IN	Integrase enzyme
INSTI's	Integrase strand transfer inhibitors
LB	Luria Broth
LTR	Long terminal repeat
MA	Matrix
MC	Mast cell
mRNA	Messenger ribonucleic acid
NC	Nucleocapsid
Nef	HIV negative regulatory factor
NHEJ	Non-homologous end joining
NK	Natural killer cell
NNRTI	Non- nucleotide reverse transcriptase inhibitor
NRTI	Nucleotide reverse transcriptase inhibitor
PBMC	Peripheral blood mononuclear cell

PBL	Peripheral blood Lymphocytes
PCR	Polymerase chain reaction
PRO	HIV protease enzyme
Pol	Polymerase
q-real- time PCR	Quantitative real time polymerase chain reaction
RAL	Raltegravir
Rev	Regulator of expression of viral proteins
RNA	Ribonucleic acid
RT	Reverse transcriptase
SAC	Southern Alberta clinic
SIV	Simian immunodeficiency virus
SU	Surface unit
Tat	HIV trans-activator
T <sub>CM</sub>	Central memory T cell
T <sub>EM</sub>	Effector memory T cell
TFIIB	Transcription factor II complex type B
TM	Transmembrane region
UNG2	Uracil DNA glycosylase 2
Vpu	Viral protein unique

## **Chapter One: Introduction**

### **1.1 HIV/AIDS:**

HIV/ AIDS (Human Immunodeficiency virus/ Acquired immunodeficiency syndrome) is a serious disease which caused the death of 1.5 million individuals around the globe (1). Africa still harbors more than 68% of all infections despite that it is only accommodating 13% of the worlds' population (2,3). In 2012, Canada has an estimated 85,000 people living with HIV (4).

HIV/AIDS is caused by an enveloped retrovirus, which was first isolated in 1983 from a lymph node biopsy of an HIV/AIDS patient with lymphadenopathy [swollen lymph nodes] (5). Lymphadenopathy was considered a precursor to AIDS (5). AIDS develops on average within five years in 20% of HIV-1 infected individuals, as the virus keeps replicating and targeting the individual's immune cells CD4+ T- cells (5). The continuous viral replication at 500-1000 RNA copies/ml and the subsequent depletion of the CD4+ cell count from the normal range between 500 and 1,600 cells/ $\mu$ l to below 200 cells/ $\mu$ l in the blood. The drop of CD4+ cell count below 200 cell/ $\mu$ l together with the occurrence of opportunistic infections are the tell-tale signs of HIV/AIDS (5,6-9). HIV-1 infection is commonly associated with hepatitis B or C virus co-infection, tuberculosis and enterocolitis (5).

HIV is a highly variable virus and there are major types and subtypes. The two major types are HIV-1 and HIV-2. HIV-1 is a wide spread epidemic variant of the virus (5), it has been classified into various groups, due to the high rate of mutations and the genetic similarities (5). HIV-1 groups consist of the outlier group (O) and the new group (N), which are found in west-central Africa and Cameroon respectively (2). The major group (M) is the dominant group that is further divided into clades or subtypes: A, B, C, D, F, G, H and K (5). Clade B is the subtype



circulating predominantly in the Americas and Western Europe (10). , HIV-2 is found primarily in Western Africa, it is considered less pathogenic as it results in a slower progression to AIDS than HIV-1 (5).

## **1.2 HIV-1 Genome and Life Cycle:**

The HIV-1 genome consists of nine open reading frames and three of them encode the Gag (Group- specific antigen), Pol (DNA Polymerase) and Env (Envelope) polyproteins, which are proteolyzed into viral proteins that form structural proteins for new virions (11) (**Figure 1**). The virus starts infecting the cell by binding to its specific receptor CD4 and co-receptors including C-C chemokine receptor type 5 (CCR5) and C-X chemokine receptor type 4 (CXCR4). The HIV envelope proteins gp120 and gp41 on the virus surface change conformation and causes the cell membrane to change and fuse with the viral envelope membrane, which allows the nucleocapsid of the virus to enter the host cell (5).The virus un-coats and starts the reverse transcription stage (catalyzed by the viral reverse transcriptase (RT)), which converts the viral RNA into a double stranded copy DNA (cDNA) containing long terminal repeats (LTRs) at each end (5) (**Figure 2**). This proviral DNA travels to the nucleus with help of the viral integrase (IN) and integrates into the host genome or stays unintegrated either as linear cDNA or circular forms (5, 11, 12). HIV-1 integrates at random in the genome flanked by the Alu elements (13). Alu elements are located in different sites of the human chromosome and they are the frequent site of mutations (13). The integrated proviral DNA starts transcribing from the 5' LTR promoter using the host transcription machinery, and transcription terminates in the 3'-LTR, which also functions as a poly-adenylation site (5).

The viral protein Tat enhances the viral gene transcription rate and it is therefore considered essential for the viral replication (2, 5). After transcription, the spliced and genomic-length RNAs (~9 kb) are transferred to the cytoplasm, which in turn is regulated by viral Rev protein, in order to be translated into the various viral proteins or in the case of the genomic transcripts packaged into the virion (14). The Env mRNA is translated to in a gp160 precursor which is cleaved to gp120 surface unit (SU) and gp41 or transmembrane region (TM) in the endoplasmic reticulum (ER), which is transported to the cell surface membrane, where the virion is assembled (11). The Gag proteins, matrix (MA), capsid (CA), nucleocapsid (NC) and p6 with Pol proteins protease (PRO), reverse transcriptase (RT) and integrase (IN) are processed from Gag and Gag-Pol polyproteins (11). They are assembled with the genomic RNA and the viral accessory proteins Vif, Vpr and Nef to form an immature virion that begins to bud from the cell surface (11). Vpu protein assists the release of the Env polyproteins by degrading the CD4 receptor (11). Nef also degrades the CD4 and promotes endocytosis, which is considered to prevent reinfection of the same cell (11). After the particle coated by the envelope is released from the cell surface, it will start the maturation phase where the viral protease cleaves the Gag and Gag-Pol polyproteins into the various individual (11). The new mature virion is then able to infect other cells (11) (Figure 2).

### **1.3 1-LTR and 2 LTR Circles Formations:**

During viral replication, the integration step of the viral DNA into the host genome is not complete and a majority of it exists as unintegrated cDNA (12). The linear cDNA is one of the unintegrated forms that the circular forms derive from (12). 1-LTR circles can be formed by a homologous recombination of the proviral DNAs at the LTRs (12, 15). Another possible explanation of this phenomenon is the ligation of interrupted reverse transcription intermediates

(12, 16). Moreover, the integration of the linear cDNA into itself can yield an internally rearranged form (17, 18). This is so-called auto-integration, where the 3'-ends of the reverse transcriptase being processed by integrase and targets sites within the viral DNA, leading to internally rearranged or less than full length DNA circles (12). In addition, the ligation of the cDNA ends by the host cell non-homologous DNA end-joining system yielding two long terminal repeats (LTR) gives rise to the 2-LTR circles (18, 19) Figure-5 depicts a schematic representation of the different proviral DNA forms. The non-homologous-end joining (NHEJ) system exists in the host nucleus as a protection mechanism against a foreign double stranded DNA (20, 21, 22). Ku is one of the NHEJ components, which associates with the viral cDNA replication (22, 23, 24). It has been found that the inactivation of the NHEJ components, such as Ku, ligase 4, DNA-PKcs or XRCC4 leads to the reduction in 2-LTR formation (3, 13, 25).

Furthermore, cellular DNA repair factors such as xeroderma pigmentosum type B (XPB) and xeroderma pigmentosum type D (XPD) were found to play a role in viral integration inhibition. These cellular helicases are part of transcription factor II type B (TFIIB) basal transcription complex that repairs the DNA nucleotide excision and the reduced function of these two components led to the degradation in retroviral cDNA and no 2-LTR formation (12, 26).

Another DNA repair factor that inhibits the viral integration are RAD 18 and RAD 52 genes (12). RAD 18 enzyme plays a role in post-replication DNA repair mechanism as it stabilizes HIV integrase (12, 27). In RAD 18 knocked out cells, the cells became more susceptible to HIV and MLV infection (12, 28). Moreover, RAD 52 is another DNA repair component that prevents the retroviral infection (12, 29). This homologous recombination (HR) repair protein increases the level of HIV-1 transduction when its expression is reduced (12, 29). It is also found that the 2-

LTR levels were reduced in RAD 52 over-expressing cells and no sign of apoptosis, indicating that RAD 52 has a direct effect only on the linear viral cDNA (12).

In addition, apolipo protein B mRNA editing enzyme catalytic polypeptide like 3G (APOBEC3G) and apolipo protein B mRNA editing enzyme catalytic polypeptide like (APOBEC3F) are the host restriction enzymes that may affect HIV unintegrated proviral DNA formation (12, 30). They mutate the virus by introducing cytidine instead of uracil in the first strand of the viral DNA synthesis, which interfere with the viral replication (12, 31). Before integration, APOBEC3F inhibits the 3' process of the viral cDNA (12, 32). Moreover, APOBEC3G generates a 6 base extension at the U5 end of the viral 3'LTR which makes the linear cDNA unsuitable for integrase function (12, 32). This process led to the reduction in 2-LTR forms by two folds in cells lacking the APOBEC3G (12, 32).

Despite this host defense mechanism, HIV transcription and thus replication can continue from 2-LTR proviral DNA forms (12). As seen in SIV infection, the 2-LTR forms were accumulated in recently infected targeted cells, suggesting viral replication (33, 34). In addition, a high level of unintegrated DNA HIV-1 DNA was found in the brains of HIV/AIDS patients with dementia (36, 37). Although this study did not distinguished between the different unintegrated DNA forms, it is supporting the study where they found a significant correlation between the presence of 1-LTR and 2-LTR forms and HIV-1 associated dementia (36, 38). In a study on T cells line infected by HIV-1, 1-LTR and 2-LTR was detected followed by syncytium formation and infectious viral particles production (36, 39). This cytopathic infection was also found in PMBCs of patients during seroconversion (undetectable HIV-1 RNA levels) as the levels of 2-LTR were high and CD4 count was low (36, 39).

Uracil DNA glycosylase 2 (UNG2) is another DNA repair factor (uracil base excision) that plays a role in stopping HIV-1 from integration into the host chromosome and might lead to 2-LTR formation. (12, 40). The role of UNG2 is still not clear as some studies found that HIV-1Vpr protein with UNG2 directly inhibit the retroviral DNA pre-integration (12, 31). However, UNG2 role in HIV-1 infection is not clear (12). In a contrary study where they found that HIV-1 DNA can tolerate a high uracil environment, which protects the virus from auto-integration (12, 41). This study suggest that 2-LTR formation is not possible under UNG2 influence and more studies are needed to know the precise role of UNG2 in the HIV-1 life cycle.

In a recent study where they blocked the HIV-1 DNA integration into the host genome using Raltegravir (RAL) (see section 1.4 for RAL mechanism), 2-LTR forms were accumulated. In comparison, the levels of 2-LTR forms in the presence of RAL were higher than the levels after the removal of RAL (42, 43). This decrease in 2-LTR forms lead to the formation of the linear HIV-1 DNA and its integration into the host genome (43). From this previous study the RAL inhibitory effect can be reversed, which demonstrate the 2-LTR role in restoring the viral replication (43). As seen in long-term HIV-1 elite suppressors who naturally control the levels of HIV replication, the levels of 2-LTR forms were increased in the absence of antiretroviral therapy (43, 44). Interestingly, the long lasting existence of 2-LTR forms in the nucleus and due to its unique feature, is used as a biomarker of ongoing HIV-1 replication and infection despite antiretroviral therapy (18, 34).

## **1.4 HIV-1 Therapy and Drug Resistance:**

### **1.4.1 Anti-HIV-1 Therapy:**

At the end of 2013, an estimated 35 million individuals over the globe were living with HIV (1). Due to the unavailability of an HIV-1 vaccine, primarily therapeutic methods have been established to control the disease (45, 46). Zidovudine (AZT - Azidothymidine) was the first antiretroviral (ART) drug to treat HIV-1(156). This monotherapy is a thymidine analog, which inhibits the viral reverse transcription by terminating the proviral DNA extension (5). These nucleoside analogs are known as nucleoside RT inhibitors (NRTI) (47). However, the relatively quick emergence of resistant HIV strains limited the benefits of AZT in slowing the progression of HIV infection to AIDS (5, 14-16).

In 1996, a combination of two antiviral drugs was recommended as an initial treatment for HIV infection, and that included two nucleoside analogues or NRTIs [AZT and didanosine (ddI)] (48, 49). This first type of combination antiretroviral therapy (cART) was found to reduce 23% of HIV related mortality and delayed the HIV progression to AIDS or death compared to AZT alone (49-51). Lamivudine (3TC) was also used in combination with AZT to treat healthcare workers or other individuals exposed to HIV infection after accidental contact with HIV-contaminated blood, tissues, or other body fluids (50, 52). In 1997, highly active antiretroviral therapy (HAART) was introduced as a combination of three drugs from different drug classes, such as the combination between two NRTIs with protease inhibitors (PI) or two nucleoside reverse transcriptase inhibitors (NRTIs) with one non- nucleoside reverse transcriptase inhibitor (NNRTI) (5, 47, 53). HAART became the standard treatment for HIV-1; for example, the combination between ddI, Lamivudine (3TC) and Efavirenz (EFV) has been highly effective in

suppressing viral replication to undetectable levels (<50 copies/ml) in the plasma; as well as in preventing HIV-related disease progression (59,60). Furthermore, HAART's effectiveness has shown significant improvement in patients' compliance to therapy, which resulted in an overall better clinical outcome (22).

Currently, there are five classes that inhibit different steps in the HIV life cycle (5). As previously mentioned, both the NNRTIs, NRTIs are in the class that inhibits the HIV reverse transcriptase step required for the virus's transition from viral genomic RNA to proviral cDNA (5, 47). Another class is the protease inhibitors that will stop the protease from cleaving the HIV polyproteins, which is important in the maturation of the virion, and results in non-infectious virus (5, 47). In addition, the fusion or entry inhibitor class blocks the fusion between the viral envelope with host cell membrane so the HIV will not enter the host cell (61). Integrase inhibitors are the fourth class of drugs that blocks the HIV proviral DNA from integrating into the host chromosome. The fifth class of drugs available are the viral attachment inhibitors. An example of this is the CCR5 attachment inhibitor, which blocks the virus from using the CCR5 co-receptor (61)

HIV treatments have helped many people around the world (61). However, apart from the costs also the problem with drug toxicity limits the number of patients who can benefit from HIV therapy (61). It has been shown that at least 15% of patients do not respond well to protease inhibitors and experience serious side effects (61). For example, Saquinavir is one of the important drugs included in highly active anti-retroviral therapies (HAARTs) and it was found to cause atherosclerosis in HIV patients (62).

### **1.4.2 Treatment of HIV-1 in Africa:**

Before HAART, AZT was the treatment of choice for HIV-1; it was not an effective therapy because it only provided the patients with approximately 6 more months to live (53). Soon after the introduction of AZT HIV-1 resistant strains emerged (53). To overcome this problem the use of two drugs were introduced, which reduced the HIV-1 viremia and drug toxicity in patients (53). For example, the combination between AZT and DDI lowered the AZT toxicity and the possibility of developing drug resistance to either one of the drugs, because in case drug resistance developed the other drug can be sufficient enough for effective treatment (53).

In most developing countries the standard HAART includes two NRTI's (AZT and 3TC) and one NNRTI's (NVP) (53, 54). In addition, the protease inhibitor is one of the important drug class included in HAART, which gives better results in managing AIDS. However, the cost of the drug makes it not available in developing countries (53, 55). In comparison, the United States of America offer HAART to HIV-1 patients when their CD4+ count fell below 350 cells/mm<sup>2</sup> or the viral load is <25,000 RNA/ml whereas in Africa the therapy is offered later in HIV-1 infection. For example, African patients are offered HAART when they show AIDS- defining indications, such as CD4+ count below 200 cells/mm<sup>2</sup> with viral load >50,000 RNA/ml (53-58). HAART is offered in some countries in Africa at late stages of HIV-1 infection, it showed high rate of mortality and increase in CD4+ cells count (53-55, 56-58, 63, 68, 69). However, HIV-1 is still considered a global health issue and Sub-Saharan Africa is still the most affected area by AIDS contributing to 70% of the total globe new infections (1). HIV positive Africans are tormented by fear of discrimination, fear of HIV- stigma and conflicts between traditions and faith- based beliefs, which makes it challenging to reach all eligible individuals to receive treatment (64, 68). Globally, 12.9 million people living with HIV and were receiving ART at the



end of 2013 (1). Under the 2013 WHO guidelines, the HIV treatment coverage in low- and middle-income countries represented only 34% (32-37%) of the 28.6 million people eligible in 2013 (66). In Africa, 25.2 million people living with HIV of them 7.6 million were receiving ART at the end of 2012 (67). Despite the rise numbers of people receiving ART in Africa, the limited resource setting raise concerns of successful treatment for AIDS in Africa (68, 69, 70). For example, 25% of HIV positive patients receiving ART do not come for follow up after a year of treatment (71). These patients have to deal with long walks to health centers or high transportation cost, hours of waiting in line to receive the medications and poor and stigmatizing consultation (71). In addition, 25% of treated patients do not successfully suppress the virus (71, 72). Moreover, key populations (men who have sex with men, sex workers, injected drugs users and transgender people are facing barriers to access of health services and low to extremely low access to antiretroviral therapy (67). At the end of 2012, men represent 40% of all the eligible people for treatment in Africa under the 2013 WHO guidelines (67). These men represent only 36% of the antiretroviral therapy recipients in Africa alone (67). In addition, an estimated of 50 young women are newly infected with HIV every hour in Africa due to sexual violence and abuse (66). There are also signs of increased unsafe sexual behaviors in some African countries which increases the burden of controlling HIV infection (66). Although the access to ART reaches 62% of pregnant women living with HIV, it is still not accessible among pregnant sex workers, transgender women and drug users (66). Furthermore, the mother to child transmission can be reduced to <5% by ART (66). As a result, 52% decrease in new HIV infections in children was achieved since 2001 until 2013 (66). In the contrast, HIV treatment coverage for children is still half of the coverage for adults in 2012 as only 647,000 children under the age of 15 were receiving ART (66). Another problematic aspect of treating HIV infected children is

among adolescents (73, 74) as they do not access HIV testing and counselling leading to the number of AIDS- related deaths to increase from 2001 to 2012 in that group (67). Similar reports from 2005 and 2012 found that the annual number of AIDS-related deaths was almost doubled in adolescents (67, 75). These facts gives the urgent need to reach all HIV-1 infected regions in Africa by increasing the efforts of building HIV services centers that includes testing, counselling and treatment as some areas still do not have HIV therapies.

In addition, HBV is another health issue alongside HIV-1 infections in South Africa (73). Overall, co-infection represent 20-30% among HIV-1 infected individual (76, 77, 78). Those patients are treated with monotherapy (lamivudine) to treat their HBV infection (73). However, the emergence of lamivudine resistance to both HIV and HBV rose and became problematic in the developing world (73). WHO guidelines to treat HIV recommended the use of Tenofovir (NRTI) and Lamivudine (NRTI) to treat HIV-HBV co infection patients, but the limited access to Tenofovir made ART unobtainable in South Africa (73). HIV-1 patients in Africa receiving monotherapy might be possible due to the limited access to HAART. Only one drug is considered ineffective against HIV-1 as the virus continues to replicate and attack the immune system.

### **1.4.3 HIV-1 Vaccines:**

The stimulation of an effective immune response against the highly mutating HIV-1 virus is one of the qualities needed in HIV-1 immunotherapy (79, 80, 81). To be protective, the HIV-1 vaccine has to induce response that acts in matter of few days before the establishment of HIV-1 latent reservoirs (79, 81, 82). HIV-1 vaccine development started soon after the virus became a wide spread health issue with more than 218 HIV vaccines going through clinical trials (79, 83-85). Only 5 HIV vaccines have been advanced to phase IIb and III clinical trials (79, 85). VAX003 and VAX004 are HIV vaccines which they have been tested in phase III clinical trials (79, 86, 87). These vaccines are bivalent recombinant HIV-1 envelope (Env) gp 120 B/E and B/B clades that induced antibodies, but did not reduce HIV-1 infection (79, 86, 87).

One of the vaccines that was advanced to phase IIb clinical trial is the adenovirus serotype 5 vector expressing HIV-1 antigens including (gag, pol and nef) genes (79,88). This vaccine was not protective against the virus, due to the selective immunity and an elevated CD8+ T cells response (79, 88). The most recent vaccine in phase IIb clinical trial was the deoxyribonucleic acid (DNA) vector expressing HIV-1 clade B Gag, Pol and Nef proteins and multi- clade Env proteins followed by a recombinant adenovirus type 5 boost, but protective immunity was not observed (79, 89).

One vaccine was successful in reducing HIV -1 acquisition, and consist a recombinant HIV-1 (env-gag-protease) canarypox vector prime and a recombinant gp 120 plus alum boost (65, 79). This vaccine was tested in clinical trials phase III but had a limited efficacy of 31% (65, 79). Following this study, it was found that Env V1-V2 immunoglobulin (Ig) G antibodies correlated with HIV reduced acquisition and IgA Env antibodies as a risk in the previous trail (79, 90, 91).

It was also found that the antibody-dependent cell-mediated cytotoxicity (ADCC) activity may have a protective effect against HIV-1 infection (79, 90, 91). For this reason, the current HIV-1 vaccines are working on stimulating cytotoxic T lymphocyte (CTL) response and antibodies (53, 79). One vaccine has been established using this approach. In macaques an SIV vaccine, inducing neutralizing antibodies was found to protect the macaques from SHIV (HIV/SIV chimera) infection (79, 92). Moreover, *in vitro* analysis showed the CTLs response was also effective against CD4+ T cells and stabilizing the viral load levels (79, 92). This vaccine seems promising in animal models, but human trials are still needed to determine the efficacy of the vaccine against HIV-1 infection (79).

In summary, so far all vaccine trials have failed or were disappointing with regard to protection, but they have given us valuable insight that are guiding the ongoing efforts in developing a vaccine. However, a vaccine will not be available in the near future, and our best weapon against HIV-1 infection will remain prevention and antiretroviral therapy.

#### **1.4.4 Drug Resistance Mechanisms:**

Despite the different HIV treatments with their clinical benefits, they are not considered a cure as they do not appear to clear the virus from the patient (5). The high HIV mutation rate of the reverse transcriptase, which is beneficial for viral immune escape, also results in the development of drug resistance to almost all classes of the drugs (5, 47). The best understood resistant mechanisms are the ones against NRTIs, NNRTIs and PIs. The NRTIs are non-extendable nucleoside analogues that stops the proviral DNA chain from growing (47). The resistance to NRTIs can occur by two mechanisms. One of them results in the increased drug discrimination by the nucleotide binding site of the reverse transcriptase (47). The other

mechanism involves mutations that prevent the NRTIs from being incorporated or increased excision from the cDNA, although the drug is bound to RT (47). NNRTIs bind to an amino acid pocket in the reverse transcriptase that allows them to block the enzyme movements required for the viral DNA to be synthesized. The resistance mutations keep the pocket closed so the NNRTIs are no longer able to interact (47). As indicated, development of drug resistance also occurs for protease inhibitors. These drugs are designed to prevent gag and gag-pol protein from being cleaved by the viral protease, which leads to a block of virion maturation and infectivity (47). However, the viral mutation changes the structure of the protease, which makes it hard for the drug to bind and block its activity (47). Raltegravir (RAL) is the only integrase inhibitor approved by the food and drugs administration (FDA) and it is one HAART component (93). RAL works on blocking the IN strand transfer reaction (93). However, the discovery of 30 integrase inhibitor mutations raises a challenge in HIV-1 treatment, since most of these mutations are located in the IN active site within the core domain which is also the binding pocket for integrase strand transfer inhibitors (INSTIs) (93). The mutations can positively affect viral capacity to replicate and all work together to either improve the fitness of the replication or/ and increase the viral resistance to integrase inhibitor (93). The rise of drug resistant mutations are problematic for treating HIV-1, but the persistence of the virus in various reservoirs and drug sanctuary sites is another problem in preventing the eradication of the virus.

In addition to continuous viral replication as a result of drug resistance mutations, HIV replication also persists in sanctuary sites, such as brain and testis (94, 95, 96). Moreover, it has also been shown that despite the successful antiretroviral therapy HIV persist in the cells of the gut associated lymphoid tissues (GALT), suggesting that the gut may also act as a sanctuary

against the antiretroviral drugs (95, 97, 98). The role of HIV-1 reservoirs will be discussed below.

### **1.5 HIV-1 Reservoirs:**

The definition of a viral reservoir is any HIV-1 infected cell with half-life longer than 1 day (99). Macrophages are considered a reservoir for HIV-1(99). Late in HIV-1 infection macrophages are prominent due to the majority of CD4+ T cells being lost (99, 100). *In vivo*, macrophages were found to be resistant to the viral cytopathic effects, which make them live longer than CD4+ T cells (99, 101). It was also found that macrophages remained persistently infected in pre- HAART era patients (102, 103-105).

Another HIV-1 reservoir is the central nervous system (CNS) (99). In the CNS, astrocytes, microglial cells contain HIV-1 DNA (106). Studies in untreated patients asymptomatic for HIV infection, the latent reservoirs were already established in the brain tissue early in infection (106). HIV-1 infects perivascular macrophages and microglial cells within the CNS (105). The central nervous system (CNS) is also considered a sanctuary for HIV for continuous replication under antiretroviral therapy, as some antiretroviral drugs cannot cross the blood- brain barrier. This continuous replication in the brains is linked to serious neurological complications, such as HIV associated dementia even under antiretroviral therapy (5, 94, 95). However, in 25-50% of HIV-1 patients receiving HAART neurocognitive impairment was not observed and patients did not show continuous viral replication in their CSF. Thus this data would suggest that CNS may not be an HIV-1 reservoir, and more investigation is needed (99, 107) However, in SIV infection neurological disease was observed in macaques and SIV DNA was detected despite HAART (60, 99).

Studies have shown that mast cells (MCs) progenitors were susceptible to HIV-1 infection (108). It was also found that stimulation of these latent infected mast cells led to the viral replication resumption, and indicates they are reservoirs for HIV-1 infection (108, 109). Further evidence in support of the concept of mast cells as HIV-1 reservoirs, is the fact that they are long lived. They also exist in all tissues close to blood vessels and epithelial interface, which exposes them to “environmental factors” (108, 110). The presence of mast cells in tissues with inflammatory conditions leads to the migrations of some mast cells to other organs (108, 111). For example, mast cells migrate to lymph nodes and spleen containing CD4+ T cells, HIV-1’s main target, which enables continuous viral dissemination (108, 111). Similarly, B-cells have the ability to capture a virus, migrate to other tissues and interact with CD4+ T cells, which make them an extracellular reservoirs for HIV-1 (112). The similarity in HIV-1 sequences obtained from peripheral blood B-cells and CD4+ T cells is the evidence for the interaction between the two cell types (113).

Follicular dendritic cells are another HIV-1 reservoir as they trap the virus with mostly intact replicative components compared to other infected cells and tissues, which enable the virus to persist for years (114).

In addition, CD34+ hematopoietic cell progenitors were shown to serve as reservoirs to latent HIV-1 infection. This latent state can be reversed to its active state using cytokines *in vitro* and *vivo* (108, 115).

## **1.6 The Immune System in the Gastrointestinal Tract and Blood:**

The gut- associated lymphoid tissue (GALT) contains mesenteric lymph nodes, Peyer’s patches in the small intestine, and follicular aggregates in the large intestine, appendix and

cecum (82,116). Lamina propria lymphocytes and intraepithelial lymphocytes are also included within GALT. In earlier studies of the GALT, the Peyer's patch dome was found to be covered by cuboidal epithelial cells expressing class II major histocompatibility complex (MHC) antigens, few goblet cells and M cells (microfold cells) (118, 119). Moreover, macrophages and dendritic cells were also found in Peyer's patches dome (118). The dendritic cells in the lamina propria of the small and large intestine are considered antigen presenting cells (118-120). In addition, Peyer's patches are enriched with B-cells with IgA surface molecules beside the predominant IgM- B cells, which makes the GALT a major site for IgA responses (118). Peyer's patches are also enriched with T-helper-inducer subset (Th) suppressor- cytotoxic T cells and contra-supressor T-cells (118). After antigen exposure, Peyer's patches generate Th and IgA-B cells that afterward will travel through the mesenteric node into the thoracic duct to enter circulation before the selective migration to the mucosal surfaces (118). After the migration of the IgA- lymphoblasts into the antigen stimulated organ, they secrete antibodies and remain in this organ until they die within a few days (118-121). In contrast, the memory cells that produce B and T cells lymphoblasts after being stimulated by antigens were found recirculating in the mucosal lymphoid tissue (37, 118). Other studies found that the lymphoblasts had the ability to distinguish high endothelial cell receptors in the colon indicating a unique specificity of the colon's homing lymphoblasts (118). However, the magnitude and persistence of the immune response in the colon is affected by the presence of antigens and antibody producing cells. (37, 118). The colon epithelial cells do not express class II MHC needed to induce T cell immune responses unless it is inflamed (118), while it is normally expressed in the small intestine (118). The different and complex immune cell expression patterns and lymphocyte components in the gastrointestinal tract play a role in HIV-1 dynamics in HIV/AIDS progression. The persistence of



the virus in the different gut tissues leads to continuous inflammation (118). This inflammation in gut tissues fuels it with new T-cells for the virus to target, which makes it hard to control the progression of HIV/AIDS (118).

In healthy individuals 80% of the total lymphocytes are found in the GALT and ~40 % of them are CD4+ T-cells (82, 116, 122). In comparison to the blood, T lymphocytes are 2-5% of total lymphocytes (116, 123, 124) which suggest a different infection rate between different compartments (116). HIV RNA was detectable in 0.01-1% of peripheral T- cells and 60% of mucosal memory CD4+ T cells during acute infection (82, 122, 129).

### **1.7 HIV-1 in the Gut:**

Abnormalities in HIV infected individuals' GI mucosa date back to the earliest observations by Kotler and colleagues, which included malabsorption and lymphocyte depletion (122). The gut associated lymphoid tissue (GALT) is the largest lymphoid organ in the body that contains the vast majority and most complex pool of immune cells (123). However, only in the last decade, it became increasingly clear that the GALT is in fact a main reservoir for viral replication, CD4+ T-cells depletion and an important compartment containing specific viral variants (95, 97, 125). Approximately, 30% of HIV/AIDS patients suffer from gastrointestinal dysfunction (GI), but the role of GALT in the HIV GI disease and the viral dynamics are still largely unknown (46, 97). Diarrhea, intestinal permeability and GI inflammation are some of the symptoms of HIV enteropathy (33). GI inflammation mediated by activated lymphocytes causes damage to the GI epithelial cells, and the degree of inflammation is found to be correlated with viral replication (122, 126). Early studies already suggested that the intestinal mucosa can be the site of HIV replication and CD4 T-cells depletion, which was further confirmed by the fact that

the GI tract was significantly depleted from CD4 T-cells early in HIV infection (122, 127, 128, 130-132). These increased viral loads lead to T-cells depletion and disease progression (5, 127). Another illustration of the effect on disease progression was the fact that HIV-1 infection of epithelial cells leads to inflammatory factor secretion (TNF- $\alpha$ , IL-6) (133). The continuous inflammatory response is considered a chronic HIV-1 infection feature (133, 134).

In a recent study, the gastric epithelial cells were suggested as a natural target for HIV-1 infection (133). HIV-1 particles were detected in the gastric epithelial cells obtained from asymptomatic and AIDS patients (133). In asymptomatic patients, a small number of HIV infected epithelial cells were found in the lamina propria (5.1% HIV-1 infected glandular acini (13.2%) whereas the numbers increased in AIDS patients, HIV-1 infected gastric epithelial cells (17.3%) HIV-1 infected glandular acini (34.2%) (133). These numbers show that the HIV-1 infected gastric epithelial cells increased in chronic HIV-1 infection (133). Furthermore, a positive correlation between the numbers of HIV infected epithelial cells from the gastric mucosa and the blood viral load was found (133). The higher the viral plasma load the higher numbers of HIV infected epithelial cells found in the gastric mucosa (133). In contrast, no correlation was found between the number of HIV-1 infected epithelial cells in the gastric mucosa and its plasma viral load (133). Many studies suggest that the gut is considered a sanctuary, where the virus can hide out and keeps replicating despite successful antiretroviral therapy, similar to what has been seen in the simian immunodeficiency virus (SIV) model (35, 95, 97, 135).

It was found that the HIV proteins have various effects on enterocytes (136, 137, 138). For example, Tat protein inhibits the uptake of glucose (97, 118). Gp120 of HIV has the ability to increase the calcium levels in the enterocytes, which leads to a decrease in the epithelial cells

ability to balance this ion (138). Moreover, HIV was found near abnormal enlarged enterocytes, which may suggest that HIV might be the reason behind the observed abnormal enterocytes differentiation (137). Studies by our lab showed that viral species in the gut tissues (esophagus-stomach- duodenum and colon) were compartmentalized, with increased viral diversity within the colon (96). Our lab also found that drug-resistant HIV variants differed in the various gut tissues compared to the blood. Moreover, after zidovudine treatment the level of resistance to this drug was increased in the colon (95). The latter finding is of interest as it has been shown that HIV-1 replication appears to continue in the colon under apparent successfully suppressive HAART. These combined observations suggest that the HIV-1 viral dynamic differs significantly amongst the different gut tissue compartments even under HAART.

### **1.8 Rationale:**

The observations by our lab and others suggest that HIV-1 replication is highly dynamic in the gut even under antiretroviral therapy. In order to get a thorough understanding of the viral dynamics in the gut of the HIV-1 infected individual, a comprehensive analysis of the levels of HIV-1 infection and replication in the gut tissues needs to be performed. To extend the previous studies the viral load (2-LTR circles and integrated HIV DNA) needs to be quantified in the different gut tissues and blood. These results will be compared with existing data from the lab and previous studies that will allow us to get a better overview off how HIV-1 dynamics (i.e. viral replication) in the GI tract and GI dysfunction are linked. A recent study by Zhu and colleagues (2011) assessed the levels of 2-LTR circles, the total HIV-1 and integrated DNA in HIV-1 infected patients during the early phase of HAART therapy, to get insight into the persistence of viral replication under therapy. They established real- time PCR methods based on methods developed by Butler et al and Brussel et al to measure the different HIV-1 proviral

DNA forms in peripheral blood mononuclear cells (PBMC's) of HIV-1 positive patients (19, 24, 139). The authors were able to easily detect changes in the 2-LTR circles levels compared to other HIV-1 DNA forms during the first 12 weeks of receiving HAART, thereby gaining insight into the persistence of viral replication under HAART in the lymphocyte reservoirs in the blood. Many studies looked into the effect of antiretroviral therapy, especially HAART on the viral loads in blood samples or other tissues, but very few studies have quantified 2-LTR circles and HIV-1 integrated DNA amounts in the different tissues of the gut (Esophagus-stomach-duodenum and colon). Moreover, we have access to unique gut tissue samples from HIV-1 infected individuals from the pre-HAART era. These samples are not ideally suitable for regular viral load analyses due to the low quantities of RNA as a result of the age of the samples and rapid degradation of RNA. Therefore, analyzing the 2-LTR proviral DNAs and integrated proviral DNA, together with the data on viral evolution our lab has already obtained, will enable novel insights into the viral replication dynamics in the gut under suboptimal therapy that has not been obtained previously. Developing reliable real-time PCR essays for the GI tract similar to those described above, will enable us to study in more detail the kinetics of HIV-1 infection under different therapies in the gastrointestinal tract.

### **1.9 Hypothesis of the Study:**

We hypothesize that HIV-1 proviral DNA (integrated and 2-LTR forms) levels vary in the different parts of the gut in HIV patients receiving ART.

**Aim 1:** Optimize the PCR conditions and the quantitative real-time-PCR protocols to determine 2-LTR forms and integrated proviruses in patient gut biopsies and blood samples.

**Aim 2:** Use the optimized protocols on patient gut biopsies and blood samples to determine how much of the different proviral DNA forms are present in each tissue (Esophagus-stomach-duodenum and colon) compared to blood.

**Aim 3:** Monitor the changes in the proviral DNA (integrated and 2-LTR) levels over time in patient gut biopsies and blood samples taken at 6-8 months intervals under different therapies.

## Chapter Two: Material and Methods

### 2.1 Patient Samples:

The samples were obtained from a cohort study (42 patients) that has been done previously at the Southern Alberta Clinic (SAC). The University of Calgary Conjoint Health Research Ethics Board (CHREB) has approved all studies (E-832). The patients enrolled were homosexual males with HIV infection and suffered from various degrees of GI dysfunction. The samples were collected between 1993-1996 before HAART was introduced at the SAC. HAART was introduced at the SAC in 1997. Gut biopsies were collected at 6-8 months intervals and for a majority of the patients, tissues were harvested 4-5 times for each patient during the period of the study. On the patients' first visit, gut biopsies (Esophagus (E), Stomach (S), Duodenum (D), and Colon (C) and blood (Plasma and PBMC) were collected, while on the subsequent second visit we collected only blood. Due to the invasive procedure of collecting the gut biopsies from the patients, the gut biopsies were collected every alternating visit. The sample type on each visit follows the same pattern is represented in Table 1. The patients' antiretroviral therapy during the study consisted of monotherapy with AZT, ddI, ddC, d4T and 3TC or a combination. In this study, we tested PBMC samples from 18 patients and gut tissues were tested from 14 patients. We also included analysis of samples taken between year 2008 and 2010 of the surviving patients from this cohort study, who are on HAART to compare our results before and after HAART. A summary of the clinical information of the HIV-1 infected patients is represented in **Table 2A-2B-2C-2D and 2E.**

**Table 1: Types of Samples on Each Visit.**

Visit 1	Visit 2	Visit 3	Visit 4	Visit 5
Gut biopsies + Blood (Plasma +PBMC)	Blood (Plasma +PBMC)	Gut biopsies + Blood (Plasma +PBMC)	Blood (Plasma +PBMC)	Gut biopsies + Blood (Plasma +PBMC)

**Table 2A: Summary of the Clinical Information of Patients #1 to #3.**

Patient ID number	Date of started therapy	Date of HIV diagnosis	Type of Antiretroviral therapy	CD4 T-cell count	HIV viral load (copies/ml)
1	06-Apr-1993	30-Jun-1986	ddl+AZT+3TC	184	500
	07-Sep-1993		AZT+ ddl	276	400
	18-Jan-1994		AZT	210	240
	31-May-1994		AZT	324	1,600
	25-Oct-1994		AZT+ ddl	253	3,300
	21-Feb-1995		AZT+ ddl	187	3,700
	06-Jun-1995		AZT+ ddl	151	730
	05-Dec-1995		AZT+3TC	214	750
2	06-Apr-1993	30-Jun-1989	ddl	187	17,000
	07-Sep-1993		d4T	40	16,000
	24-Jan-1994		-	40	130,000
	03-May-1994		-	6	26,000
	13-Sep-1994		-	12	
3	06-Apr-1993	30-Jun-1989	ddl	144	20,000
	07-Sep-1993		ddl	187	1,200
	25-Jan-1994		AZT	162	210,000
	03-May-1994		AZT	120	220,000
	13-Sep-1994		AZT	77	430,000
	17-Jan-1995		-	96	210,000
	09-May-1995		D4T	82	54,000
	24-Oct-1995		AZT	69	110,000
	Ther3TC				

**Table 2B: Summary of the Clinical Information of Patients #5 to #14.**

Patient ID number	Date of started therapy	Date of HIV diagnosis	Type of Antiretroviral therapy	CD4 T-cell count	HIV viral load (copies/ml)
5	13-Apr-1993	30-Jun-1991	ddl	340	250
	14-Sep-1993		ddl	399	1,400
	18-Jan-1994		ddl	286	400
	10-May-1994		ddl	400	2,500
	27-Sep-1994		ddl	340	28,000
	21-Feb-1995		ddl	315	6,800
	20-Jun-1995		ddl	275	26,000
	20-Jun-1995		ddl	239	46,000
	03-Oct-1995		ddl		
7	20-Apr-1993	30-Jun-1992	ddl	294	34,000
	21-Sep-1993		ddl	240	4,800
	22-Feb-1994		ddl	234	90,000
	06-Sep-1994		ddl	187	110,000
	28-Mar-1995		AZT	146	180,000
	04-Jul-1995		AZT	141	140,000
	24-Oct-1995		AZT	148	120,000
	24-Oct-1995		AZt+ ddc	188	7,028
	06-Feb-1996		AZT+ ddc		
8	20-Apr-1993	30-Jun-1988	ddl	432	2,100
	14-Sep-1993		ddl	360	1,400
	11-Jan-1994		ddl	450	3,500
	10-May-1994		ddl	384	20,000
	15-Nov-1994		ddl	325	23,000
	07-Mar-1995		ddl	376	7,900
	04-Jul-1995		-	372	28,000
	10-Oct-1995		-	310	22,000
14	11-May-1993	30-Jun-1986	ddl	540	4,900
	14-Sep-1993		ddl	520	6,100
	11-Jan-1994		ddl	672	3,400
	21-Jun-1994		ddl	494	4,300
	04-Oct-1994		ddl	588	16,000
	02-May-1995		ddl	510	14,000
	10-Oct-1995		ddl	519	11,000
	06-Feb-1996		ddl	491	3,900



**Table 2C: Summary of the Clinical Information of Patients #16 to 20.**

Patient ID number	Date of started therapy	Date of HIV diagnosis	Type of Antiretroviral therapy	CD4 T-cell count	HIV viral load (copies/ml)
16	25-May-1993	30-Jun-1989	ddl	690	250
	26-Oct-1993		ddl	594	400
	01-Feb-1994		ddl	575	400
	17-May-1994		ddl	520	400
	17-Oct-1994		ddl	576	400
	17-Mar-1995		ddl	4165	400
	13-Jun-1995		ddl	688	1,000
	12-Dec-1995		ddl	466	400
	12-Dec-1995		ddl	466	400
18	26-May-1993	30-Jun-1990	ddl	104	6,000
	09-Sep-1993		ddl	112	26,000
	13-Jan-1994		ddl	120	370,000
	12-May-1994		ddl	100	320,000
	22-Sep-1994		ddl	90	430,000
	16-Feb-1995		ddl	97	15,000
	22-Jun-1995		ddl	115	12,000
	02-Nov-1995		AZT+ ddc	82	14,000
	02-Nov-1995		AZT+ ddc	82	14,000
19	01-Jun-1993	30-Jun-1991	ddl	77	8,000
	14-Oct-1993		AZT	78	6,800
	25-Jan-1994		AZT	22	200,000
	03-May-1994		AZT	38	110,000
	15-Nov-1994		AZT	42	46,000
	28-Mar-1995		AZT	19	9,400
	27-Jun-1995		AZT	17	47,000
	03-Oct-1995		AZT	82	20,000
	-		-	-	-
20	08-Jun-1993	30-Jun-1988	ddl	252	83,000
	20-Oct-1993		ddl	330	6,900
	04-Jan-1994		ddl	198	14,000
	03-May-1994		ddl	140	120,000
	06-Sep-1994		ddl	63	330,000
	31-Jan-1995		ddl	30	210,000
	09-May-1995		ddl	49	280,000
	03-Oct-1995		ddl	46	190,000
	03-Oct-1995		ddl	46	190,000

**Table 2D: Summary of the Clinical Information of Patients #22 to #39.**

Patient ID number	Date of started therapy	Date of HIV diagnosis	Type of Antiretroviral therapy	CD4 T-cell count	HIV viral load (copies/ml)
22	21-Jun-1993	30-Jun-1989	ddl	170	8,900
	26-Oct-1993		ddl	153	45,000
	27-Feb-1994		ddl	180	77,000
	21-Jun-1994		ddl	128	50,000
	21-Nov-1994		ddl	112	14,000
	07-Mar-1995		ddl	156	6,000
	03-Oct-1995		ddl	149	46,000
	20-Feb-1996		ddl	103	9,000
	23		08-Jun-1993	30-Jun-1989	AZT
26-Oct-1993		AZT	150		16,000
01-Mar-1994		AZT	104		130,000
18-Oct-1994		-	162		26,000
24	15-Jun-1993	30-Jun-1990	ddl	462	1,800
	16-Sep-1993		ddl	480	400
	06-Jan-1994		ddl	450	400
	20-May-1994		ddl	512	400
	27-Oct-1994		ddl	512	400
	20-Mar-1994		ddl	560	400
	20-Jun-1995		ddl	570	400
	17-Oct-1995		ddl	444	1,900
31	22-Jun-1993	30-Jun-1988	ddl	182	80,000
	23-Nov-1993		ddl	80	170,000
	21-Jun-1994		ddl	30	33,000
	29-Nov-1994		ddl	18	180,000
	29-Mar-1995		ddl	7	179,999
			ddl		
39	20-Jul-1993	30-Jun-1989	AZT	304	32,000
	12-Oct-1993		AZT	240	270,000
	04-Jan-1994		AZT	182	310,000
	03-May-1994		AZT	98	1,300,000
	13-Sep-1994		AZT	20	64,000
			-		

**Table 2E: Summary of the Clinical Information of Patient # 57 and #60.**

Patient ID number	Date of started therapy	Date of HIV diagnosis	Type of Antiretroviral therapy	CD4 T-cell count	HIV viral load (copies/ml)
57	29-Mar-1994	30-Jun-1989	AZT	957	620
	18-Oct-1994		AZT	952	500
	21-Feb-1995		AZT	594	400
	04-Jul-1995		AZT	726	400
	03-Oct-1995		AZT	551	1,200
	16-Jan-1996		AZT	748	400
	04-Jun-1996		AZT	722	250
	60		17-Sep-1994	30-Jun-1988	AZT
13-Jan-1995		AZT+ ddl	240		4,800
28-May-1995		AZT+ ddl	234		90,000
28-Oct-1995		AZT+ ddl	187		110,000
10-Jan-1996		AZT+ ddl	146		180,000
05-May-1996		AZT+ 3TC	141		140,000
17-Sep-1996		AZT+ 3TC	148		120,000
		AZT+ 3TC	188		7,028

## **2.2 Nucleic Acid Extraction from PBL and Biopsies:**

The chromosomal DNA and viral DNA was isolated using Trizol Reagent (Invitrogen, Burlington ON) from the different gut tissue biopsies and PBL (5, 21, 34, 140). Previous work in our lab showed that the quality of the RNA isolated varied, and therefore the work in this thesis focused on the use of the chromosomal DNA and viral DNA as template for the quantitative PCR approaches described below. Previous studies in our lab showed a consistent ability to amplify HIV-1 proviral DNA from these samples.

## **2.3 Construction of Positive Controls for Quantification of Total HIV-1 Proviral DNA, 2-LTR and Integrated Proviral DNA Forms:**

The PCR and the quantification real-time PCR protocol were conducted on the following positive control plasmids (pNL4-3, 2-LTR circle, integrated HIV). The plasmid pNL4-3

containing the complete proviral DNA genome of HIV strain NL4-3 in a pUC19 background, has been obtained from the HIV/AIDS reagent program (141) (**Figure 3**). This plasmid was used for the optimization of the PCRs to quantify the total amounts of HIV proviral DNA (total, integrated and 2-LTR forms). For the control of the 2-LTR forms and Alu-integrated proviral HIV-1 DNA, plasmids were synthesized by Eurofin MWG operon ([www.operon.com](http://www.operon.com)) using the LTR sequence of pNL4-3 obtained from gene bank (AF324493.1). Moreover, the sequences used by Zhu et al for the Alu repeat was used in the integrated proviral DNA plasmid control. Sequences and plasmid maps are given in (**Figures 4 and 5**).

#### **2.4 *E.coli* Heat Shock Transformation with (pNL4-3, integrated HIV- DNA and 2-LTR Plasmids):**

To propagate the control HIV template containing plasmids (see section 2.3), plasmids were transformed to *E. Coli* using the following protocol. Frozen competent cells of *E. coli* Top 10 cells were thawed on ice. The plasmid of interest were added to the competent cells and incubated on ice for 15-30 minutes. Afterwards, the mixture was giving a heat shock at 42°C for 30 seconds then placed on ice for at least 5 minutes. 1 ml of LB (Luria Broth) medium (antibiotic-free) was added to the mixture and left to shake at 37°C. After 1 hour, the mixture was centrifuged for 1 minute. The pellet was resuspended with 100µl of LB medium. Then, the mixture was transferred on LB agar containing 100 µg/ml of ampicillin and incubated overnight at 37°C. The colonies were picked and grown overnight in 3 ml of LB with ampicillin. Plasmid was isolated from these cultures using the SIGMA- Gene Elute plasmid mini prep kit (PLN350-1KT). The suggested extra wash step was performed in order to purify the plasmids from any salt and residues that can interfere with the PCR reaction and DNA was eluted in water. The OD 260

nm was measured from which the concentration in copies per  $\mu\text{l}$  of the plasmid DNA was calculated using the known molecular weight of each of the plasmids.

## **2.5 PCR Primers and Probes:**

Primer sequences used in this research were based on those published work (19, 24, 139). The total HIV proviral DNA primers amplify the region of the HIV linear DNA between the left LTR sequence and the 5' end of the gag gene. 2-LTR proviral DNA primers cross the junction generated by ligation of the DNA ends. Furthermore, the integrated proviral primers of the first round are complementary to the HIV LTR and the chromosomal Alu repeats, whereas the second primers amplify the LTR and gag gene of HIV. The locations of the primers and probes for the various PCRs used in this research are illustrated in Figure 6 .We also ordered “mutant” primers to compensate for any of the point mutations that exist between the various published sequences of HIV strains. These “mutant” primers and probes sequences were based on the prototype B-clade HIV strain NL4-3 (**Table 3**).

**Table 3: The Primers and Probes Sequences.**

Type of primers and probes	Primers
Total HIV DNA	(MH531) F: TGTGTGCCCGTCTGTTGTGT (MH532-original) R: GAGTCCTGCGTCGAGAGAGC (MH532-mutated) R: GAGTCCTGCGTCGAGAGATC (LRT-P*) P: FAM-CAGTGGCGCCCGAACAGGGA-TAMRA
2LTR	(MH535-original) F: AACTAGGGAACCCACTGCTTAAG (MH535- mutated) F: AGCTAGGAACCCACTGCTTAAG (MH536-original) R: TCCACAGATCAAGGATATCTTGTC (MH536- mutated) R: CCCCACAGATCAAGGATATCTTGTC (MH603rd,*-Original)P: FAM-AAAGCTTGCCTTGAGTGCTTCAAGTAGTGT-TAMRA (MH603rd,*-mutated) P:FAM-AAAGCTTGCCTTGAGTGCTTCAAAGTAGTGT-TAMRA
Integrated DNA	(L-M667) F:ATGCCACGTAAGCGAAACTGGCTAACTAGGGAACCCACTG
First Round PCR	Alu1: TCCCAGCTACTGGGGAGGCTGAGG Alu2: GCCTCCCAAAGTGCTGGGATTACAG LamdaT: ATGCCACGTAAGCGAAACT
Second Round PCR	(AA55M) R: GCTAGAGATTTCCCACTGACTAA (LRT-P*) P: FAM-CAGTGGCGCCCGAACAGGGA-TAMRA

The yellow highlight= The base pair is different than the original.

(T)= The base pair is missing compared to original.

The green highlight= The base pair is an extra than the original.

All the original primers and probes sequences were previously published (19, 24, 139)

## 2.6 Conventional Polymerase Chain Reaction (PCR):

First we used a conventional PCR approach to test and optimize the PCR conditions for all primers using the control plasmids as templates. We used a standard PCR protocol with a mixed reaction of 25  $\mu\text{l}$  containing 2.5  $\mu\text{l}$  10X PCR buffer, 2.5  $\mu\text{l}$  (10mM) dNTP's, 1.25  $\mu\text{l}$  (50mM)  $\text{MgCl}_2$ , 1  $\mu\text{l}$  of each (10mM) primer, 0.3  $\mu\text{l}$  Taq polymerase, 9.2  $\mu\text{l}$   $\text{H}_2\text{O}$  and 1  $\mu\text{l}$  of DNA target under the following conditions: 95°C for 10 min, followed by 40 cycles of 95°C for 30s, 60°C for 1 min, and 70°C for 1 min, then 72°C for 5 min and 4°C for hold (**Table 4**). A similar reaction mixture was used to test the total HIV primers and the integrated HIV DNA and the 2-LTR controls. All PCRs were performed using the Bio-Rad T100 thermal cycler.

For the integrated HIV-1 DNA, the first round conditions were as follows: 95°C for 8 min, 12 cycles of amplification at 95°C for 10 s, 60°C for 10 s, and 72°C for 170 s, then 72°C for 5 min and 4°C to hold based on published protocol (186). One-tenth of the 1<sup>st</sup> round PCR product was transferred to a new tube for the 2<sup>nd</sup> round PCR conditions that were the same as the conditions described above (**Table 5**).

**Table 4: Standard PCR Cycling and Reaction Conditions:**

Standard PCR set up (total HIV, 2-LTR )	Standard PCR Cycling Conditions
2.5 µl 10X PCR buffer	95°C for 10 min
2.5 µl dNTP's	95°C for 30
1.25 µl MgCl <sub>2</sub>	60°C for 1 min } 40 cycles
1 µl of each primer	70°C for 1 min
0.3 µl Taq polymerase	72°C for 5 min
9.2 µl H <sub>2</sub> O	4°C for hold
2 µl of DNA target	

**Table 5: Standard Cycling and Reaction Conditions for Integrated Proviral DNA PCR:**

Standard PCR set up	Standard PCR cycling conditions (First Round)
2.5 µl 10X PCR buffer	<b>(First round):</b>
2.5 µl dNTP's	95°C for 8 min
1.25 µl MgCl <sub>2</sub>	95°C for 10 s } 12 cycles
1 µl of each primer	60°C for 10 s }
0.3 µl Taq polymerase	72°C for 170 s
9.2 µl H <sub>2</sub> O	72°C for 5 min
2 µl of DNA target	4° to hold
	<b>(Second round):</b>
	95°C for 10 min
	95°C for 30 s } 40 cycles
	60°C for 1 min }
	70°C for 1 min
	72°C for 5 min
	4°C for hold



## 2.7 Real-Time PCR:

Real-time PCRs were performed in a 25  $\mu$ l solution containing 2.5  $\mu$ l of DNA target, 12.5  $\mu$ l of SsoAdvanced™ Universal Probes Supermix (Bio-Rad #172-5281), 1  $\mu$ l of each primer and 0.5  $\mu$ l of probe under the following conditions: 95°C for 10 min, followed by 40 cycles of 95°C for 15 s and 60°C for 1 min CFX multiplex PCR machine (**Table 6**). For the integrated HIV-1 DNA, the first round of PCR was conducted with the following conditions: 95°C for 8 min, and then 12 cycles of amplification at 95°C for 10 s, 60°C for 10 s, and 72°C for 170 s (**Table 7**). One-tenth of product from the first round PCR was transferred to a new tube for the q –real-time PCR quantification analysis (**Table 8**). For the total and 2-LTR HIV-1 proviral DNA only one round of real- time PCR was performed. A standard curve was created for each run using 1:10 in serial dilutions in triplicate of our plasmid standards.

**Table 6: Total HIV-1 and 2-LTR proviral DNA Quantification PCR Conditions:**

PCR reaction setup	PCR cycle conditions
2.5 $\mu$ l DNA target	95°C for 10 min
12.5 $\mu$ l Master Mix	Followed by 40 cycles of:
1 $\mu$ l of each primer	95°C for 15 s
0.5 $\mu$ l of probe	60°C for 1 min

**Table 7: Integrated HIV-1 proviral DNA quantification (first round) PCR conditions:**

PCR reaction setup	PCR cycle conditions
2.5 µl 10X PCR buffer	95°C for 8 min
2.5 µl dNTP's	Followed by 12 cycles of:
1.25 µl MgCl <sub>2</sub>	95°C for 10 s
1 µl of each primer	60°C for 10 s
0.3 µl Taq polymerase	72 °C for 170 s
9.2 µl H <sub>2</sub> O	
2 µl of DNA target	

**Table 8: Integrated HIV-1 DNA quantification (second round) PCR conditions:**

PCR reaction setup	PCR cycle conditions
2.5 µl DNA target	95°C for 10 min
12.5 µl Master Mix	Followed by 40 cycles of:
1 µl of each primer	95°C for 15 s
0.5 µl of probe	60°C for 1 min

**2.8 Optimized Polymerase Chain Reaction (PCR) primers and Probes:**

In addition to the previously published probes described in the previous chapter, we also had “mutant” primers and probes sequences based on the prototype B-clade HIV strain NL4-3 as our plasmid controls sequences were obtained from this strain. In order to investigate the optimal conditions and the effect of the mutations in the primers and probes on the detection of the total

HIV-1 proviral DNA forms, we tested both the published primers and probes and compared them to mutant ones.

### **2.8.1 Optimized Conventional-PCR:**

After using the standard PCR protocol we made modifications including changes in temperature, reagent concentration and DNA dilution. We optimized our 25  $\mu$ l PCR reaction mix to contain 2.5  $\mu$ l 10X PCR buffer, 0.5  $\mu$ l (10 mM) dNTP's, 1.  $\mu$ l (50mM )MgCl<sub>2</sub>, 1  $\mu$ l of each (10 mM ) primer, 0.15  $\mu$ l Taq polymerase, 17.85  $\mu$ l H<sub>2</sub>O and 1  $\mu$ l of DNA target under the following conditions: 95°C for 10 min, followed by 40 cycles of 95°C for 30s, 60°C for 1 min, and 70°C for 1 min, then 72°C for 5 min and 4°C for hold (**Table 9**). This optimized protocol was used in testing the primers of the total HIV, 2-LTR, integrated DNA (second round) using the previously constructed plasmids controls. Again the Bio-Rad T100 thermal cycler was used in the optimization process.

For the integrated HIV-1 DNA, the first round conditions were as follows 95°C for 8 min, followed by 12 cycles of 95°C for 10s, 60°C for 10s, and 72°C for 170s, then 72°C for 5 min and 4°C for hold (**Table 9**) (186). The second round PCR set up and conditions were the same as the previously described protocol (**Table 9**).

For the 2-LTR we also used another optimized protocol which was as follows 94°C for 5 min, followed by 35 cycles of 94°C for 1 min, 57°C for 30s, and 70°C for 30s, then 72°C for 5 min and 4°C for hold (**Table 9**).

**Table 9: Optimized PCR Cycling and Reaction Conditions.**

PCR set up	PCR cycling conditions
2.5 µl PCR buffer 0.5 µl dNTP's 1 µl MgCl <sub>2</sub> 1 µl of each primer 0.15 µl Taq polymerase 17.85 µl H <sub>2</sub> O 1 µl DNA target	<p><b>Total HIV(pNL4-3) and the 2- LTR control but the annealing is 57:</b></p> 95°C for 10 min 95°C for 30 s } 40 cycles 60°C for 1 min } 70°C for 1 min 72°C for 5 min 4°C for hold
2.5 µl PCR buffer 0.5 µl dNTP's 1 µl MgCl <sub>2</sub> 1 µl of each primer 0.15 µl Taq polymerase 17.85 µl H <sub>2</sub> O 1 µl DNA target  (The second round contains DNA from the first round product).	<p><b>The integrated DNA control ( first round):</b></p> 95°C for 8 min 95°C for 10 s } 12 cycles 60°C for 10 s } 72°C for 170 s 72°C for 5 min 4° to hold  <p><b>(Second round):</b></p> 95°C for 10 min 95°C for 30 s } 40 cycles 60°C for 1 min } 70°C for 1 min 72°C for 5 min 4°C for hold

### 2.8.2 Optimized Quantitative Real-Time Polymerase Chain Reaction:

The CFX96 4 system machines (BioRad) were used for real-time PCRs. First, we assessed our primers using Syber green as real-time PCR detection master mixes, with and without chromosomal DNA added to our plasmid standard. Then, we tested the primers using SsoAdvanced™ Universal Probes Supermix (Bio-Rad #172-5281) with and without chromosomal DNA added to our plasmid standard. The assays were performed in 25 µl volume containing 5 µl of DNA target, 12.5 µl of Supermix 1 µM of primers and 0.2 µM of probe under the following conditions: 95°C for 30 s, followed by 40 cycles of 95°C for 10 s and 60°C for 30s (**Table 10**).

For the integrated HIV-1 DNA, the first round was conducted using conventional PCR as previously described under the following conditions: 95°C for 8 min, and then 12 cycles of amplification at 95°C for 10 s, 60°C for 10 s, and 72°C for 170 s (**Table 11-12**).

A standard curve was created for each run using 1:10 serial dilutions of our plasmids. In addition, the chromosomal DNA from Jurkat cell line was extracted using Trizol described above. The Jurkat cell line is a human T lymphoblastoid cell line obtained from a male patient with acute T cell leukemia (142). The added concentration of chromosomal DNA was 50 ng/µl into the real-time PCR reactions at the same volume of the plasmid. The mixture of chromosomal DNA and plasmid controls containing HIV-1 sequence in our real-time PCR reactions created an environment for the primers containing competitive host DNA that could prevent binding to the targeted DNA, which mimics the patients' samples environment. The limit of detection of each run was calculated with and without the chromosomal DNA (Jurkat) to test the real-time PCR sensitivity under both conditions.

Furthermore, we tested different dilutions of patients' samples ranging from (2-200 ng) to approach the optimal DNA concentration in our PCR reactions (**Figure 19**).

**Table 10: Total HIV and 2-LTR Proviral DNA Optimized Quantification PCR Conditions.**

PCR reaction setup	PCR cycle conditions
5 µl DNA target	95°C for 30 s
12.5µl Master Mix	Followed by 40 cycles of:
1 µM of primers	95°C for 10s
0.2 µM of probe	60°C for 30 s

**Table 11: The Integrated HIV-1 Proviral DNA Optimized Quantification (First Round) PCR Conditions.**

PCR reaction set up	PCR conditions
5 µl DNA target	95°C for 8 min
12.5µl Master mix	Followed by 12 cycles of:
1 µl of each primer	95°C for 10 s
0.5 µl of probe	60°C for 10 s
	72 °C for 170 s

**Table 12: The Integrated HIV-1 Proviral DNA Optimized Quantification (Second Round) PCR Conditions.**

PCR reaction setup	PCR cycle conditions
5 µl DNA target	95°C for 30 s
12.5 µl Master mix	Followed by 40 cycles of:
1 µl of each primer	95°C for 10 s
0.5 µl of probe	60°C for 30 s

## 2.9 Approaches to Overcome Quantitative Real- Time PCR Inhibition:

To avoid possible inhibitory effects in our samples during PCR, such as, bile salt, complex polysaccharides, collagen, heme, urea, hemoglobin, lactoferrin, and immunoglobulin G (IgG). (143-153), we treated our patients gut tissues samples the same way as stools. It was suggested by previous studies that stool samples can be treated with bovine albumin serum (BSA) to neutralize the inhibition factors (100-151). For this reason in our approach to overcome inhibition in our samples we added 1.25  $\mu$ l (10 mM) BSA (100-151) (**Table 13**).

**Table 13: Quantification Real- Time PCR with BSA Conditions:**

PCR set up reaction	PCR cycle conditions
5 $\mu$ l DNA target	95°C for 30 s
12.5 $\mu$ l Master mix	Followed by 40 cycles of:
1 $\mu$ l of each primer	95°C for 10 s
0.5 $\mu$ l of probe	60°C for 30 s
1.25 $\mu$ l BSA	

## Chapter Three: Results

### 3.1 Conventional PCR Optimization:

We started our optimization steps using the constructed plasmids as our control templates. The annealing temperatures used to optimize the conventional PCR ranged from (50 -60°C) and the optimal temperature was 60°C for both the total HIV and integrated proviral DNA PCR protocol. The optimal annealing temperature was 57°C for 2-LTR proviral DNA PCR protocol. The expected band size for the total HIV proviral DNA is 150 bp, 2-LTR proviral 200 bp and the integrated proviral DNA band size is 180bp (**Figure 7, 8 and 9**). Furthermore, the limit of detection of each run was calculated based on our dilution series. The total HIV proviral DNA limit of detection was 500 viral copy/ng. Similarly, the limited of detection of 2-LTR proviral DNA was 500 viral copy/ng. The limit of detection for the integrated proviral DNA was 600 viral copy/ng (**Figure 7, 8 and 9**). Moreover, we tested different volumes of 25 or 50 mM MgCl<sub>2</sub> and we found that the optimal volume is 1 µl of 50 mM in the 25µl PCR reaction, resulting in a final concentration of 1 mM of MgCl<sub>2</sub>.

### 3.2 Quantitative Real- Time PCR Optimization:

After obtaining the optimal conditions for the conventional PCR, we tested our positive controls in real- time PCRs to establish standard curves for each run. Representative quantitative real- time PCR standard curves of each run using Syber green are shown in **Figure10, 12 and 13**. The annealing temperature used was the same as the previously published protocol (i.e. 60 °C). However, we used 57 °C for 2-LTR proviral DNA to keep it consistent with our optimization process that showed it was the optimal annealing temperature for the conventional PCR. We also calculated the limit of detection per ng of host DNA and it was as follows: total



HIV proviral = 5 viral copy number/ng, 2-LTR= 5 viral copy number/ng and the integrated proviral DNA= 6 viral copy number/ng (**Figure 13-14 and 15**). Compared to the conventional PCR, quantitative real- time PCR is more sensitive and able to detect HIV-1 proviral DNA forms to <10 viral copy number/ng. **Figure 16, and 18** shows quantitative real- time PCR standard curves of each run after adding chromosomal DNA. We did not see any difference in the limit of detection after adding chromosomal DNA from Jurkat cells with the purified plasmid. We expected that it would be possible that the sensitivity of the quantitative real- time PCR could be lower due to chromosomal DNA competing with the primers for the targeted DNA, but this was not the case.

**Figure 19** illustrates the different dilutions of our tissue sample ranging from 2-200 ng of DNA were tested and we saw no difference in detecting HIV-1 proviral DNA forms. To mitigate lower detection due to the age of the samples or the input of DNA we decided to use our samples with their initial input concentrations (100-400 ng), to increase the change of detecting HIV proviral DNA.

### **3.3 Bovine Albumin Serum to Neutralize the Inhibitory Factors in Patients Samples:**

We selected samples that had different concentrations ranged between 100 to 400 ng from various tissues (PBMC-esophagus-colon). To eliminate possible inhibitory factors in our samples we used different concentration of BSA. **Figure 20** illustrates the effect of BSA on the detection of total HIV via real- time PCR in patient # 57. In patient # 57 gut tissues (i.e. esophagus-stomach-duodenum and colon), the BSA treatment revealed more copies of the total HIV-1 proviral DNA. However, the viral copy numbers were still considered low. The same as patient # 57, in patient # 16 the BSA treatment revealed the total HIV-1 proviral DNA in the patients'

samples that were negative before adding BSA, but still at a very low level. We also tested the effect of BSA in 2-LTR proviral DNA real-time PCR for patient # 3 (**Figure 21**), as 2-LTR proviral DNA was detectable and quantifiable without BSA in this patient's samples. After adding BSA, the 2-LTR was only detectable but not quantifiable suggesting no noticeable increase in the detection limit, but rather a negative effect. Other patients (# 5, 24 and 57) were also tested and there was no difference in viral copy numbers with or without BSA. Similarly, patients # 57 and 20 showed no difference in viral copy numbers for the integrated proviral DNA. For the colon visit 5 of patient # 19 the viral DNA was low before using BSA and there was no difference in detecting the integrated proviral DNA after adding BSA, and the level detected remained not quantifiable (**Figure 21**). From these observations we concluded that adding BSA did not alter any of the results obtained previously, and suggested that the difficulty in detecting the different HIV-1 DNA forms was probably not due to PCR inhibitors that could be neutralized by BSA within the sample.

### **3.4 HIV-1 Proviral Quantification in PMBC's:**

18 HIV-1 infected patients were tested for the HIV-1 proviral DNA (total, 2-LTR and integrated) in PBMC samples. We used the same real-time PCR assay described previously. 8/18 patients were positive for total HIV-1 proviral DNA (**Figure 22**). The HIV-1 proviral DNA was detected in samples collected at different time-points from patients while they were on ART (AZT or ddI). For instance, patient # 20 was receiving AZT and we detected total HIV-1 proviral DNA in visit 2 and 3. Patient #19 was also receiving AZT during visit 5, and patient # 39 we were able to detect total HIV-1 proviral DNA in visit 3. On the other hand, patient #18 was treated with ddI during this study and we detected total HIV-1 proviral DNA in visit 1, visit 3 and visit 4. Furthermore, patient #22 was only detectable for total HIV-1 proviral DNA in visit 1.

Patient # 7 was detectable in visit 3 and receiving ddI. Patient #23 visit 7 was detectable for total HIV-1 proviral DNA as well as patient # 24 visit. **Figure 23** shows the total HIV-1 proviral DNA quantification in the PMBC's.

Moreover, 2-LTR proviral DNA was found in PBMC's of 5/18 patients. This was similar to our results of testing for total proviral DNA, in which various samples collected at various time-points were detectable for 2-LTR while receiving ART. In the ddI treatment group, for instance patient # 14. 2-LTR proviral DNA was detected in visit 7 whereas patient# 18 visit 6, 7 and 9 were positive. Patient # 22 visit 7 and patient 23 visit 4 were positive. As for AZT group, which include patient # 20 the 2-LTR DNA forms were found in visit 8 and patient # 39 visit 3 and 7 see (**Figure 24**).

Furthermore, 2/18 patients were positive for integrated HIV-1 proviral DNA in their PBMC's. Patient #22, receiving ddI was positive for the integrated HIV-1 proviral DNA in visit 1 and visit 2. Patient #39 receiving AZT was positive in visit 3 (**Figure 25**). These analyses revealed highly variable levels of HIV DNA amongst the different patients and no specific pattern in HIV DNA levels amongst different treatment groups could be identified. However, these results showed our assays could detect the different HIV DNA forms in patient samples, and could be used for the analysis of on chromosomal DNA isolated from gut tissue of HIV-1 infected patients.

### **3.5 The Presence of Various Types of HIV-1 DNA in Gut Tissues of HIV Infected Patients:**

To study the virus dynamic in the gut different tissues, samples were obtained from patients either receiving zidovudine (AZT) or dideoxyinosine (ddI) and we focused on analyzing the levels of HIV-1 proviral DNA (total HIV, 2-LTR and integrated DNA) from different gut tissues (esophagus, stomach, duodenum and colon). For the 18 patients tested, biopsies were collected

from ~6 months intervals. PBMC's were also tested from these patients. All patients were part of previous cohort study and the clinical information is summarized in (Table 2A, 2B, 2C, 2D, 2E).

The gut tissues (esophagus, stomach, duodenum and colon) were tested for the presence of HIV-1 DNA using the PCR procedures for total, 2-LTR, and integrated HIV-1 proviral DNA. It was found that each tissue varied highly in the distribution of the presence of HIV-1 DNA among HIV infected patients (Figure 26). For instance, HIV-1 DNA was most easily detected in the colon, while the frequency of detecting total HIV-1 DNA was the lowest in the stomach of most patients. Interestingly, 2-LTR forms and integrated DNA were mostly detectable in the stomach.

### **3.6 Quantitation of Total HIV-1 Proviral DNA Levels in Different Gut Tissues:**

Total HIV-1 proviral DNA amounts were assessed using our quantitative-real-time PCR procedure. The total HIV-1 DNA detected in our results reflects the integrated and unintegrated proviral DNA, which represent the overall level of infection of the tissue. Levels of the total HIV-1 DNA fluctuated from visit to visit in most of our patients. In general, most the total HIV levels detected in most patients were low between 1-98 viral copies/ng. For 4/18 patients the difference between their levels for each visit was observed (Figure 27). Of interest was patient #23 who was receiving AZT during the study period and we observed very low proviral DNA copy numbers ranging from 16 to 32 viral copy number/ng. At visit 1 and 3 total HIV-1 proviral DNA was detected in the colon, but during later visits we were unable to detect any total HIV-1 proviral DNA. Similar fluctuations were observed in the other gut tissues of patient # 23, with very low proviral DNA copy numbers. Figure 29 illustrates the fluctuating levels of total HIV-1 proviral DNA in patients #23 and #14. Patient #14 was receiving ddI during this study and we

detected total HIV-1 proviral DNA in most of the gut tissues except the duodenum from various visits the levels were as low as 1 viral copy number/ng. Of interest was patient #20 who was on zidovudine treatment during the first 4 visits, and then switched to ddI from the 5<sup>th</sup> to the 7<sup>th</sup> visit. At visit 5 after switching to ddI we did not detect any total HIV-1 DNA in any of the gut tissues. However, we did detect proviral DNA in visit 7. These differences could be the result of the switch in antiretroviral therapy. Furthermore, the rest of the tissues tested in the patients (#19-31-39-18-24-22-5) showed detectable total HIV-1 DNA ranging between 1-23 viral copy number/ng. The viral copy numbers were very low and we did not see any difference in viral load between the antiviral treatment received (AZT or ddI).

In general, regardless of the approach used total HIV-1 DNA was more readily detectable for all patients at visit 3. It was found that 11/18 patients were positive for total HIV-1 DNA at visit 3, in the colon, 7/12 patients of the duodenum, 8/12 of the esophagus, and 5/12 patients were also positive at visit 3 in the stomach (**Figure 28**). This could be an effect of differential effects of mono antiretroviral therapy on the different gut compartments. **Table 14, 15 and 16** shows detectable and quantifiable total HIV proviral DNA in all patients gut tissues and visits.

### **3.7 Quantification of 2-LTR Proviral DNA Levels in the Different Gut Tissues:**

For quantifications of 2-LTR proviral HIV-1 DNA levels, we first identified 2-LTR positive samples, by conducting a regular nested PCR for 2-LTR HIV DNA. The positive samples (5/18 positive patients) were subsequently used to quantify the 2-LTR proviral HIV-1 DNA levels using our quantitative real- time PCR approach.

The 2-LTR proviral DNA was detected at various visits from all the different gut tissues and levels ranged from 1 to  $9 \times 10^{11}$  viral copy number/ng. **Figure 30** shows how 2-LTR proviral DNA levels fluctuated in patients # 57 and # 24. In patient #57 (receiving AZT) the 2-LTR proviral DNA was found in most of the gut tissues except for the esophagus, and levels fluctuated between visits. The same fluctuation in 2-LTR HIV DNA levels were found in the stomach and colon of patient # 24 who was receiving ddI. The 2-LTR levels detected from both patients were high. In contrast, 2-LTR proviral DNA levels were low in the stomach of patient # 5 who was also receiving ddI during the period of this study. For patient # 18, the stomach was the only tissue with detectable 2-LTR forms but the levels were not quantifiable. The same pattern of detectable but not quantifiable levels of 2-LTR proviral DNA were found in patients # 23 and #39, both of which were on AZT. **Table 17 and 18** illustrates the detectable and quantifiable 2-LTR in all the patients visit from the gut tissues.

These results in this select set of patients, would suggest that both drugs (AZT and ddI) did affect the levels of detection for 2-LTR proviral DNA in a similar way in the different gut tissues. Interestingly, high levels of 2-LTR proviral DNA were found, but we argue against high levels of replication in the gut tissues of most of our patients examined in this study.

### **3.8 Quantification of Integrated Proviral HIV-1 DNA Levels in the Gut Tissues:**

Integrated proviral DNA was detected in 8/18 patients. Again a regular PCR approach was used to select the positive patients, before quantification by real- time PCR similar to the approach as the 2-LTR assay. Depending on the patient tissue sample the levels of the integrated DNA ranged between 15 to  $\sim 2266$  viral copy number/ng. However, no pattern was found identifying tissues that had consistently higher integrated DNA levels than others in the patients

studied. For instance, in patient # 5 receiving ddI, the integrated proviral DNA copy numbers were low copy numbers in the stomach at visit 7 (29 viral copy number/ng) whereas the colon visit 3 showed higher DNA copy numbers (2266 viral copy number/ng), that subsequently dropped to below the detection limit in the next visit. **Figure 31** shows the integrated proviral DNA levels in patients 5 and 14. In patient #14 the integrated proviral DNA was detected in the esophagus at visit 5 and 7. **Table 19 and 20** shows the patients' tissue samples from various visits with detectable and/or quantifiable integrated proviral DNA. For patients # 16, 18, 22 and 24 who were receiving ddI during their visits, the integrated proviral DNA levels fluctuated. Interestingly, in patients # 19 and 20 (receiving AZT at the time of their positive visits) only integrated proviral DNA was detectable (**Table 20**).

Similar to the analysis of the other proviral DNA types, integrated proviral DNA levels varied among the different gut tissues, visits, and patients. We did not see any difference in detecting the integrated proviral DNA from both AZT and ddI patients. Although, the majority of the quantifiable levels were collected from patients on ddI.

## Chapter Four: Discussion and Conclusions

Our study's aim was to gain an insight into the dynamics of HIV replication in patients receiving ART. Currently, HAART is the standard treatment in the developed world, and untreated patients are very rare at the SAC clinic in Calgary. As ART (i.e. monotherapy) is suboptimal as an anti-HIV treatment, patients on ART are interesting as they would closely represent the patients that are untreated or suboptimal treated for HIV. In the gut tissues HIV-1 DNA can persist as integrated and unintegrated. The total HIV-1 proviral DNA represents the viral dissemination in the gut tissues, 2-LTR forms are considered biomarkers for viral replication and the integrated proviral DNA represents the viral latent infection (24). In this research, we established real-time PCR assays to quantify the various forms of HIV-1 proviral DNA (total, 2-LTR and integrated) in different gastrointestinal tract tissues (esophagus, stomach, duodenum and colon). We monitored the changes in the proviral DNA levels between visits, and included the PBMCs of the infected patients in order to compare the viral dynamics in the blood compartment and the gut tissues.

We found that 2-LTR proviral DNA was most frequently detected in the esophagus and stomach and the levels varied between patients and at different time points. Of interest, the 2-LTR levels were found to be high ( $4 \times 10^6$ -  $9 \times 10^{11}$  viral copy number/mg) in two of our patients (#57 and #14 in their colon and stomach. However, since the levels of the 2-LTR proviral DNA detected was not consistently high at different time points, we considered this data was not a conclusive indicator for viral replication in our patients. It is possible that the age of our samples is one of the technical difficulties that challenged the detection and quantification of the 2-LTR proviral DNA. Alternatively, during DNA extraction the majority of the circular form of 2-LTR



proviral DNA might have been lost due to its low molecular weight making it difficult to detect and quantify

Similar to the 2-LTR forms, the integrated proviral DNA levels were highly variable but were frequently found in most of the gut tissues, except for the esophagus. A possible explanation for the low levels detected is the unique form of the integrated proviral DNA, as it is part of the host chromosomal DNA. This might make it difficult to detect integrated proviral DNA due to the competition of the chromosomal DNA for the primers, or it may be harder to fully denature in the denaturation step of the PCR and thus making it inaccessible for the primers. Another possibility is that the gut tissue samples were taken from random sites in the different tissues, and each biopsy might contain different amount of lymphoid tissue. This combined with lower CD4<sup>+</sup> T-cells due to the immune depletion could explain the big difference in levels of 2-LTR and integrated proviral DNA detected between the various samples (33, 116, 82). Other HIV-1 cell reservoirs might also play a role, as the gut tissues might have highly variable amounts of HIV-1 infected cells other than CD4<sup>+</sup> T-cells, such as, lymphoid tissue, dendritic cells, macrophages, B-cells and mast cells.

Analysis of the PBMC showed a very limited detection of HIV. Only 5 patients were positive for the different proviral DNA forms and the levels varied, but in general they were low. Despite receiving ART (either AZT or ddI) the frequency of detecting or quantifying HIV-1 proviral DNA forms should not have been affected as even under HAART proviral DNA can be detected in PBMC (24). As our PCR methods were very sensitive we do not suspect issues with the PCR method itself, but other factors beyond technical issues may have affected the detection and quantification of the HIV-1 proviral DNA forms.

A study by Henrich et al (2013), looked at the different distribution of memory T-cells subsets in the blood and gut tissues (ileum and rectum) (154). They found that the central memory T-cell ( $T_{cm}$ ) were the most prevalent subset in the peripheral blood, making them the most dominant contributor as HIV-1 DNA reservoir in patients with higher CD4+ T-cell counts. Similarly, our patients had relatively high CD4+ T-cell counts, thus we assume that our findings of HIV-1 proviral DNA levels from our PBMC samples might have been derived from central memory T-cells. Due to the longevity and the low level of the central memory T-cells we were only able to detect HIV-1 proviral DNA in these cells, resulting in the lower levels of proviral DNA in our study (154). The Henrich study also found that the effector memory T-cells ( $T_{EM}$ ) were most frequently found in gut tissues and they considered them the most likely contributor as HIV-1 DNA reservoir in the ileum and rectum. In our analyses we did not include the ileum or rectum directly and we did not distinguish between T-cell subsets. However, this study gave an alternative explanation to our findings. Presumably, the HIV-1 proviral DNA levels from the gut tissues might have originated from the effector memory T-cells (155). Other studies have shown that the half- life of effector T-cells is shorter than central memory T-cells. CD4+ and CD8+ ( $T_{EM}$ ) cells were persistently found for years after antigen exposure due to either ( $T_{EM}$ ) cells maturation from ( $T_{CM}$ ) cells or homeostatic proliferation (135, 139, 140). These finding can explain our ability to detect HIV-1 proviral DNA from PBMC's and the gut tissues albeit at low levels.

The colon is considered to be an important site for HIV replication even under treatment. This can be explained by for example the fact that AZT has a short life and low diffusion in the colon. AZT also has the same kinetics in lymph nodes as in the colon, which explains our findings of the more frequent detection of HIV-1 proviral DNA forms in other tissues beside the

colon. Additionally, the tissues that were high in HIV-1 proviral DNA levels might have been enriched with cells from the lymph nodes (33-158). This explains why in patient # 23 receiving AZT, the HIV DNA was found in the esophagus, duodenum and colon.

In a previous study, ddI was found to also be rapidly metabolized (51). This would explain why both AZT and ddI had the same effect on the detection of the proviral DNA forms in our study. Similarly in patients that switched from ddI to AZT, we were also able to detect the integrated proviral DNA. Our results clearly show that detection of the proviral DNA forms does not seem to be affected by AZT and ddI, which would be consistent with the earlier mentioned pharmacokinetics of the drugs. However due to the small sample size further investigation with additional patient samples will be needed.

The low levels of total HIV-1 proviral DNA in gut tissues is consistent with previous studies where showing that total HIV decreases within 48 weeks under HAART. Our patients were under suboptimal ART, and even the latent infection might have persisted beyond the 48 weeks and we were able to detect the integrated and total proviral DNA in higher copy numbers. In a study by Josefsson and colleagues, it was found that HIV-1 DNA frequencies were low in naïve T-cells of the blood and GALT (159). In this study it was found that in inactivated CD4 T-cell the levels of HIV DNA was higher than integrated DNA in activated cells as they rapidly die as a result of viral cytopathic effects or host effector mechanisms. Again in our study we cannot distinguish the T -cells type in our samples, but our findings of low DNA levels might be due to the detection of proviral DNA present in naïve T-cells (142-159)

The rapid decrease in HIV-1 RNA and DNA in the blood and gut was observed in an SIV/HAART study (33). As our patients were on ART higher levels of proviral DNA was

expected in the blood. However, even with ongoing viral replication only 1% of the CD4+ cells in blood in untreated patients get infected with HIV-1 (160). These findings also explain our low levels of HIV DNA from the blood derived DNA in our patients.

Another study found that HIV-1 infection of blood and GALT were higher in patients who initiated therapy during chronic infection compared to acute/early infection (116, 161, 162). This study would support our findings of integrated proviral DNA in our patients' tissues as they were on ART for two or three years after being diagnosed with HIV-1, can therefore be considered chronically infected.

The levels of the HIV-1 proviral DNA forms in our gut tissues and PBMC samples was the opposite to our expectations. Earlier studies of SIV/ HIV showed that in untreated animals, total HIV-1 and 2-LTR proviral DNA were detected in all tissues studied (PBMC, spleen, lymph node and gut). After 28 days of HAART these levels were reduced significantly compared to 14 days of treatment. However, HAART had no effect on 2-LTR proviral DNA levels in lymphoid tissues and spleen, and high could be detected (73). 2-LTR proviral DNA forms are considered stable and persistent in non-dividing cells and they can be easily detected in our samples due to their high CD4+ T-cells counts (18, 43, 163). Other studies showed that 2-LTR forms are lost because of cells division, and for this reason they are not easily detectable in the total CD4+ T-cells which would be consistent with some of our data (12, 164).

Total HIV-1 proviral DNA decreases in the PBMC's after HAART, but no significant change was found in the levels of the integrated proviral DNA (166). The highest integrated proviral DNA from this study was 1260 copies/  $10^6$  PBMC's, hence the expectation of high levels in our samples. As mentioned previously in chapter 1, Dr. Zhu and et al (24) study on PMBC's after 12

weeks of HAART, showed detectable HIV-1 proviral DNA forms in high levels. All these studies combined and a previous study by our lab, which showed increased viral diversity and increased AZT resistance in the gut tissues (especially the colon) would suggest that high levels of HIV-1 proviral DNA forms and high levels of replication and integration in the gut tissues. The lower levels of proviral DNA observed in our studies let us to explore technical issues as a possible explanation to these lower levels.

The first step in our study was to optimize PCR conditions to ensure that the primers that were used in previous studies are able to amplify the targeted HIV-1 proviral DNA. After that, we tested the primers in the real-time PCR and we optimized the conditions to get reproducible standard curves. We tested the primers using already published probes to quantify the HIV-1 proviral DNA forms. We also tested our real-time PCR by adding the chromosomal DNA with the positive controls, as it is possible for the primers and probes to react differently in a “clean” sample containing only targeted DNA. However, when the primers and probes were “challenged” with chromosomal DNA to mimic the samples environment, they were still able to detect the targeted DNA forms and we did not see any differences in the detection limit of Syber green or probes. After we established the real-time assays we tested different dilutions of our patient samples. For example, the 2 ng dilution of the patients’ samples was frequently found positive for the different HIV-1 proviral DNA forms, however, half of that positive results were not quantifiable. We saw the same pattern in the other dilutions, and sometimes the higher the dilution the more frequent the positive results detected. For this reason the initial concentration of each sample varied (i.e. 40-200 ng) was used to quantify the HIV-1 proviral DNA. Based on these analysis we do not believe that there is an inherent technical problem with our real-time PCR approaches.

Furthermore, we tried to neutralize inhibitory factors in our assays that might interfere with the detection and quantification of the different HIV-1 proviral DNA forms. We added Bovine albumin serum (BSA) to our samples used in the quantitative real-time PCR assay (151-153). Our samples of the gut tissues might contain the same type of inhibitors present in stool samples (i.e. bile salts- complex polysaccharide, lipids and urate). These inhibitors should be neutralized by BSA (153). We also included PBMCs samples in these analyses as they might contain heme, hemaglobin and adding BSA has been found to neutralize these PCR inhibitors (146, 147). However, the results showed no dramatic changes in the HIV-1 proviral DNA forms detection levels before or after adding BSA. The overall levels were found to be low in the same order of magnitude in both assays with or without BSA. From this we concluded that the low levels we detected were not the results of inhibitory factors in our patients' samples. The DNA was isolated from samples that had been stored at -80 °C for a long time which could have led to the technical difficulties in detecting the HIV-1 proviral DNA levels. Another possible technical difficulty was the samples preparation itself, as the 2-LTR proviral DNA could have been lost during the DNA extraction process, which should be more efficient with chromosomal DNA and not episomal 2-LTR DNA forms. We concluded that the age of the samples and DNA extraction process may be possible reasons behind the limited and low detection of total HIV-proviral DNA and warrant further investigation before any definitive conclusions can be drawn from our study

In this study we were able to detect the total proviral DNA in most of the patients, and most of the gut different tissues. The total HIV-1 proviral DNA detected might have been in the linear, full length unintegrated form, which could be the most prevalent in active or resting CD4 T-cells as it was most frequently detected when compared to the other DNA forms (2-LTR and integrated). Although, the total proviral DNA was easily detectable, the levels were still low in

all of the different gut tissues and patients visits. Interestingly, visit 3 was frequently positive for total HIV-1 proviral DNA in most of the gut tissues, which might suggest that the samples were prepared in better conditions which helped the detection and quantification of total HIV-1 proviral DNA. Regardless of potential technical issues, the colon was the most commonly proviral DNA positive, which might be due to the low infusion of the drugs in the colon leading to continued viral replication. .

In conclusion, our study gave some insight into the kinetics of HIV-1 in the gut tissues under ART. We were able to detect and quantify HIV-1 proviral DNA (total, 2-LTR and integrated DNA) despite the technical difficulties. Our results indicate that HIV-1 is disseminated differently among the gut tissues. 2-LTR proviral DNA which is supposed to account for <10 % of the total unintegrated DNA. However, despite their low levels in our study, their role as biomarkers for ongoing replication cannot be underestimated. A previous study, showed that unintegrated HIV DNA can transcribe viral genes, such as Vpr, independently promoting transcription from unintegrated DNA, in addition to Tat transcription (12, 70, 165). Other studies have also reported that 2-LTR proviral DNA is active, but they are not the only source of the viral transcription levels (12, 167, 168, 169). Overall, all the unintegrated HIV DNA are considered transcriptionally active template, but more studies are needed to understand their role and dynamics in HIV-1 infection. (12).

Although we only studied a small number of patients, our study showed no difference in the effect of AZT or ddI in detecting HIV-1 proviral DNA forms, and we were able to detect them in various gut tissues and various visits of HIV-1 infected patients. More studies are needed to determine the effect of monotherapy on HIV-1 kinetics in the gut. In addition, the low levels

of proviral DNA clearly indicate the viral persistence in reservoirs in the gut which is considered an obstacle for viral eradication (33, 146, 156, 166)

Our results with regard to HIV-1 proviral DNA forms levels did not correlate with the viral loads or CD4+ T-cells count as our patient samples had high viral loads and CD4+ T- cells count, which would lead us to expect high DNA levels detection in our samples. Our results did not allow us to make a firm conclusion about the HIV-1 proviral DNA form levels in the gut tissues, but they did show the various forms were present in the gut tissues. It is important to continue our HIV-1 studies under ART, and compare those to patients in sub- Sahara Africa, where there are millions of HIV-1 patients receiving sub optimal therapies due to the expensive nature of antiretroviral drugs and lack of access, which could resemble our observation of our “historical” patients on monotherapy.

Our lab in previous studies encountered difficulties in extracting sufficient high quality viral RNA from our gut tissues samples, we therefore directed our study to quantify proviral DNA, as it is still can give an insight of HIV-1 dynamics in the gut tissues. Although technical difficulties such as DNA quality may have challenged our ability to detect HIV-1 proviral DNA forms in our samples. Our optimization and our studies with the positive controls revealed that our assays can successfully amplify and quantify the various proviral HIV-1 DNA forms.

To put to rest the issues of the quality of the DNA we suggest isolating fresh DNA from our samples and a better DNA extraction method such as phenol-chloroform, as it has a better yield of episomal DNA and potential cleaner DNA, which could increase our ability detect the different HIV-1 DNA forms.



We also suggest to conduct the experiments using cell cultures such as Jurkat cell line as they are leukemic T-cell line, which can be infected with HIV-1 and treat them with monotherapies (AZT or ddI) , and subsequently monitor the HIV-1 proviral DNA forms levels at different time points. Although this method may not give the dynamic of HIV-1 in the gut tissues, but it will increase our understanding of HIV-1 dynamics under ideal ART conditions.

Finally, as we do have optimal real time PCR assays to quantitate proviral HIV-1 DNA forms, it would be of interest to extend our studies to African countries, and conduct this research on a larger scale with gastrointestinal tissues and blood samples from HIV-1 infected patients receiving suboptimal HAART to obtain further insight in the dynamics of HIV-1 infection in that important group of patients.

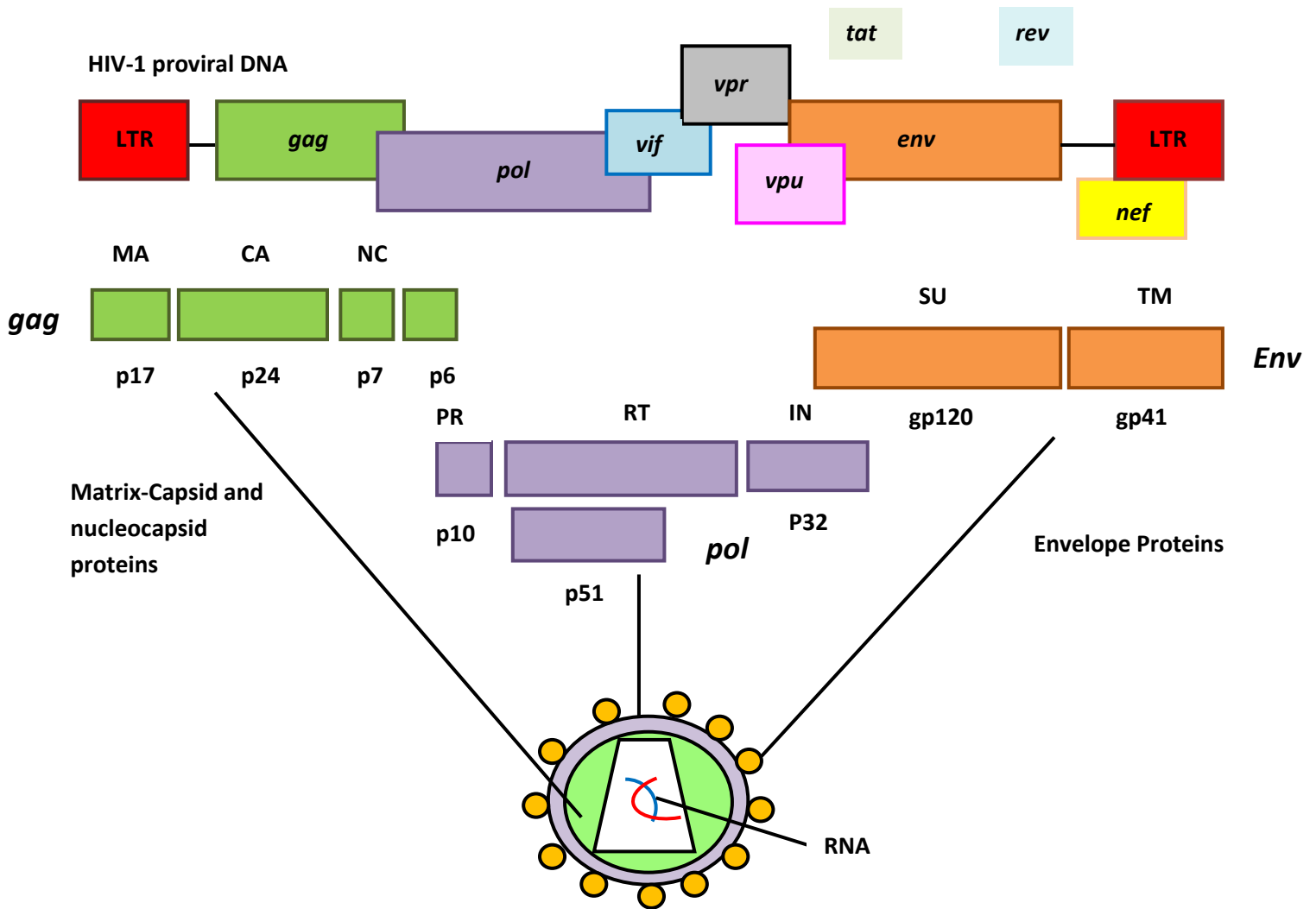


**Figure 1:** A lantzematic Representation of the HIV-1 Genome. It has nine open reading frames.

Three of the open frames encode the Gag, Pol and Env polyproteins that subsequently are proteolytically cleaved into the individual proteins to form structure a new virion (170).

Gag proteins:

- (MA) matrix
- (CA) capsid
- (NC) nucleocapsid

Envelope proteins:

- (SU) surface or gp120
- (TM) transmembrane or gp41

Pol proteins:

- (PR) protease
- (RT) reverse transcriptase
- (IN) integrase

Accessory proteins:

- (Tat and Rev) gene regulatory
- (Vif) increases viral infectivity
- (Vpr) viral protein
- (Vpu) assist the virion release
- (Nef) prevent reinfection of the same cell

**Figure 2:** A Schematic Representation of the HIV-1 Life Cycle. The virus starts infecting the cell by binding to its specific receptors CCR5 and CXCR4 on the host cell and fuses the viral envelope with the host cell membrane. This allows the rest of the virus to enter the cell. The virus un-coats and starts the reverse transcription resulting in double stranded proviral DNA that travels to the nucleus and integrates to the host genome. Then, the transcription begins to make new virions. After the virus is released from the cell, the virus starts the maturation stage. In this stage, the protease starts to cleave the virion proteins, which gives the virus its final mature structure that is able to infect another cell (171).

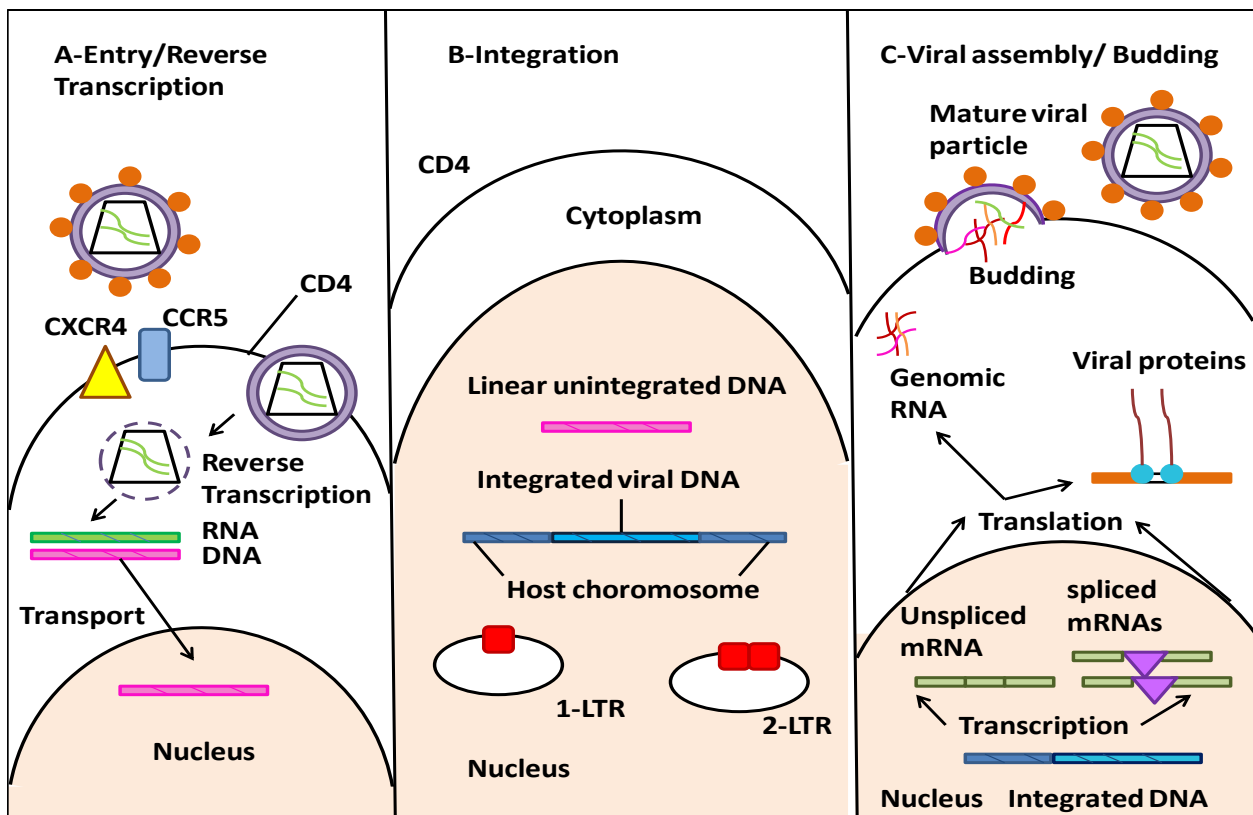


**Figure 3:** A Schematic Representation of pNL4-3 Plasmid Map. The plasmid has a pUC backbone. It is commonly used in vitro for genetic manipulation of HIV-1 proviral sequence (141). This plasmid was used as positive control in the real- time PCR assays to quantify total HIV-1 proviral DNA.

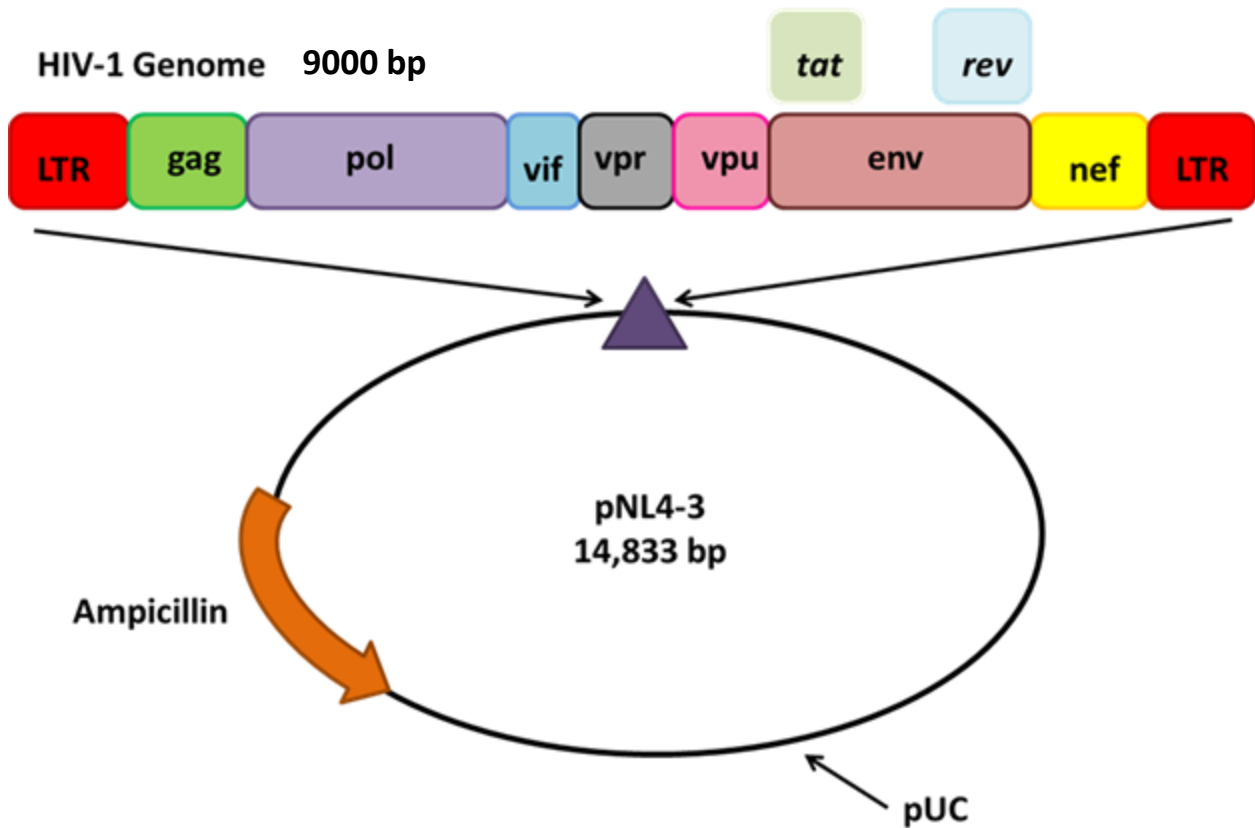


**Figure 4:** A Schematic Representation of 2-LTR Plasmid Map. **[A]** The HIV-1 proviral linear DNA structure before integration. **[B]** The integration of the linear cDNA into itself can yield an internally rearranged form. This so-called auto-integration, where the 3'-ends of the reverse transcriptase being processed by integrase and targets sites within the viral DNA, leading to internally rearranged or less than full length DNA circles. In addition, the ligation of the cDNA ends by the host cell non-homologous DNA end-joining system yielding two long terminal repeats (LTR) gives rise to the the 2-LTR circles **[C]** The pEX-A plasmid was constructed similar to the HIV-1 2-LTR circles to be used as a control (17). The 2-LTR sequence was obtained from the pNL4-3 plasmid that is commercially available from (<http://www.operon.com/default.aspx>).

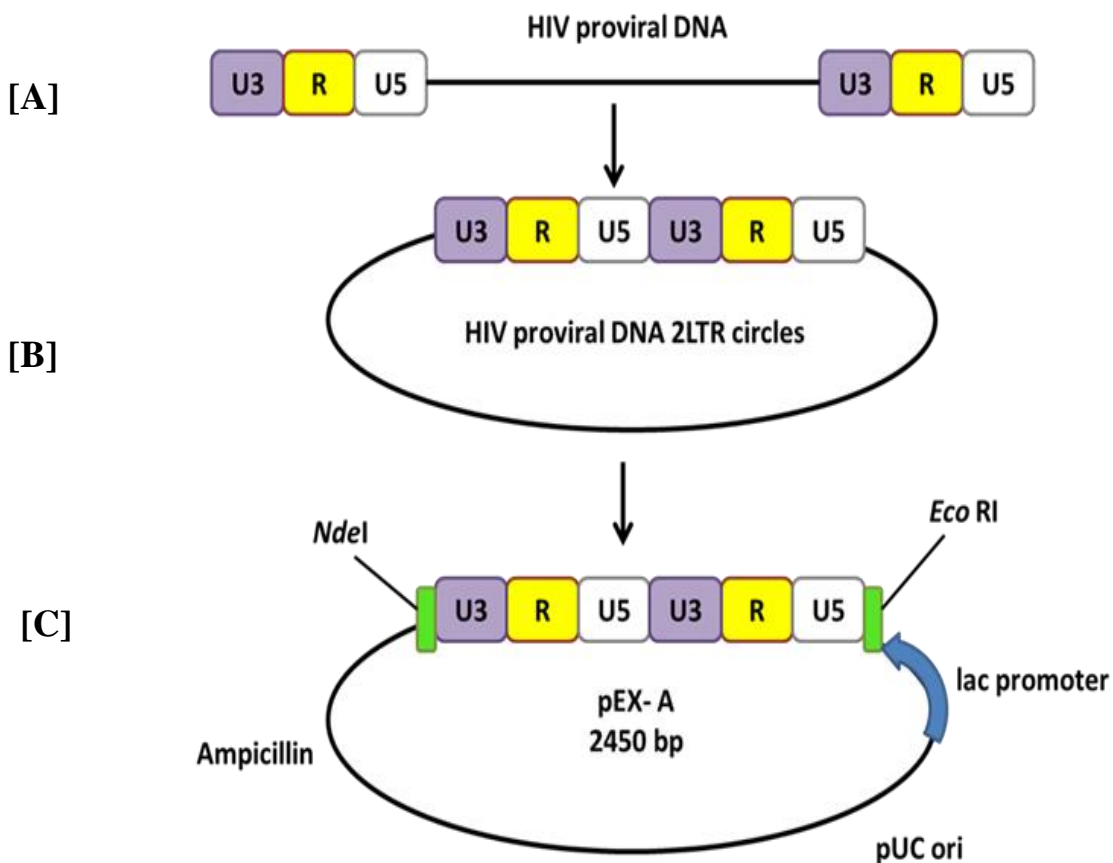


**Figure-5:** A Schematic Representation of the Integrated DNA Map. The plasmid was constructed to resemble the HIV-1 integrated proviral DNA. LTR and gag genes were obtained from pNL4-3 sequence and inserted in the pCR-TOPO vector. The Alu element sequence obtained from the gene bank number HQ709124.2 (<http://www.ncbi.nlm.nih.gov/genbank/>).The plasmid was used as a control for detecting the HIV-1 integrated DNA and ordered from (<http://www.operon.com/default.aspx>)

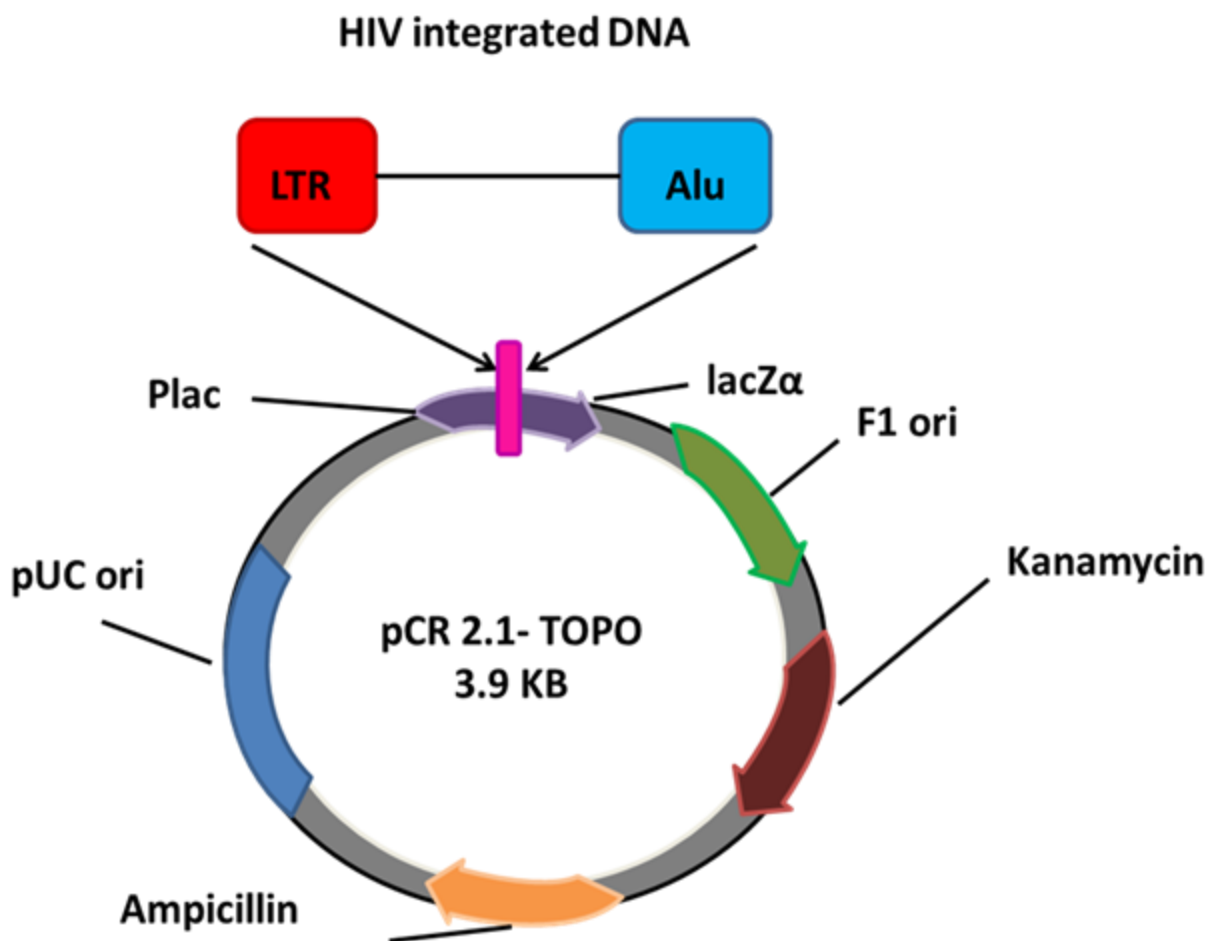
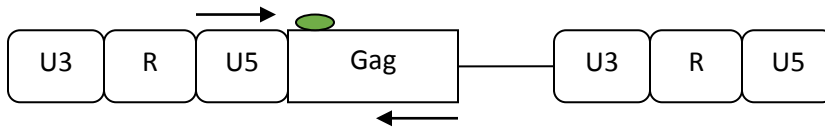
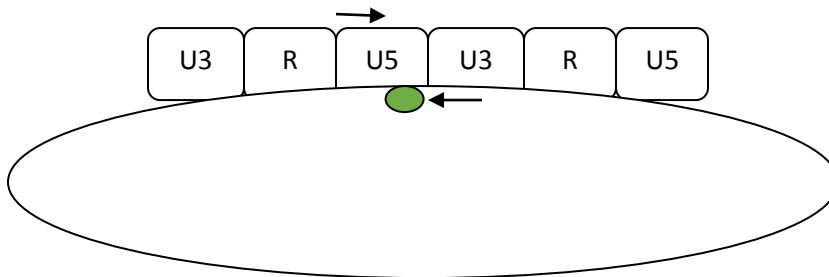


**Figure 6:** A schematic Representation of the Locations of the PCR Primers in the HIV DNA (172).

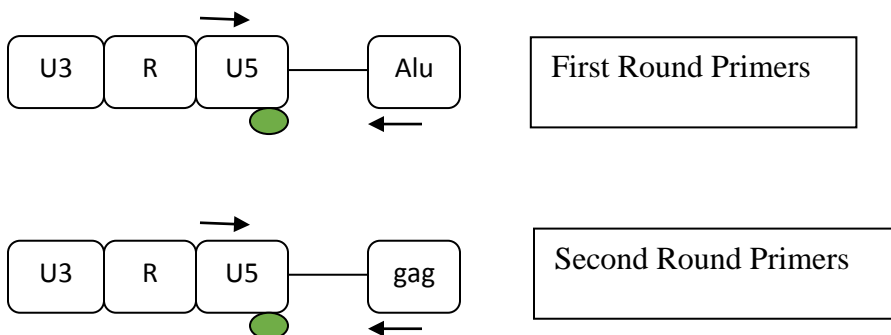
[A] Total HIV primers amplify the region of the HIV linear DNA between the left LTR sequence and the 5' end of the gag gene.



[B] To quantify the 2-LTR levels the primers used cross the junction generated by ligation of the DNA ends.



[C] Integrated provirus quantification primers are complementary to the HIV LTR and the chromosomal Alu repeats.



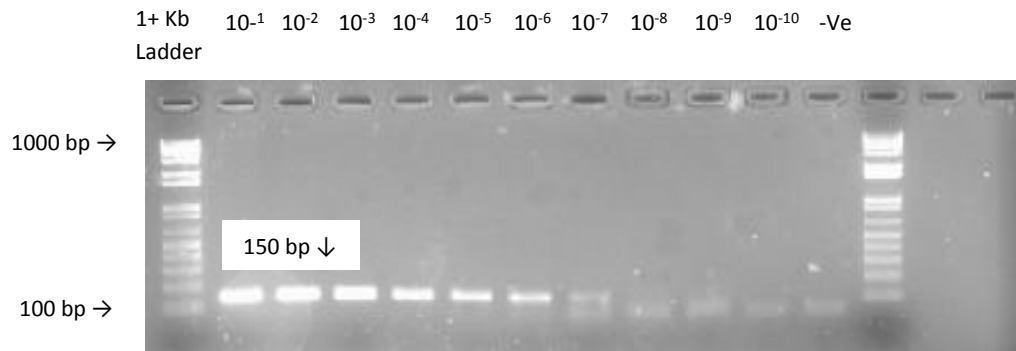


**Figure 7:** Detection of Amplified Total HIV-1 Proviral DNA by Conventional PCR. The plasmid used as a positive control resulted in the expected size 150bp for the total HIV-1 proviral DNA. The lower limit of detection was calculated as 500 viral copy number/ng.



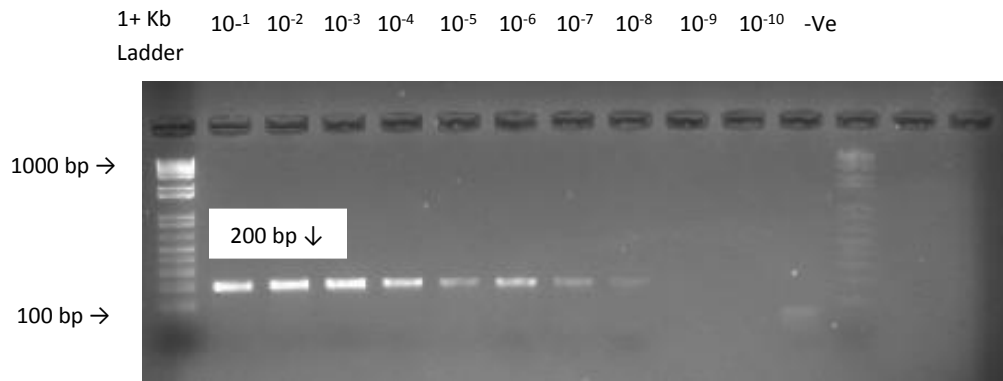


**Figure 8:** Detection of Amplified 2-LTR Proviral DNA by Conventional PCR. The plasmid used as a positive control gave the desired 200 bp band expected for 2-LTR proviral DNA. The lower limit of detection was calculated as 500 viral copy numbers/ng.

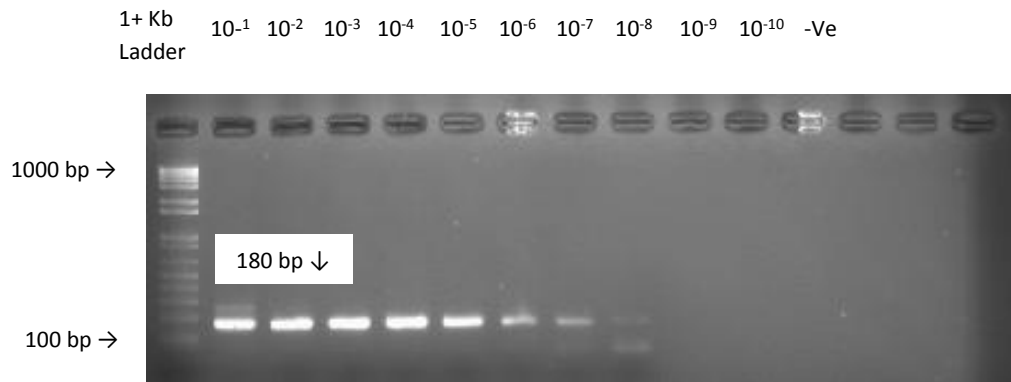


**Figure 9:** Detection of Amplified Integrated Proviral DNA by Conventional PCR. The plasmid used as a positive control amplified the desired 180bp band. The lower limit of detection was also calculated at 600 viral copy number/ng.

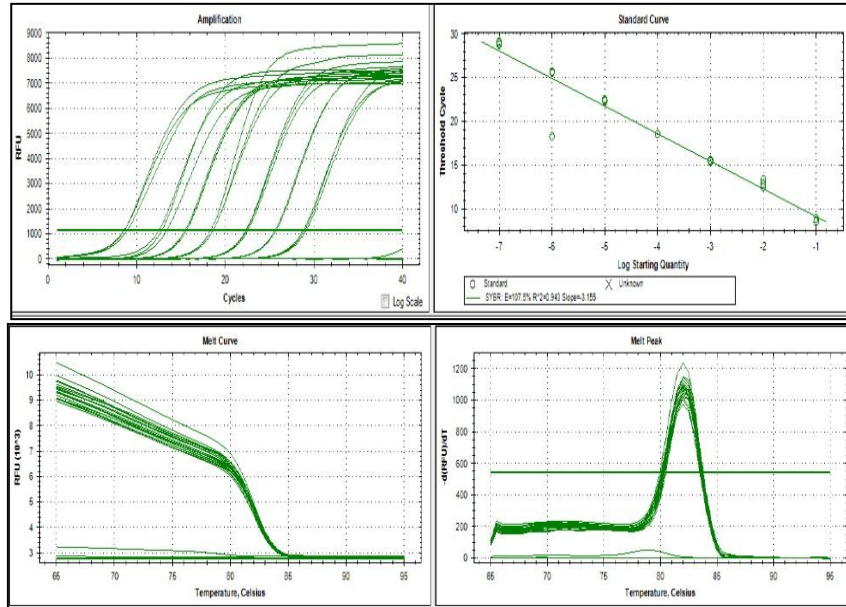


**Figure 10:** Total HIV Proviral DNA Syber Green Real- Time PCR Standard Curve. Total HIV-1 proviral DNA standard and melting temperature curves showing the appropriate amplicon. The lower limit of detection was 5 viral copy numbers/ng.

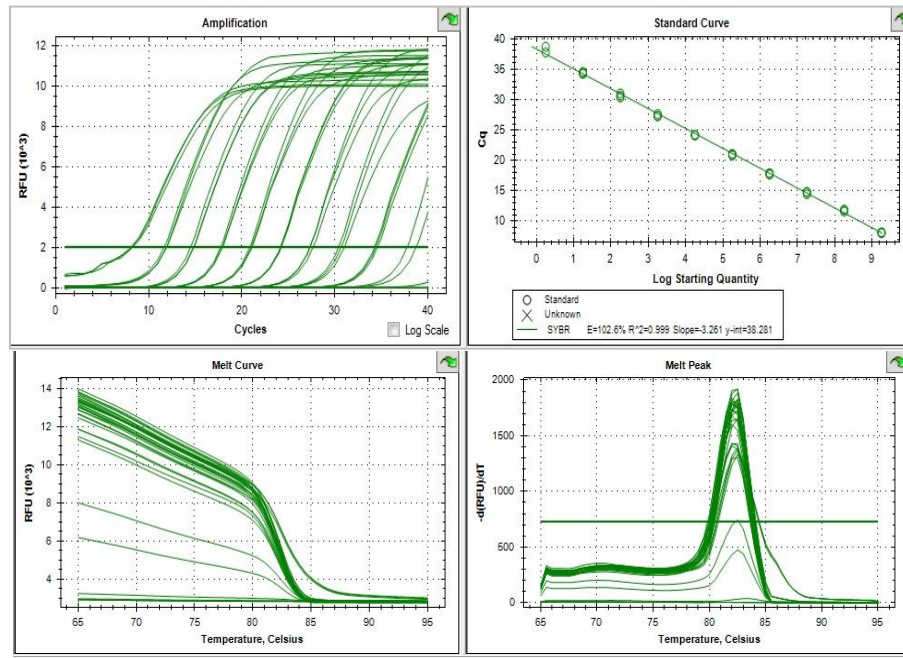


**Figure 11:** 2-LTR Proviral DNA Syber Green Real- Time PCR Standard Curve. 2-LTR proviral DNA standard and melting curves showing the appropriate amplicon. The lower limit of detection was 5 viral copy

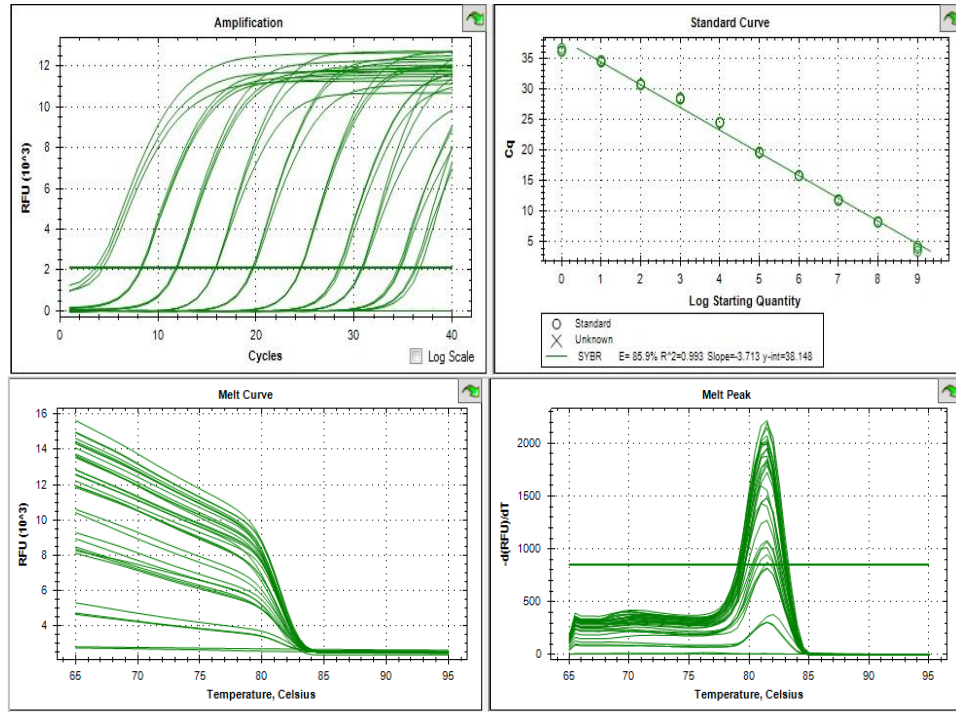


**Figure 12:** The Integrated Proviral DNA Syber Green Real- Time PCR Standard Curve. The integrated proviral DNA standard and melting curves showing the limit of detection of 6 viral copy number/ng.

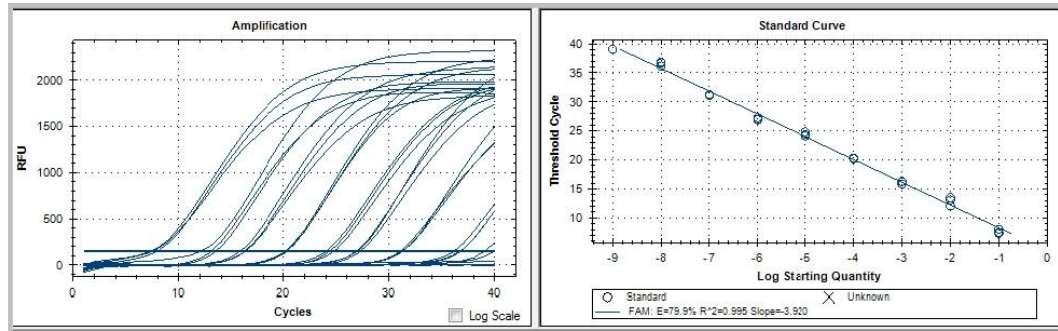


**Figure 13:** Optimization of Total HIV-1 Proviral DNA Detection by Real- Time PCR. Total HIV-1 proviral DNA positive standard curve using previously described primers and probe with the average limit of detection of 5 viral copy numbers/ng

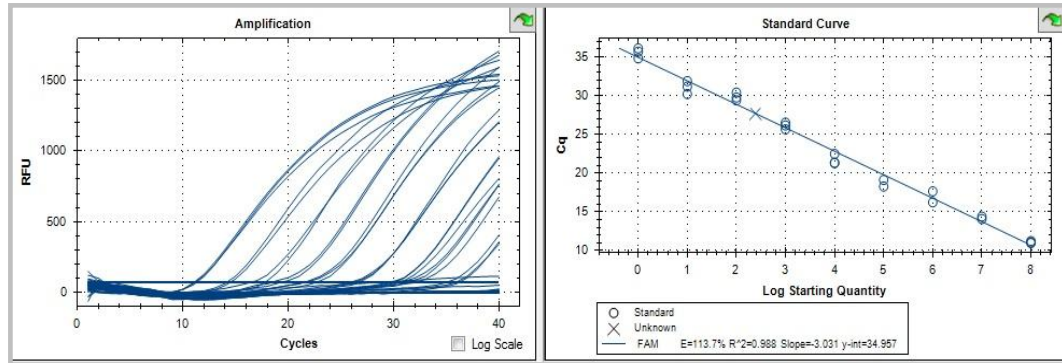


**Figure 14:** Optimization of 2-LTR Proviral DNA Detection by Real- Time PCR. 2-LTR proviral DNA standard curve giving an average of 5 viral copy numbers for the limit of detection.

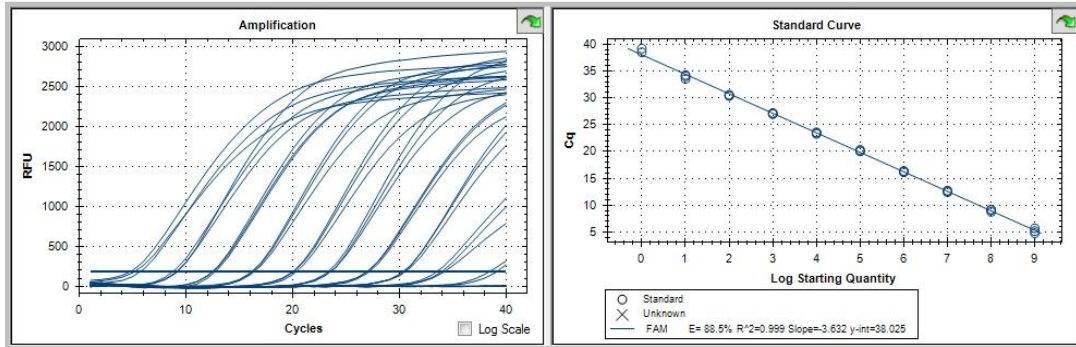


**Figure 15:** Optimization of the Integrated Proviral DNA Detection by Real- Time PCR. Integrated proviral DNA standard curve was positive for the desired product giving an average limit of detection low as 6 viral copy numbers/ng.



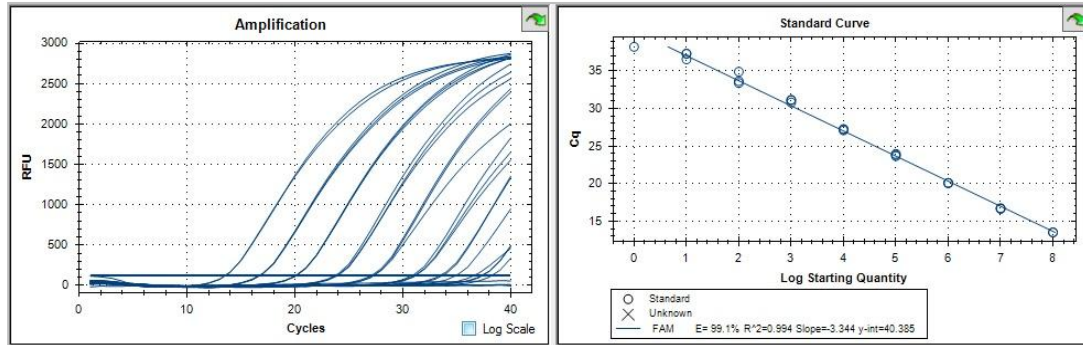


**Figure 16:** Optimization of Total HIV Proviral DNA Detection by Real- Time PCR Mixed with Chromosomal DNA. The total HIV-1 proviral DNA positive standard curve mixed with chromosomal DNA giving an average limit of detection of 5 viral copy numbers/ng the same as the analysis without chromosomal DNA

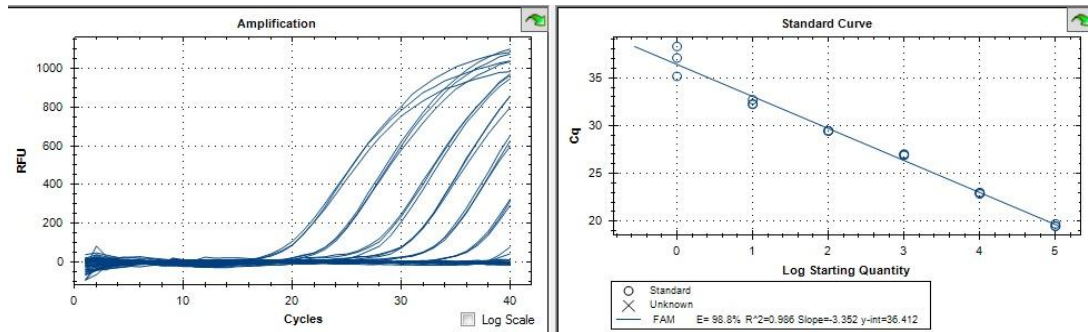


**Figure 17:** Optimization of 2-LTR Proviral DNA Detection by Real- Time PCR Mixed with Chromosomal DNA. The positive standard curve mixed with chromosomal DNA gave the lower limit of detection of 5 viral copy numbers/ng the same as the analysis without chromosomal DNA

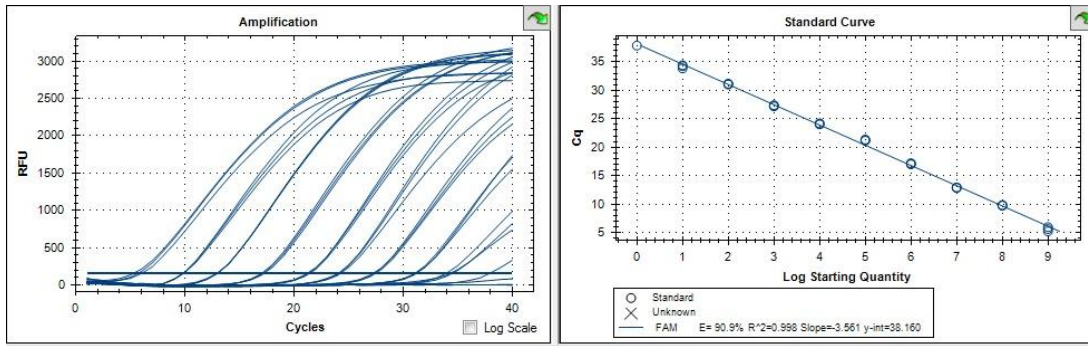


**Figure 18:** Optimization of the Integrated Proviral DNA Detection by Real- Time PCR Mixed with Chromosomal DNA. The standard curve gave the lower limit of detection of 6 viral copy numbers/ng.

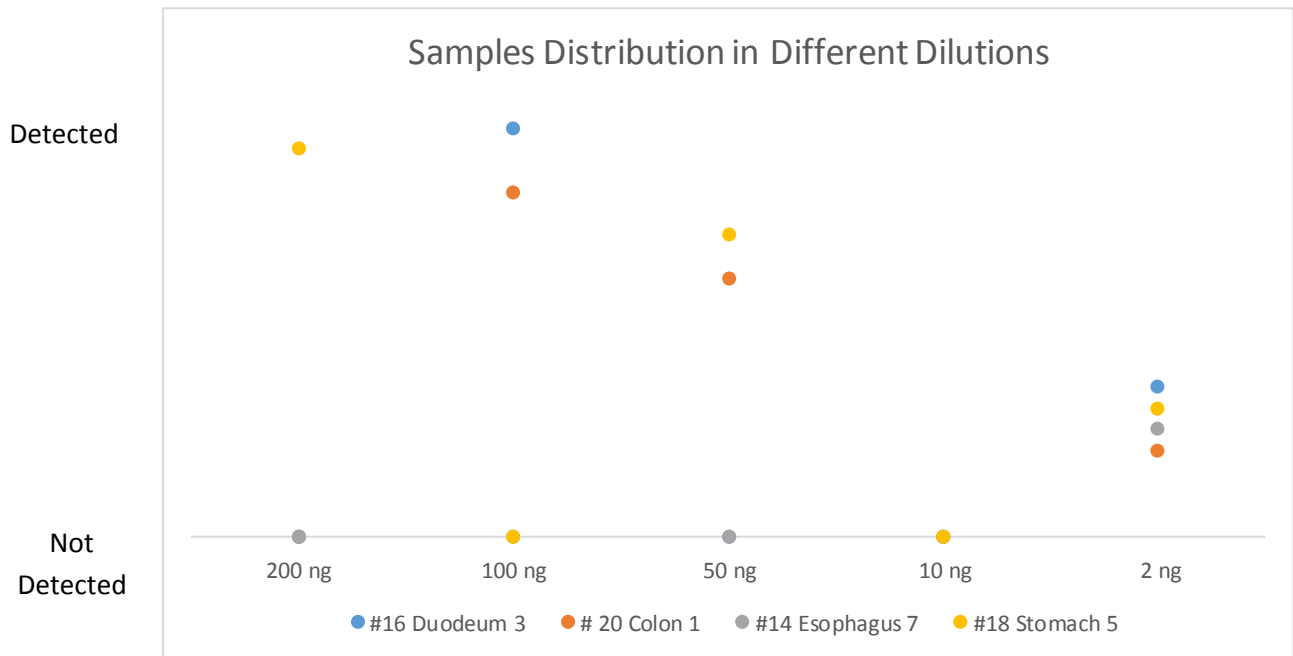


**Figure 19:** Samples Dilutions from Various Gut Tissues to Test for the Optimal DNA Concentration. Total HIV-1 proviral DNA was tested on patient # 16 duodenum Visit 3 and patient # 20 Colon dilutions. 2-LTR proviral DNA was tested on patients # 14 esophagus visit 7 and patient # 18 stomach visit 5. For all patients total HIV-1 proviral DNA was detectable in various dilutions. The 2 ng concentration seems to be giving the most positive results, however two of the results were outside of the standard curve.

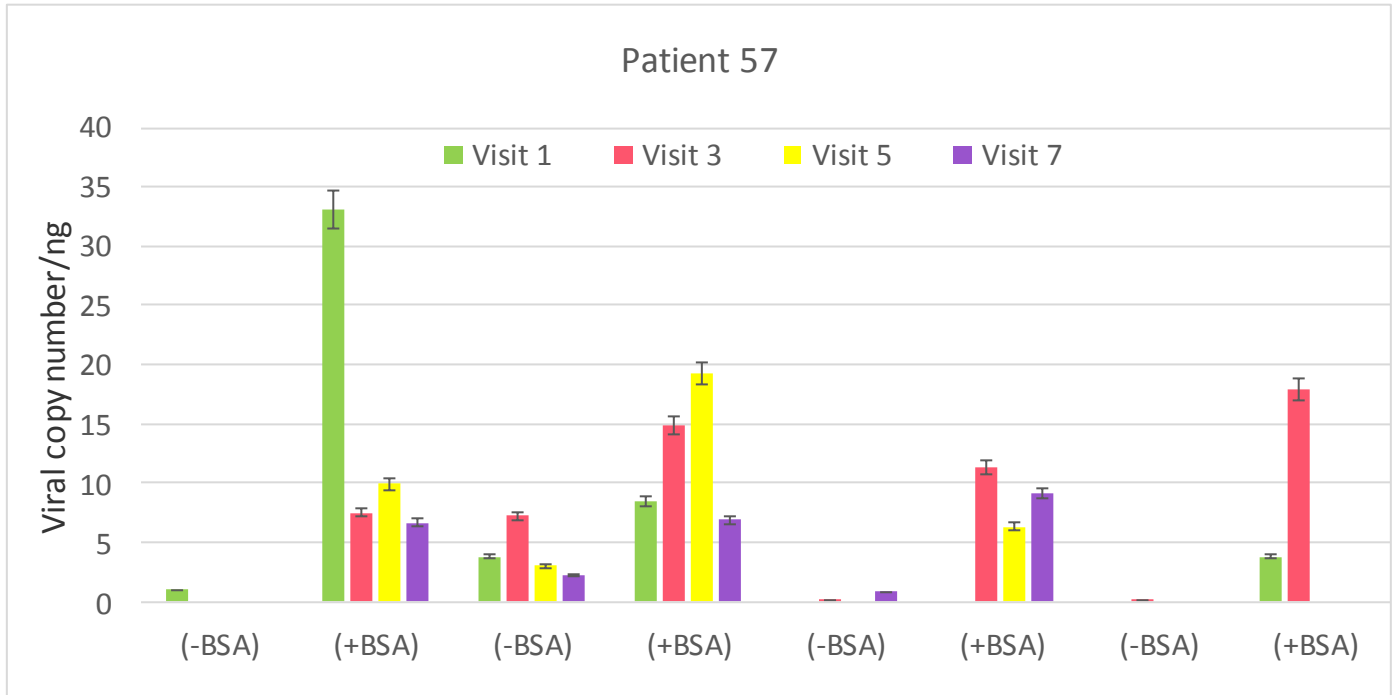


**Figure 20:** Total HIV-1 proviral DNA detection by real time PCR without/with the presence of BSA. To determine the effect of potential inhibitors we added BAS to our assays. In comparison, the total HIV-1 proviral DNA with BSA might have an effect as some tissues were negative before using BSA. However,

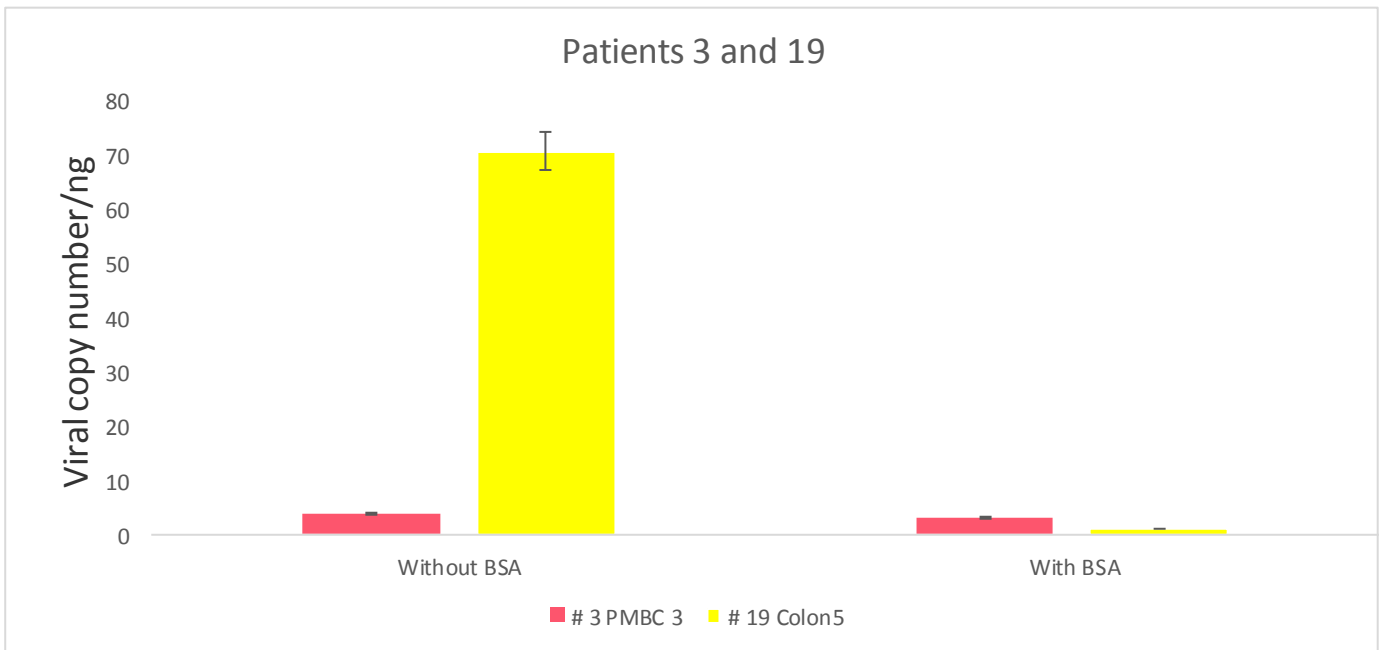


**Figure 21:** 2-LTR and integrated proviral DNA detection by real time PCR without/with the presence of BSA. . To determine the effect of potential inhibitors we added BAS to our assays. 2-LTR proviral DNA was tested on patient #3 PBMC visit 3 and integrated proviral DNA was tested on patient #19 Colon visit 5. The results of both of the proviral DNA forms were not affected by BSA as they remained detectable with even lower levels after adding BSA.

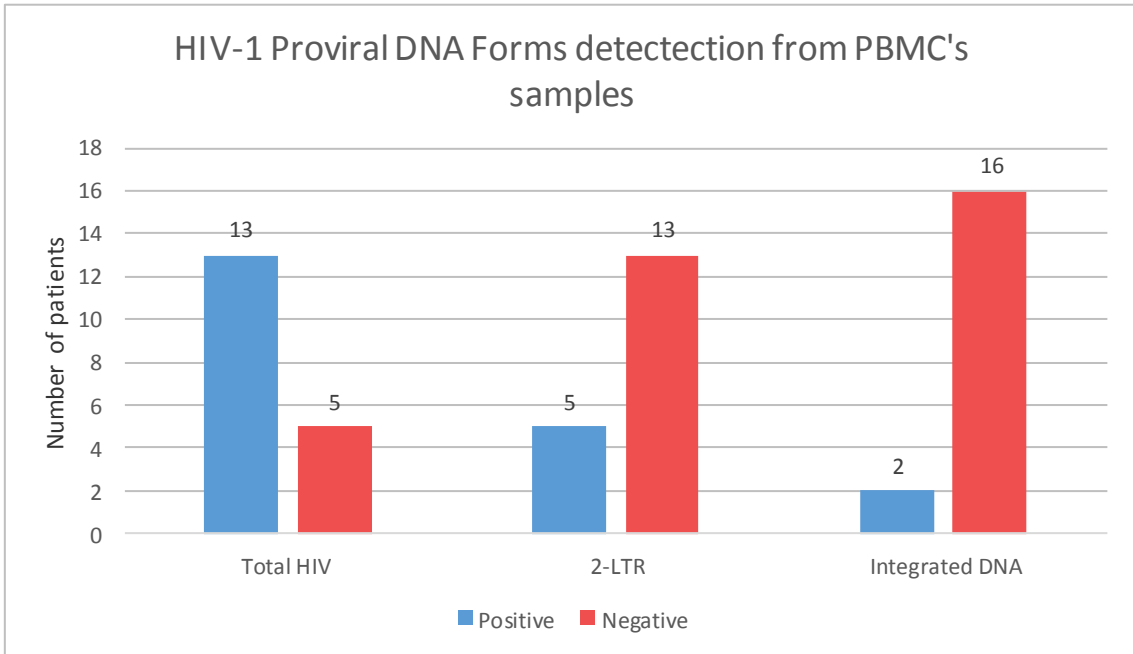


**Figure 22:** HIV-1 proviral DNA forms detection from PBMC's of HIV-1 infected patients. 72% of the patients were positive for total HIV proviral DNA, 27% were positive for 2-LTR proviral DNA and 11% of the patients were positive for the integrated proviral DNA.

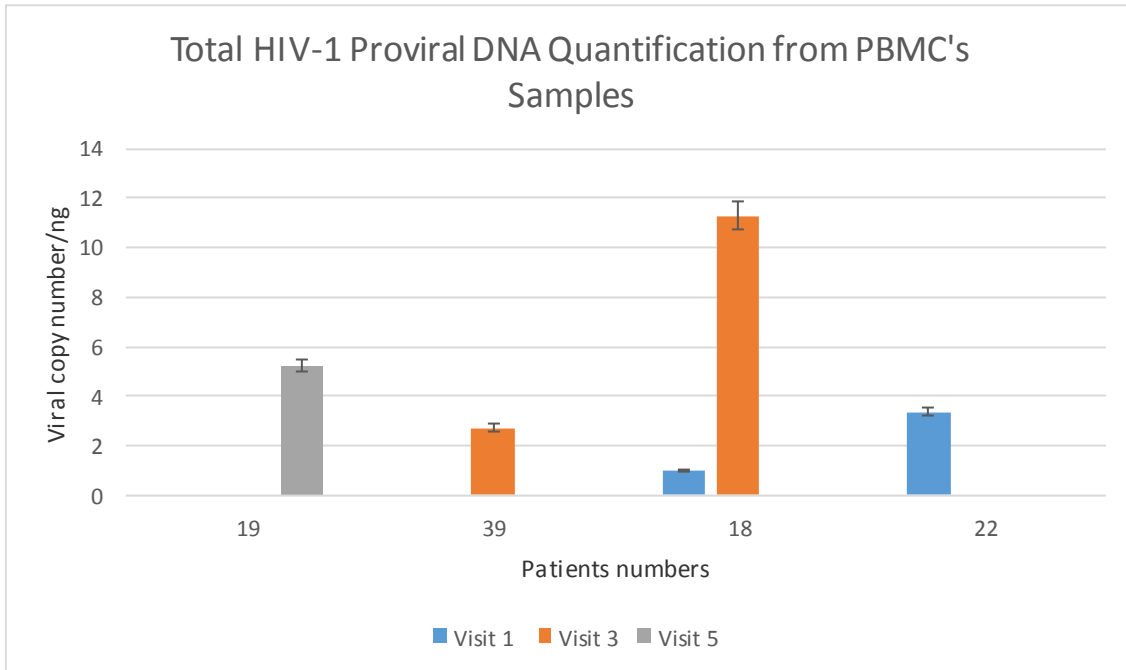


**Figure 23:** Total HIV-1 proviral DNA quantification from PMBC's of HIV-1 infected patients. 4/13 of the positive patients were detectable and quantifiable for the total HIV-1 proviral DNA. The patients' different treatments had not effect on the levels of detection as it was low for both AZT and ddI patients.



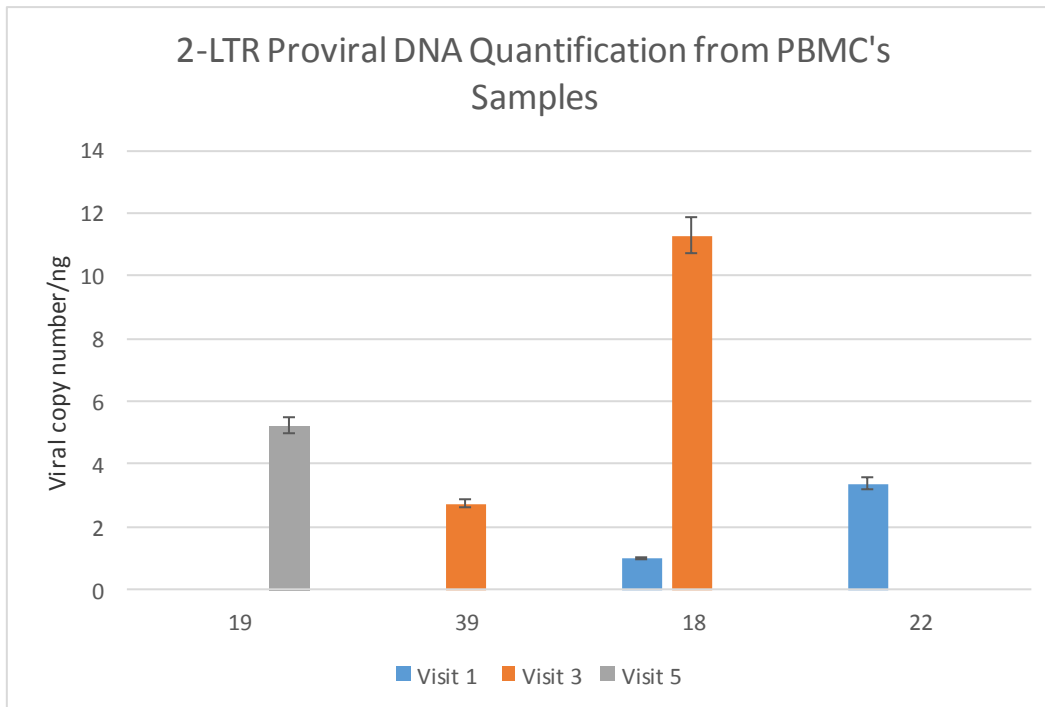


**Figure 24:** 2-LTR proviral DNA quantification from PBMC's of HIV-1 infected patients. 4/5 of positive patients were detectable and quantifiable for 2-LTR proviral DNA. The patients' different treatments had no effect on the levels of detection as it was low for both AZT and ddI patients.

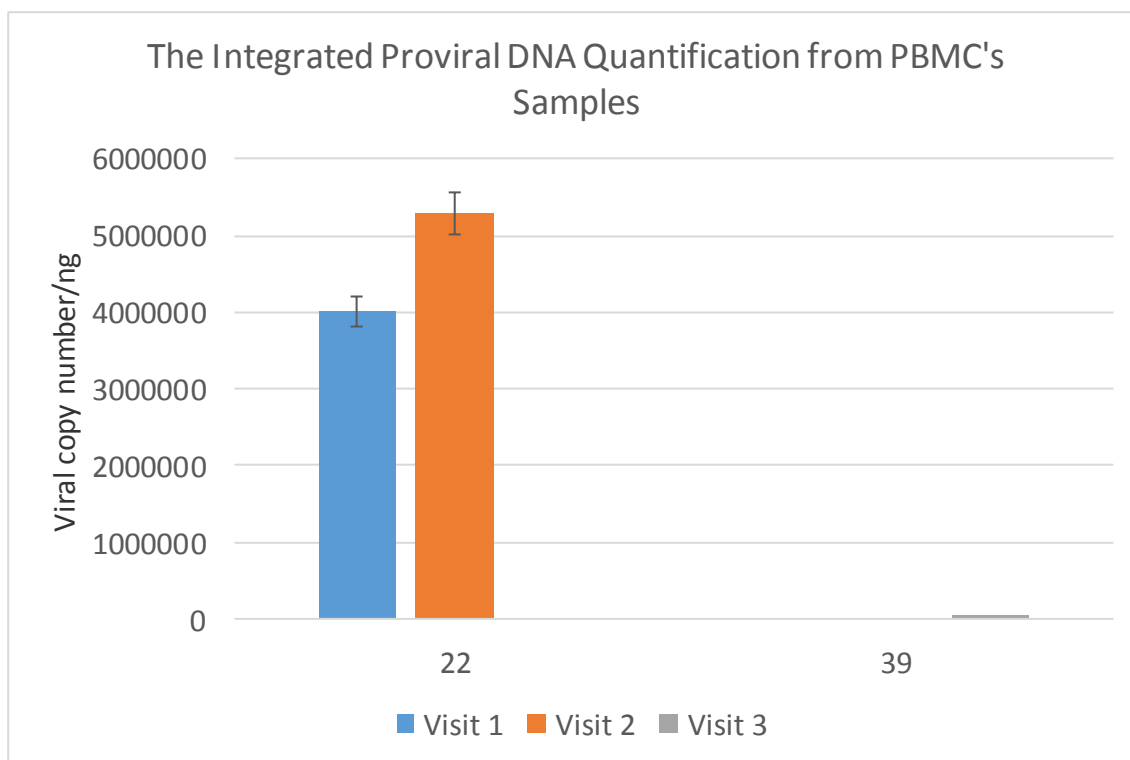


**Figure 25:** The integrated proviral DNA quantification from PBMC's of HIV-1 infected patients. 2/2 of positive patients were detectable and quantifiable for the integrated proviral DNA. The patients' different treatments seems to have an effect on the levels of detection as it was low for AZT and high in DDI patients. However, the limited numbers of patients cannot confirm that affect.

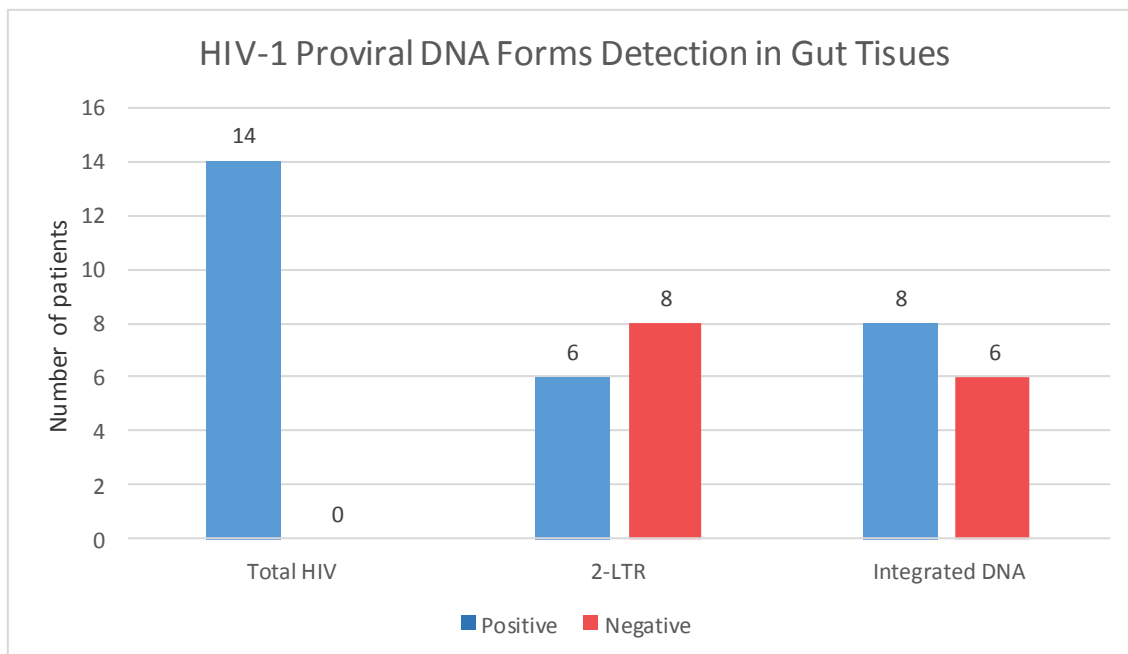


**Figure 26:** HIV-1 proviral DNA forms detection in the gut different tissues of HIV-1 infected patients: 14 out of 14 tested patients were positive for the total HIV-1 proviral DNA. 6 out of 14 patients were positive for the 2-LTR DNA form and 8 out of 14 patients were positive for the integrated proviral DNA.

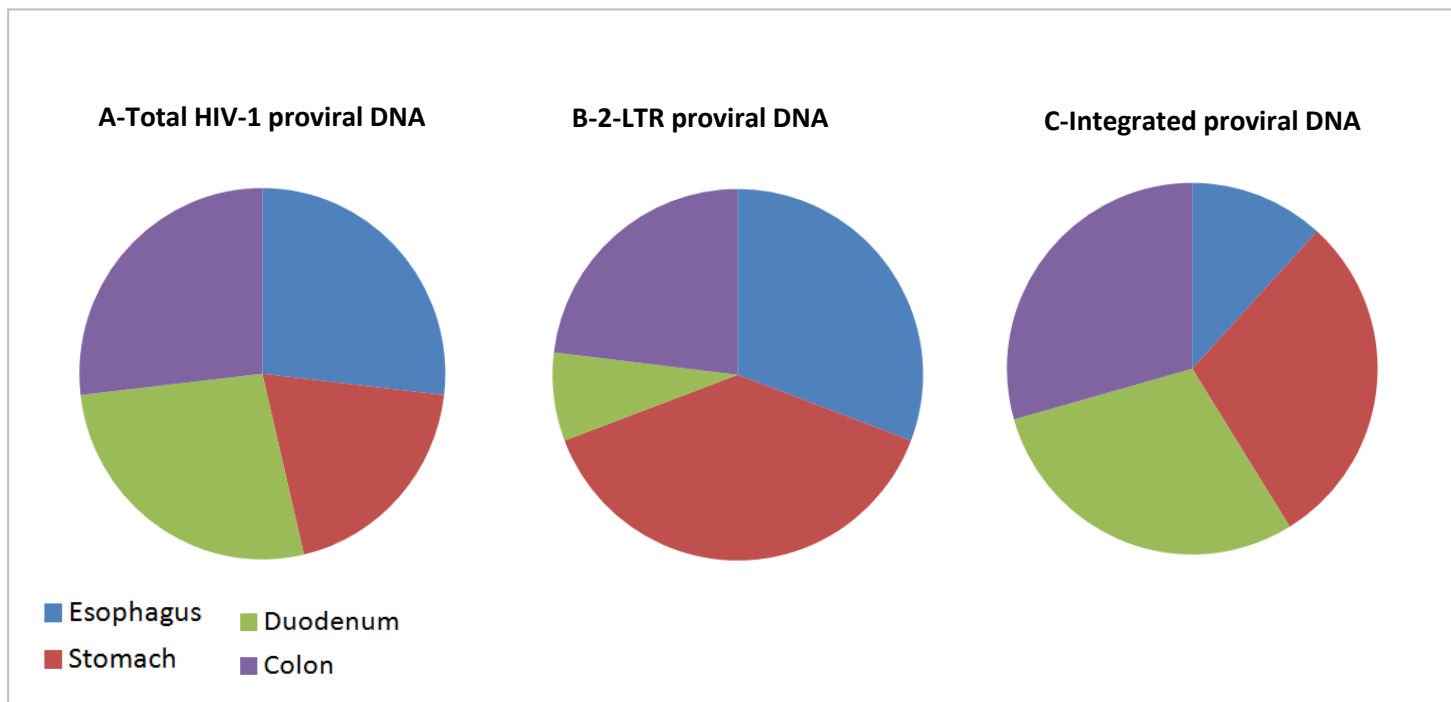


**Figure 27:** HIV-1 DNA distribution in gut tissues of HIV-1 infected patients: **A-** represents the total HIV proviral DNA from the patients' samples with the esophagus and the colon being the most detectable tissues among the rest of the gut tissues. **B-**The distribution of the 2-LTR proviral DNA was found most frequently in our patients' esophagus and stomach. The duodenum and colon were the least detectable tissues. **C-** The integrated proviral DNA was also found mostly in the stomach, duodenum and colon with the esophagus being the least detectable tissue among the gut different tissues.

**Table 14:** Positive gut tissue samples for total HIV-1 proviral DNA from AZT group various visits.

Patient Number	Type of Tissue	Visit 1	Visit 3	Visit 5	Visit 7
23	Esophagus	++	++	+	-
	Stomach	-	-	-	-
	Duodenum	-	++	-	-
	Colon	++	++	-	-
39	Esophagus	-	+	-	-
	Stomach	-	-	-	-
	Duodenum	-	-	-	-
	Colon	-	++	-	-
57	Esophagus	+	+	+	+
	Stomach	+	+	+	+
	Duodenum	NA	++	++	NA
	Colon	NA	+	+	NA

(++) Detected and quantified (-) Negative

(+) Detected only (N/A) Not available

Patients # 23, 39 and 57 received AZT only during this study. Total HIV-1 proviral DNA was detectable and quantifiable more frequently in visit 3 of the esophagus, duodenum and colon. Although, the ability to quantify the total HIV-1 proviral DNA in the other visits of the gut tissues was limited, our assay was able to detect it in our patients' samples.

**Table 15:** Positive gut tissue samples for total HIV-1 proviral DNA from ddI group various visits.

Patient Number	Type of Tissue	Visit 1	Visit 3	Visit 5	Visit 7
5	Esophagus	-	-	+	-
	Stomach	+	-	-	-
	Duodenum	-	+	+	-
	Colon	-	+	+	-
14	Esophagus	-	-	-	++
	Stomach	++	-	-	++
	Duodenum	-	-	-	+
	Colon	-	++	-	-
16	Esophagus	-	-	++	-
	Stomach	-	-	-	-
	Duodenum	-	-	-	-
	Colon	-	-	-	-
22	Esophagus	+	+	+	+
	Stomach	+	+	-	+
	Duodenum	-	+	+	-
	Colon	-	+	+	-
24	Esophagus	+	+	-	+
	Stomach	+	+	-	+
	Duodenum	-	+	+	-
	Colon	-	-	+	-
31	Esophagus	-	-	-	-
	Stomach	-	-	-	-
	Duodenum	-	-	+	-
	Colon	-	++	-	-

(++) Detected and quantified (-) Negative

(+) Detected only (N/A) Not available

Patients # 5, 14, 16, 22, 24 and 31 received ddI only during this study. Total HIV-1 proviral DNA was detectable and quantifiable more frequently in the stomach and colon. The assay detected the total HIV-1 proviral DNA from various visits of the patients' gut tissues and no trending was observed.

**Table 16:** Positive gut tissue samples for total HIV-1 proviral DNA from switched treatment group various visits.

Patient Number	Type of Tissue	Visit 1	Visit 3	Visit 5	Visit 7
18	Esophagus	-	-	-	-
	Stomach	-	-	-	-
	Duodenum	-	++	++	-
	Colon	-	++	-	-
19	Esophagus	-	-	++	-
	Stomach	-	-	-	++
	Duodenum	-	-	-	-
	Colon	-	-	-	-
20	Esophagus	++	++	-	-
	Stomach	-	-	-	+
	Duodenum	-	-	-	-
	Colon	++	++	-	++

(++) Detected and quantified (-) Negative

(+) Detected only (N/A) Not available

Patients # 18 received ddI during 6 visits and switched to AZT+ ddc. For this patient, the duodenum and colon were the only detectable and quantifiable for total HIV-1 proviral DNA, and visit 3 was more frequently found positive. Moreover, patient #19 received ddI on the first visit and switched to AZT during this study. The total HIV-1 proviral DNA was detectable and quantifiable in the Esophagus and Stomach for this patient. In addition, 20 received AZT during 4 visits and switched to ddI during this study. Total HIV-1 proviral DNA was detectable and quantifiable more frequently in the esophagus and colon and most frequently in visit 3. In conclusion, the switching between AZT and ddI did not affect the detection of total HIV-1 proviral DNA as various tissues were detectable and quantifiable. The frequent detection on visit 3 might be due to a better DNA purity.

**Table 17:** Positive gut tissue samples for 2-LTR proviral DNA from AZT group various visits.

Patient Number	Type of Tissue	Visit 1	Visit 3	Visit 5	Visit 7
23	Esophagus	+	-	-	-
	Stomach	+	+	-	-
	Duodenum	-	+	-	-
	Colon	+	+	-	-
39	Esophagus	+	+	-	-
	Stomach	+	+	-	-
	Duodenum	-	-	+	-
	Colon	+	+	-	-
57	Esophagus	-	-	-	-
	Stomach	+	+	++	+
	Duodenum	-	+	+	++
	Colon	+	++	-	-

(++) Detected and quantified (-) Negative

(+) Detected only (N/A) Not available

Patients # 23, 39 and 57 were receiving AZT during this study. The total HIV-1 proviral DNA were detectable and quantifiable in patient #57 stomach visit 5, duodenum visit 7 and colon visit 3. These same tissues were detectable but not quantifiable in the other visits. Patients 23 and 39 were detectable for total HIV-1 proviral DNA more frequently in visit 1 and 3 of the esophagus and stomach.



**Table 18:** Positive gut tissue samples for 2-LTR proviral DNA from ddI and switched treatment group various visits.

Patient Number	Type of Tissues	Visit 1	Visit 3	Visit 5	Visit 7
5	Esophagus	-	+	+	-
	Stomach	-	+	++	-
	Duodenum	-	-	-	-
	Colon	-	-	-	-
24	Esophagus	-	-	-	+
	Stomach	++	-	-	-
	Duodenum	-	-	-	-
	Colon	-	++	-	-
18	Esophagus	-	-	-	-
	Stomach	-	-	+	-
	Duodenum	-	-	-	-
	Colon	-	-	-	-

(++) Detected and quantified (-) Negative

(+) Detected only (N/A) Not available

Patients # 5, 24 and 18 were receiving ddI during this study. The 2-LTR proviral DNA was detectable and quantifiable in the stomach and colon from various visits. The esophagus was only detectable in the visit 3 and 5 from patients # 5. The stomach was also detectable for 2-LTR proviral DNA in visit 5 from patient # 18 who were receiving ddI during this visit.

**Table 19:** Positive gut tissue samples for the integrated proviral DNA from ddI group various visits.

Patient Number	Type of Tissue	Visit 1	Visit 3	Visit 5	Visit 7
5	Esophagus	-	-	-	-
	Stomach	-	-	-	++
	Duodenum	-	-	-	-
	Colon	-	++	-	-
14	Esophagus	-	-	++	++
	Stomach	-	-	-	++
	Duodenum	-	-	-	-
	Colon	-	-	+	-
16	Esophagus	-	-	-	-
	Stomach	++	-	-	-
	Duodenum	-	-	++	-
	Colon	-	-	-	-
22	Esophagus	-	-	-	-
	Stomach	-	-	++	-
	Duodenum	-	-	-	-
	Colon	-	-	-	-
24	Esophagus	-	-	-	-
	Stomach	++	-	-	-
	Duodenum	-	-	-	-
	Colon	-	-	-	-

(++) Detected and quantified (-) Negative

(+) Detected only (N/A) Not available

Patients #5, 14, 16, 22, and 24 were receiving ddI during this study. The integrated proviral DNA was detectable and quantifiable most frequently in the stomach from various patients' visits. The detection of the integrated proviral DNA was varied from patients to another and from visit to another from the same patient.

**Table 20:** Positive gut tissue samples for the integrated proviral DNA from switched treatments group various visits.

Patients Number	Type of Tissue	Visit 1	Visit 3	Visit 5	Visit 7
18	Esophagus	-	-	-	-
	Stomach	-	-	-	-
	Duodenum	-	-	-	-
	Colon	-	-	++	-
19	Esophagus	-	-	-	+
	Stomach	-	-	+	-
	Duodenum	-	-	+	-
	Colon	-	+	+	-
20	Esophagus	-	-	-	-
	Stomach	-	-	-	-
	Duodenum	-	-	+	-
	Colon	-	-	-	-

(++) Detected and quantified (-) Negative

(+) Detected only (N/A) Not available

Patient #18 was receiving ddI during visit 5 of the colon, which was the only visit detected and quantified for the integrated proviral DNA. Patient # 19 was receiving AZT during the positive visits for the integrated proviral DNA and most of the gut tissues were only detectable from various visits. Patient # 20 was receiving ddI during visit 5 of the duodenum. In conclusion, the various gut tissues were detectable from various visits. The switching between AZT and ddI had no effect in the detection of the integrated proviral DNA and the challenge was in the structure of the DNA.

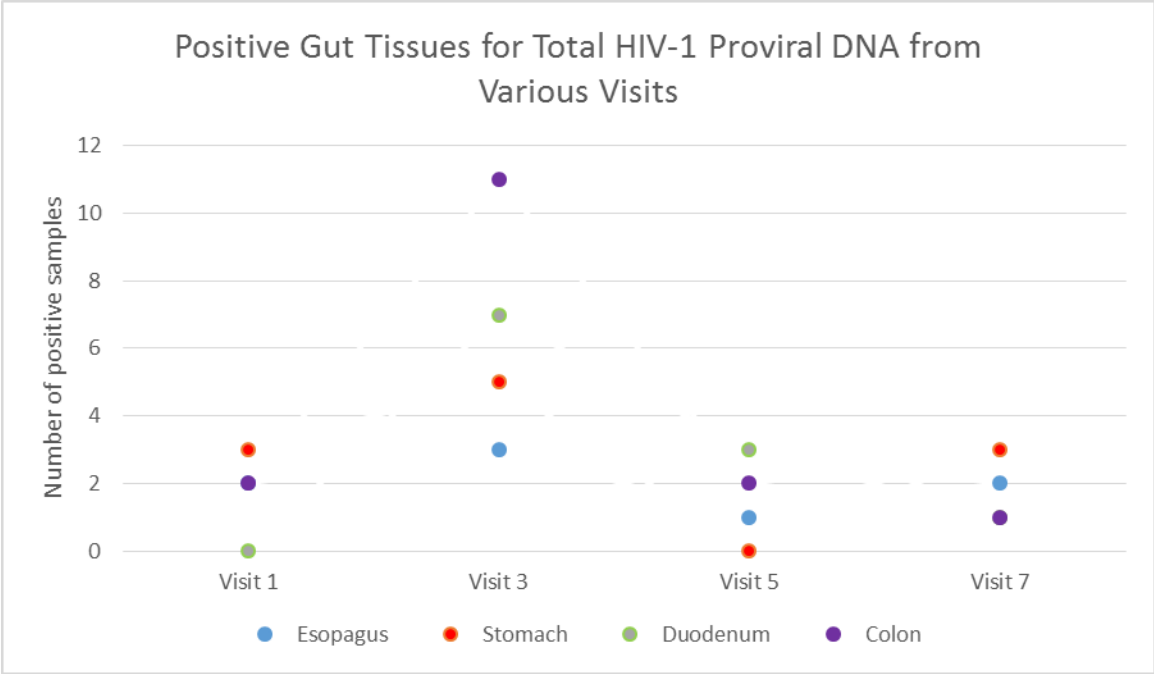


**Figure 28:** All positive gut tissue samples for the total HIV-1 proviral DNA from various visits. Visit 3 was the most detectable for total HIV-1 proviral DNA from all of the gut tissues. This pattern might have to do to the DNA purity at this visit and also the effect of monotherapy on the different gut compartments.

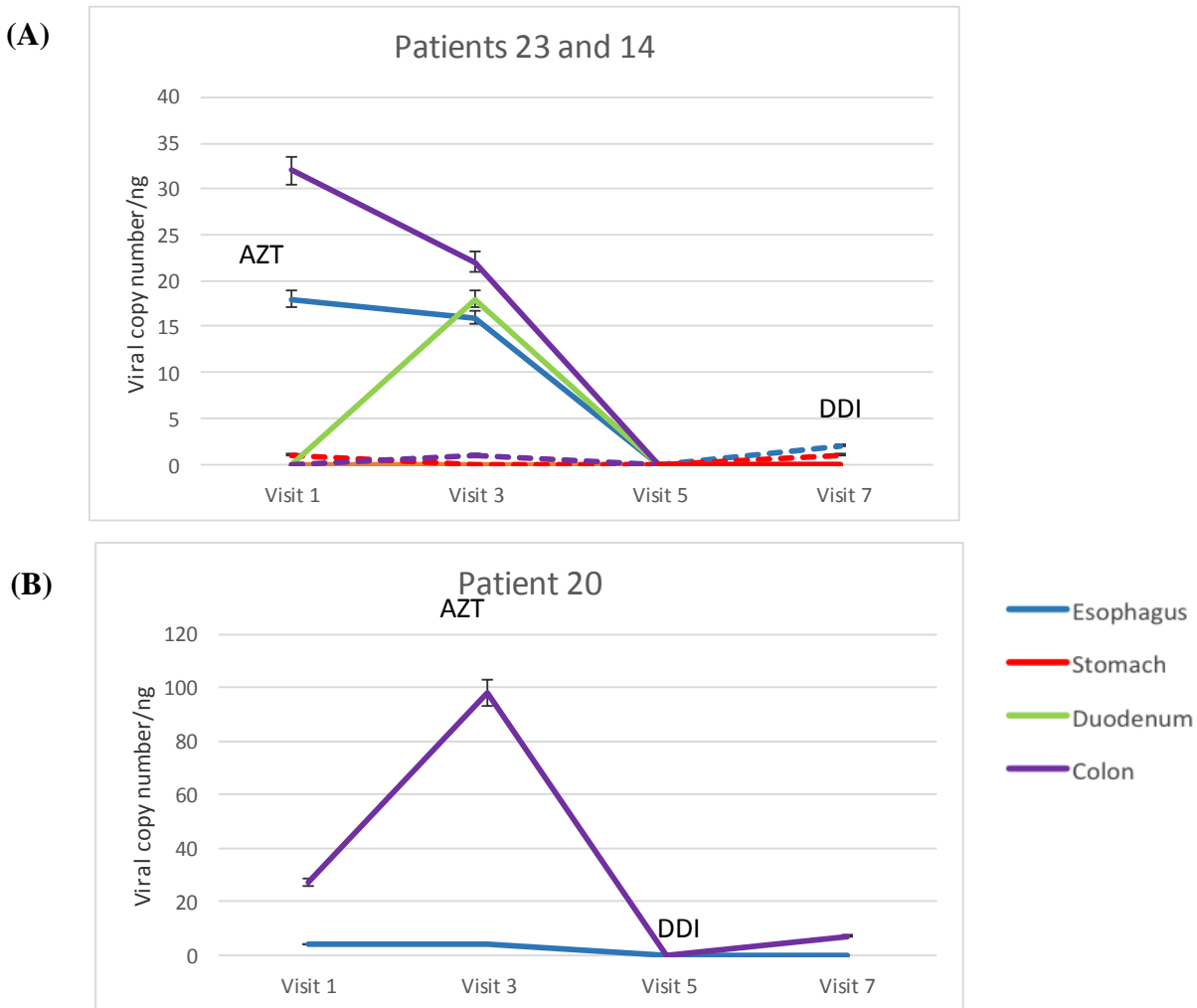


**Figure 29:** Comparison of Total HIV-1 proviral DNA levels in the gut tissues from HIV-1 infected patients: **(A)** Patient #23 received AZT (solid line) the levels of the total HIV-1 proviral DNA fluctuated between the visits of the esophagus, duodenum and colon. The same pattern was also found in the esophagus and the stomach of patient #14 (dashed line) who received ddI. **(B)** Patient #20 was receiving AZT and switched to ddI in visit 5. The total HIV-1 proviral DNA levels fluctuated in the esophagus and colon, which seems that switching to ddI affected the levels of total HIV-1 proviral DNA.

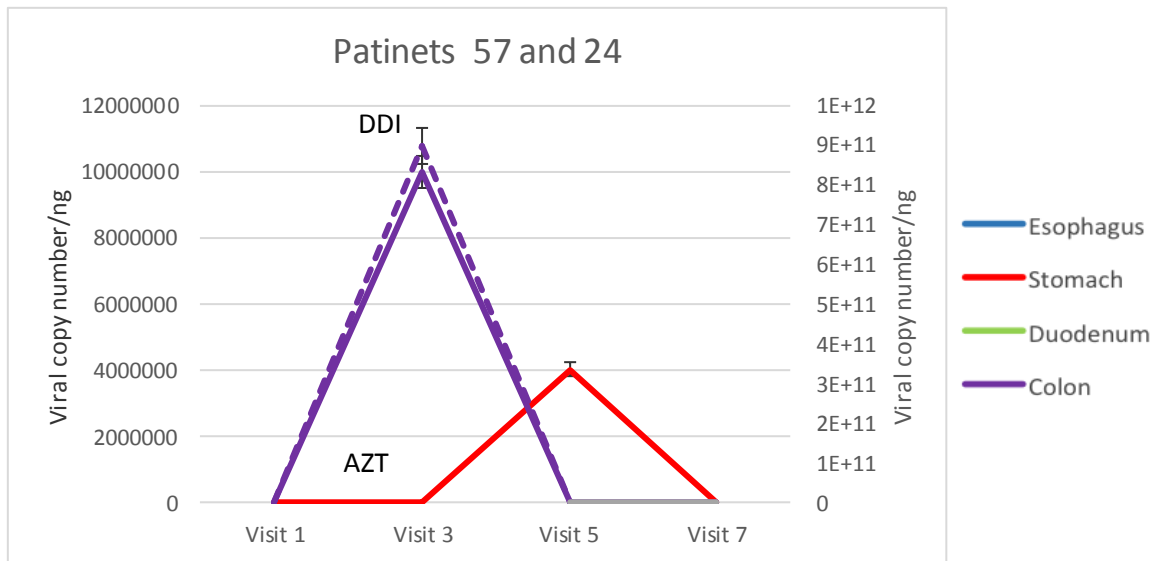


**Figure 30:** 2-LTR proviral DNA levels in the gut tissues from HIV-1 infected patients. Patient 57 (solid line) received AZT and the levels of the 2-LTR fluctuated between the visits of the stomach and colon. The same fluctuation was found in the stomach visit of patient #24 receiving ddi (dashed line). Both drugs had the same fluctuated levels of 2-LTR proviral DNA, and high viral copy number.

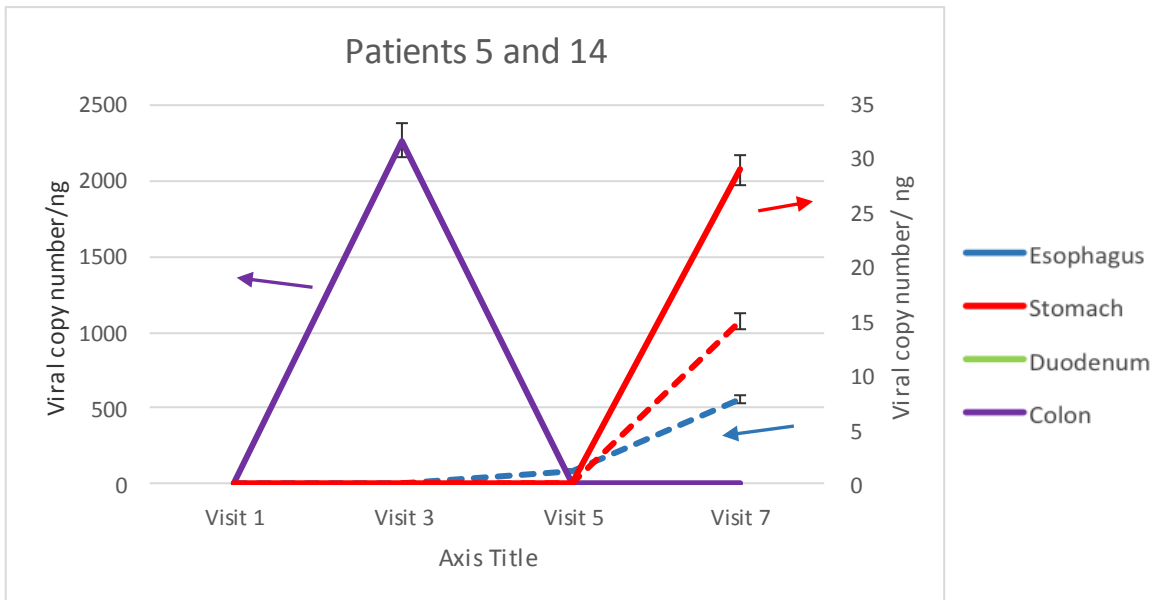


**Figure 31:** The integrated proviral DNA levels in the gut tissues from HIV-1 infected patients: Both patients 5 (solid line) and 14 (dashed line) were receiving ddI in in the different tissues of both patient. This analysis showed that the integrated proviral DNA level fluctuated in the various gut tissues.

The colored arrows point towards the appropriate axis for the sample.

## References

1. **World Health Organization (WHO)**. 2014. HIV/ AIDS: Key facts. Media center.
2. **Shao Y and Williamson C**. 2012. The HIV epidemic: Low- to middle-income communities. *Cold spring harbor perspectives in medicine*. Dio: 10. 1101.
3. **UNAIDS**. 2010. UNAIDS reports on the global HIV epidemic: 2010. The global heroin market. *World Drug red Report*. p.p. 37-63
4. **UNAIDS**. 2015, HIV and AIDS estimate 2012.
5. **Shors T**. 2009. *Understanding viruses*. USA: Jones and Bartlett publishers, LLC.
6. **Center for Disease Control and Prevention (CDC)**. 2011. Ten great public health achievements-worldwide, 2001-2010. *Weekly* 60 (24): 814-818.
7. **Center for Diseases Control and Prevention (CDC)**. 2015. About HIV/AIDS: what are the stages of HIV/AIDS?.
8. **Katzenstein DA, Hammer SM, and et al**. 1996. The relation of virologic and immunologic markers to clinical outcomes after nucleoside therapy in HIV- infected adults with 200 to 500 CD4 cells per cubic millimeter. *The New England journal of medicine* 335: 1091-1098.
9. **Miller MD, Wang B, Bushman FD**. 1995. Human immunodeficiency virus type 1 preintegration complexes containing discontinuous plus strands are competent to integrate in vitro. *J Virol* 69:3938-3944.
10. **Junqueira DM, de Medeiros R and et al**. 2011. Reviewing the history of HIV-1: Spread of subtype B in the Americas. *Plos one* dio: 10. 1371.
11. **Frankel AD, and Young JAT**. 1998. HIV-1: Fifteen proteins and an RNA. *Annual review* 67:1-25.
12. **Sloan RD and Wainberg MA**. 2011. The role of unintegrated DNA in HIV infection. *Retrovirology* 8:52.
13. **Rowold DJ and Herrera RJ**. 2000. Alu elements and human genome. *Genetica* 108:57-72.
14. **Fischl MA, Richman DD and et al**. 1990. The safety and efficacy of zidovudine (AZT) in the treatment of subjects with midly symptomatic human immunodeficiency virus type 1 (HIV) infection. *Ann Intern Med* 112: 727-737.
15. **Farnet C, Haseltine W**. 1991. Circularization of human immunodeficiency virus type 1 DNA in vitro. *J Virol* 65:6942-6952.
16. **Moore RD, Hidalgo J and et al**. 1991. Zidovudine and the natural history of the acquired immunodeficiency syndrome. *The New England journal of medicine* 324:1412-1416.
17. **Butler Li L, Olvera JM, Yoder K, Mitchell RS, Butler SL, Lieber MR, Martin SL, and Bushman FD**. 2001. Role of the non-homologous DNA end joining pathway in retroviral infection. *EMBO J*. 20:3272–3281.
18. **Butler SL, Johnson EP, and Bushman FD**. 2002. Human immunodeficiency virus cDNA metabolism: Notable stability of two-long terminal repeat circles. *Journal of virology* dio: 10. 1128. 76: 3739-3747.
19. **Butler SL, Mark S.T and et al**. 2001. A quantitative assay for HIV DNA integration in vivo. *Nature medicine* 7: 631-634.
20. **Bukrinsky MI, Sharova N, Dempsey MP, Stanwick TL, Bukrinskaya AG, Haggerty S, Stevenson M**. 1992. Active nuclear import of human immunodeficiency virus type 1 preintegration complexes. *Proc Natl Acad Sci USA* 89:6580-6584.
21. **Shoemaker C, Goff S, Gilboa E, Paskind M, Mitra SW, Baltimore D**. 1980. Structure of a cloned circular Moloney murine leukemia virus DNA molecule containing an inverted segment: implications for retrovirus integration. *Proc Natl Acad Sci USA* 77:3932-3936.



22. **Nacro B, Zoure E, and et al.** 2012. Pharmacology and immune-virologic efficacy of once- a-day HAART in Africa HIV-infected children: ANRS 12103 pase II trail. Retrieved on 4 June, 2012 from <http://www.who.int/bulletin/volumes/89/6/10-081646/eng/>
23. **Zheng Y, Ao Z, Wang B, Danappa Jayappa K, Yao X.** 2011. Host protein Ku70 binds and protects HIV-1 integrase from proteasomal degradation and is required for HIV replication. *J Biol Chem* 286:17722-17735.
24. **Zhu W, Jiao Y, and et al.** 2011. Rapid turnover of 2-LTR HIV-1 DNA during early stage of highly active antiretroviral therapy. *Plos one* dio:10. 1371.
25. **Katsambas A C and Lotti T M.** 2003. European hand book of dermatological treatments. Germany: Springer-Verlag Berlin Heidelberg.
26. **Deng W and Roberts SG.** 2007. TFIIB and the regulation of transcription by RNA polymerase II. *Chromosoma* 116:417-429.
27. **Mulder LC, Chakrabarti LA and Muesing MA.** 2002. Interaction of HIV-1 integrase with DNA repair protein hRad18. *J Biol Chem* 277:27489-27493.
28. **Lloyd AG, Tateishi S, Bieniasz PD and et al.** 2006. Effect of DNA repair protein Rad18 on viral infection. *PLoS Pathog* 2: e40.
29. **Lau A, Kanaar R, Jackson SP and O'Connor MJ.** 2004. Suppression of retroviral infection by the RAD52 DNA repair protein. *EMBO J* 23:3421-3429.
30. **Doms R W and Trono D.** 2000. The plasma membrane as a combat zone in the HIV battlefield. *Genes Dev* 14:2677-88.
31. **Ahn J, Vu T, Novince Z and et al.** 2010. HIV-1 Vpr loads uracil DNA glycosylase-2 onto DCAF1, a substrate recognition subunit of a cullin 4A-ring E3 ubiquitin ligase for proteasome-dependent degradation. *J Biol Chem* 285:37333-37341.
32. **Mbisa JL, Barr R, Thomas JA and et al.** 2007. Human immunodeficiency virus type 1 cDNAs produced in the presence of APOBEC3G exhibit defects in plus-strand DNA transfer and integration. *J Virol* 81:7099-7110.
33. **Bourry O, Mannioui A, Sellier P and et al.** 2010. Effect of short-term haart on siv load in macaque tissues is dependent on time initiation and antiviral diffusion. *Retrovirology* 7:78
34. **Sharkey M E, Teo I, Greenough N and et al.** 2000. Persistence of Episomal HIV-1 infection intermediates in patients on highly active anti-retroviral therapy. *Nat Med* 6:76-81.
35. **Dinosa JB, Rabi SA, Blankson JN, Gama L and et al.** 2009. A SIV-infected macaque model to study viral reservoirs that persist during highly active antiretroviral therapy. *J Virol* 83:9247-54.
36. **Teo I ,Veryard C, Barne H and et al.** 1997. Circular Forms of Unintegrated Human Immunodeficiency Virus Type 1 DNA and High Levels of Viral Protein Expression: Association with Dementia and Multinucleated Giant Cells in the Brains of Patients with AIDS. *Journal of Virology*. P.2928-2933.
37. **Pang S, Koyanagi Y, Miles S, Wiley C, Vinters HV and Chen IS.**1990. High levels of unintegrated HIV-1 DNA in brain tissue of AIDS dementia patients. *Nature* 343:85–89.
38. **Pierce NF, Cray WC Jr.** 1982. Determinants of localization, magnitude and duration of a specific mucosal IGA plasma cell response in enterically immunized rats. *J Immunol* 128:1311-5.
39. **Jurriaans, S, de-Ronde A, Dekker J, Goudsmit J, Cornelissen M.** 1992. Analysis of human immunodeficiency virus type-1 LTR-LTR junctions in peripheral blood mononuclear cells of infected individuals. *J. Gen. Virol.* 73:1537–1541.

40. **Fenard D, Houzet L, Bernard E and et al.** 2009. Uracil DNA Glycosylase 2 negatively regulates HIV-1 LTR transcription. *Nucleic Acids Res* 37:6008-6018.
41. **Yan N, O'Day E, Wheeler LA and et al.** 2011. HIV DNA is heavily uracilated, which protects it from autointegration. *Proc Natl Acad Sci USA* 108:9244-9249.
42. **Emiliani S, Mousnier A, Busschots K, Maroun M, Van Maele B, Tempe D and et al.** 2005. Integrase mutants defective for interaction with LEDGF/p75 are impaired in chromosome tethering and HIV-1 replication. *J Biol Chem* 280:25517-23.
43. **Sylvain Thierry, Soundasse Munir, Eloïse Thierry and et al.** 2015. Integrase inhibitor reversal dynamics indicate unintegrated HIV-1 DNA initiate *de novo* integration. *Retrovirology* 12:24
44. **Graf EH, Mexas AM, Yu JJ, Shaheen F, Liszewski MK, Di Mascio M and et al.** 2011. Elite suppressors harbor low levels of integrated HIV DNA and high levels of 2-LTR circular HIV DNA compared to HIV+ patients on and off HAART. *Plos Pathog* 7:e1001300.
45. **Bansal GP, Malaspina A and Flores J.** 2010. Future paths for HIV vaccine research: Exploiting results from recent clinical trials and current scientific advances. *Curr Opin Mol Ther* 12:39-46.
46. **Kotler DP.** 2005. HIV infection and the gastrointestinal tract. *Aids* 19:107-17.
47. **Clavel F.** 2004. Mechanism of HIV drug resistance: a primer. *The PRN Notebook* 9:3-7.
48. **Carpenter CCJ, Fischl MA, Hammer SM, Hirsch MS and et al.** 1996. Antiretroviral therapy for HIV infection in 1996. Recommendations of an international panel. *JAMA* 276:146-54
49. **Egger M, Hirschel B and et al.** 1997. Impact of new antiretroviral combination therapies in multicentere study. *BMJ* 315:1194-9.
50. **CAESAR Coordinating Committee.** 1997. Randomised trial of addition of lamivudine or lamivudine plus loviride to zidovudine-containing regimens for patients with HIV-1 infection: the CAESAR trial. *Lancet* 349:1413-21.
51. **Delta Coordinating Committee.** 1996. Delta: a randomised double-blind controlled trial comparing combinations of zidovudine plus didanosine or zalcitabine with zidovudine alone in HIV-infected individuals. *The Lancet.* 348: 283-291.
52. **Medlineplus.**2012.Lamivudine.<http://www.nlm.nih.gov/medlineplus/druginfo/meds/9696011.html>
53. **Mboup S, Musonda R, Mhalu F and et al.** 2006.Disease and Mortality in Sub-Sahara Africa 2<sup>nd</sup> edition. The international bank for reconstruction and development /the world bank.
54. **Laurent C, Diakhaté N, Gueye NFN and et al.** 2002. The Sengalsee government antiretroviral therapy initiative: an 18 month follow up study. *AIDS.* 16: 1363-70.
55. **Coetzee D, Hilderbrand K, Boule A and et al.** 2004. Outcomes after two years of providing antiretroviral treatment in Khayelitsha, South Africa. *AIDS.* 18:887-95.
56. **Djomand G, Roles T, Ellerbrock T and et al.** 2003. Virologic and Immunologic outcomes ans progromatic challenges of an antiretroviral treatment pilot project in Abidjan. Côte d'Ivoire. *AIDS.* 17:S5-S15.
57. **Weidle PJ, Malamba S, Mwebaze R and et al.** 2002. Assessment of a pilot antiretroviral drug therapy program in Uganda: Patients response, survival and drug resistance. *Lancet.* 360:34-40.
58. **Wester CW, Kim S, Bussmann H and et al.** 2005. Initial response to highly active antiretroviral therapy in HIV-1C infected adults in Public sector treatment program in Botswana. *Journal of Acquired immune Dificiency Syndrome.* 40: 336-43.

59. **Evering TH, Mehandru SM and et al.** 2012. Absence of HIV evolution in the gut associated lymphoid tissue from patients on combination antiretroviral therapy initiated during primary infection. *Plos pathogen* 10:1371.
60. **Zink MC, Brice AK, Kelly KM and et al.** 2002. A novel Simian immunodeficiency virus model that provides insight into mechanisms of human immunodeficiency virus central nervous system disease. *Journal Neurovirol* 8 (Suppl2): 42-48.
61. **Robinson H, Zinkus D.** 1990. Accumulation of human immunodeficiency virus type 1 DNA in T cells: results of multiple infection events. *J Virol* 64:4836-4841.
62. **Baliga RS, Lui C, Hoyt DG and et al.** 2004. Vascular endothelial toxicity induced by HIV protease inhibitor. *Cardiovascular Toxicology* 4:199-206.
63. **Laurent-Crawford AG, Hovanessian AG.** 1993. The cytopathic effect of human immunodeficiency virus is independent of high levels of unintegrated viral DNA accumulated in response to superinfection of cells. *J Gen Virol* 74(Pt 12):2619-2628.
64. **Grinstead OA, van der Straten A.** 2000. Counsellors' perspectives on the experience of providing HIV counselling in Kenya and Tanzania: the Voluntary HIV-1 Counselling and Testing Efficacy Study. *Aids Care*. 12(5):625-42.
65. **Rerks-Ngarm S, Pitisuttithum P, Nitayaphan S and et al.** 2009. Vaccination with ALVAC and AIDSVAX to Prevent HIV-1 Infection in Thailand. *N Engl J Med* 361(23):2209-2220.
66. **UNAIDS.** AIDS by the Numbers.2013.
67. **UNIADS.** 2013. Access to antiretroviral therapy in Africa: Status report on progress towards the 2015 targets.
68. **Pottie k, Bamoueni S, Alas A and et al.** 2010. Treating HIV in Africa: case report from rural Congo. *Canadian family physician*. 56: 434-437.
69. **Joint United Nations Programme on HIV/AIDS [website].** 2007 AIDS epidemic update. Geneva, Switz: Joint United Nations Programme on HIV/AIDS and World Health Organization; 2008. Available from: [www.unaids.org/en/KnowledgeCentre/HIVData/EpiUpdate/EpiUpdArchive/2007/default.asp](http://www.unaids.org/en/KnowledgeCentre/HIVData/EpiUpdate/EpiUpdArchive/2007/default.asp). Accessed 2009 Oct 7.
70. **Powell HA and et al.** 1994. Proteinase inhibition of the detection of *Listeria monocytogenes* in milk using the polymerase chain reaction. *Lett.Appl. Microbiol.* 18, 59–61.
71. **Ellman Tom.** 2015. Demedicalizing AIDS prevention and treatment in Africa. *The new England Journal of Medicine* 10:1056.
72. **South Africa National AIDS Council.** Progress report on national strategic plan for HIV, TB and STIs (2012-2016).
73. **Bisceglie A, Maskew M, Schulze D and et al.** 2010.HIV-HBV coinfection among South African patients receiving antiretroviral therapy. *Antiretroviral therapy*. 10:3851.
74. **Bukrinsky M, Stanwick T, Dempsey M, Stevenson M.** 1991.Quiescent T lymphocytes as an inducible virus reservoir in HIV-1 infection. *Science* 254:423-427.
75. **UNAIDS.** 2013. Estimates and WHO, HIV and Adolescents: Guidance for HIV testing and counselling and care for adolescents living with HIV. WHO Geneva.
76. **Hoffmann CJ, Thio CL.** 2007. Clinical implications of HIV and hepatitis B co-infection in Asia and Africa. *Lancet Infect Dis* 7(6):402-9.
77. **Luetkemeyer A.** hepatitis B and HIV co-infection. 2010. HIV in site.
78. **Uneke CJ, Ogbu O, Inyama PU and et al.** 2005. Prevalence of hepatitis-B surface antigen among blood donors and human immunodeficiency virus-infected patients in Jos, Nigeria. *Mem Inst Oswaldo Cruz* 100(1):13-6.

79. **Mann J and Ndung'u T.** 2015. HIV-1 Vaccine immunogen design strategies. *Virology journal* 10:1186.
80. **McMichael AJ, Borrow P, Tomaras GD, Goonetilleke N, Haynes BF.** 2010. The immune response during acute HIV-1 infection: clues for vaccine development. *Nat Rev Immunol.* 10
81. **Picker LJ, Hansen SG, Lifson JD.** 2012. New paradigms for HIV/AIDS vaccine development. *Annu Rev Med* 63:95-111. (1):11-23.
82. **Mehandru S and et al.** 2004. Primary HIV-1 infection is associated with preferential depletion of CD4+ T lymphocytes from effector sites. *J. Exp. Med* 761-770.
83. **McElrath MJ and Haynes BF.**2010. Induction of immunity to human immunodeficiency virus type-1 by vaccination. *Immunity* 33(4):542-554.
84. **Esparza J.** 2013. A brief history of the global effort to develop a preventive HIV vaccine. *Vaccine.* 31(35): 3502-3518.
85. **McMichael A, Picker LJ, Moore JP, Burton DR.** 2013. Another HIV vaccine failure: where to next? *Nat Med* 19(12):1576-1577
86. **Flynn NM, Forthal DN, Harro CD, Judson FN, Mayer KH, Para MF.** 2005. Placebo-controlled phase 3 trial of a recombinant glycoprotein 120 vaccine to prevent HIV-1 infection. *J Infect Dis* 191(5):654-665.
87. **Pitisuttithum P, Gilbert P, Gurwith M and et al.** 2006. Randomized, double-blind, placebo-controlled efficacy trial of a bivalent recombinant glycoprotein 120 HIV-1 vaccine among injection drug users in Bangkok. *Thailand J Infect Dis* 194(12):1661-1671.
88. **Kantor B, Ma, H, Webster- Cyriaque, J, Monahan, PE, and Kafri T.** 2009. Epigenetic activation of unintegrated HIV-1 genomes by gut associate short chain fatty acids and its implications for HIV infection. *PNAS* doi: 10.1073.
89. **Hammer SM, Sobieszczyk ME, Janes H and et al.**2013. Efficacy trial of a DNA/rAd5 HIV-1 preventive vaccine. *N Engl J Med* 369 (22):2083-2092.
90. **Haynes BF, Gilbert PB, McElrath MJ and et al.**2012. Immune-correlates analysis of an HIV-1 vaccine efficacy trial. *N Engl J Med* 366(14):1275-1286.
91. **Tomaras GD, Ferrari G, Shen X and et al.** 2013. Vaccine-induced plasma IgA specific for the C1 region of the HIV-1 envelope blocks binding and effector function of IgG. *Proc Natl Acad Sci U S A* 110(22):9019-9024.
92. **Wiley R, Nason MC, Nishimura Y, Follmann DA, Martin MA.** 2010. Neutralizing antibody titers conferring protection to macaques from a simian/human immunodeficiency virus challenge using the TZM-bl assay. *AIDS Res Hum Retroviruses* 26(1):89-98.
93. **Mbisa J, Martin SA and Cane PA.** 2011. Pattern of resistance development of integrase inhibitor in HIV. *Infection and drug resistance* 10:2147.
94. **Pomerantz RJ.** 2003. Reservoirs, sanctuaries and residual disease: the hiding spots of HIV-1. *HIV Clin Trails* 4: 137-143.
95. **van Marle G, Church DL, and et al.** 2010. Higher levels of Zidovudine resistant HIV in the colon compared to blood and other gastrointestinal compartments in HIV infection. *Retrovirology* 7:74.
96. **van Marle G, Gill MJ, Kolodka D and et al.** 2007. Compartmentalization of the gut viral reservoir in HIV-1 infected patients. *Retrovirology* 4:87.
97. **Chun TW, Nickle DC, and et al.** 2008. Persistence of HIV in Gut- associated lymphoid tissue despite long-term antiretroviral therapy. *The journal of infectious diseases* 197:714-20.

98. **Guadalupe M, Sankaran S, George MD and et al.** 2006. Viral suppression and immune restoration in the gastrointestinal mucosa of Human Immunodeficiency Virus Type 1-infected patients initiating therapy during primary or chronic infection. *J Virol* 80:8236-8247.
99. **Eisele E and Siliciano R.** 2012. Redefining the viral Reservoirs that Prevent HIV-1 Eradication. *Immunity* 10:1016.
100. **Grashi T, Brown CR, Endo Y and eat al.** 2001. Macrophages are the principle reservoir and sustain high virus laods in rhesus macaques after the depletion of CD4+ T cells by a highly pathogenic simian immunodeficiency virus/HIV type 1 chimera (SHIV): Implications for HIV-1 infection of humans. 2001. *Proc natl acad sci usa.* 98:658-663.
101. **Gartner S, Markovits P, Markovits DM and et al.** 1986. The role of mononuclear phygocytes in HTLV-III/LAV infection. *Science* 233:215-219.
102. **Hufert FT, Schmitz J, Schreiber M and eat al.** 1993. Human Kupffer cells infected with HIV-1 in vivo. *Journal of acquired immune deficiency syndrome* 6:772-777.
103. **Koenig S, Gendelman HE, Orenstein JM and et al.** 1986. Detection of AIDS virus in macrophages in brain tissue from AIDS patients with encephalopathy. *Science.* 233:1089-1093.
104. **Mcllory JC, Autran B, Cheynier R and et al.** 1996. Low infection frequency of macrophages in the spleens of HIV+ patients. *Red. Viro.* 147:115-121.
105. **Wiley CA, Schrier RD, Nelson JA and et al.** 1986. Cellular localization of human immunodeficiency virus infection within the brains of acquired immune deficiency syndrome patients. *Proc. Nalt. Acad.Sci. USA.* 83:7089-7093.
106. **Thompson K, Cherry CL, Bell JE and et al.** 2011. Brain Cell reservoir s of latent virus in presymptomatic HIV-infected individuals. *The American journal of pathology.* 10:1016.
107. **Heaton RK, Clifford DB, Franklin DR and et al.** 2010. HIV-associated neurocognitive disorders persist in the ear of potent antiretroviral therapy: Charter study. *Neurology* 75:2087-2096.
108. **Bulfone-Paus S.** 2013. Mast Cells as Reservoirs for HIV Latency. *Journals of Immunodeficiency and Disorders* 2:1.
109. **Sundstrom JB, Ellis JE, Hair GA, Kirshenbaum AS, Metcalfe DD and et al.** 2007. Human tissue mast cells are an inducible reservoir of persistent HIV infection. *Blood* 109: 5293-5300.
110. **Okayama Y, Kawakami T.** 2006. Development, migration, and survival of mast cells. *Immunol Res* 34: 97-115.
111. **Wang HW, Tedla N, Lloyd AR and et al.** 1998. Mast cell activation and migration to lymph nodes during induction of an immune response in mice. *J Clin Invest* 102:1617-1626.
112. **Moir S, Malaspina A, Li Y and et al.** 2000. B Cells of HIV-1–Infected Patients Bind Virions through Cd21–Complement Interactions and Transmit Infectious Virus to Activated T Cells. *The journal of cell biology* 10:1084.
113. **Malaspina A, Moir S, Nickle DC and et al.** 2002. Human Immunodeficiency Virus Type 1 Bound to B Cells: Relationship to Virus Replicating in CD4+ T Cells and Circulating in Plasma. *Journla of Virology.* 10:1128.
114. **Keele BF, Tazi L, Gartner S and et al.** 2008. Characterization of the Follicular Dendritic Cell Reservoir of Human Immunodeficiency Virus Type 1. *Journal of Virology* 10: 1128.
115. **Carter CC, Onafuwa-Nuga A, McNamara LA, Riddell J 4th, Bixby D and et al.** 2010. HIV-1 infects multipotent progenitor cells causing cell death and establishing latent cellular reservoirs. *Nat Med* 16: 446-451.

116. **Costiniuk CT and Angel JB.** 2012. Immunodeficiency virus and the gastrointestinal immune system: does highly active antiretroviral therapy restore gut immunity? *Mucosal Immunology* 5, 596–604.
117. **Cheroutre H and Madakamutil L.** 2004 Acquired and natural memory T cells joining forces at the mucosal front line. *Nat. rev. Immunol.* 4, 292-300.
118. **Doe WF.** The intestinal immune system.1989. *Gut* 30:1679-1685.
119. **Owen RL, Jones AL.** Epithelial cell specialization within human Peyer's patches: An ultrastructural study of intestinal lymphoid follicles. *Gastroenterology* 1974; 66: 189-203.
120. **Spalding DM, Koopman WJ, Eldridge JH, McGhee JR, Steinman RM.** Accessory cells in murine Peyer's patch. 1986. Identification and Enrichment of a functional dendritic cell. *J Exp Med* 157: 1646-59.
121. **Husband A, Gowans JL.** 1978. The origin and antigen-dependent distribution of IgA-containing cells in the intestine. *J Exp Med* 148: 1146-60.
122. **Brenchley JM, Douek DC.** 2008. HIV infection and the gastrointestinal immune system. *Mucosal Immunol.* 10: 1038.
123. **Mowat A, Viney J.** 1997. The anatomical basis of intestinal immunity. *Immunol. Rev.* 156, 145–166.
124. **Gray G, Buchbinder S, Duerr A.** 2010. Overview of STEP and Phambili trial results: two phase IIb test-of-concept studies investigating the efficacy of MRK adenovirus type 5 gag/pol/nef subtype B HIV vaccine. *Curr Opin HIV AIDS* 5(5):357-361.
125. **Poles MA, Boscardin WJ and et al.** 2006. Lack of Decay of HIV-1 in Gut-associated lymphoid tissue reservoirs in maximally suppressed individuals. *Acquired immune defi syndr* 43:65-68.
126. **Mehandru S, et al.** 2007. Mechanisms of Gastrointestinal CD4+ T-cell depletion during acute and early human immunodeficiency virus type 1 infection. *J. Virol* 81:599–612.
127. **Brenchley JM, Schacker TW, Ruff EL and et al.** 2004. CD4+ T cell depletion during all stages of HIV disease occurs predominantly in the gastrointestinal tract. *J Exp Med* 749-759.
128. **Mattapallil JJ and et al.** 2005. Massive infection and loss of memory CD4+ T cells joining forces at the mucosal front line. *Nat. Rev. Immunol.* 4: 292-300.
129. **Clayton F, et al.** 1992. Rectal mucosal pathology varies with human immunodeficiency virus antigen content and disease stage. *Gastroenterology* 103:919–933
130. **Clayton F, Snow G, Reka S, Kotler DP.** 1997. Selective depletion of rectal lamina propria rather than lymphoid aggregate CD4 lymphocytes in HIV infection. *Clin. Exp. Immunol* 107:288–292.
131. **Kotler DP, Reka S, Clayton F.** 1993. Intestinal mucosal inflammation associated with human immunodeficiency virus infection. *Dig. Dis. Sci* 38:1119–1127.
132. **Ullrich R, Zeitz M and et al.** 1992. Enteric immunologic abnormalities in human immunodeficiency virus infection. *Semin Liver Dis* 12:167–174.
133. **Liu R, Huang L, Li J and et al.** 2013. HIV Infection in Gastric Epithelial Cells. *The journal of infectious Diseases* 10:1093.
134. **Giorgi JV, Hultin LE, McKeating JA and et al.** 1999. Shorter survival in advanced human immunodeficiency virus type 1 infection is more closely associated with T lymphocyte activation than with plasma virus burden or virus chemokine coreceptor usage. *J Infect Dis* 179: 859-70.
135. **Yukl SA, Gianella S, Sinclair E, Epling L, Li Q and et al.** 2010. Differences in HIV burden and immune activation within the gut of HIV-positive patients receiving suppressive antiretroviral therapy. *J Infect Dis* 202: 1553–1561.

136. **Canani RB, et al.** 2006. Inhibitory effect of HIV-1 Tat protein on the sodium-D-glucose symporter of human intestinal epithelial cells. *AIDS* 20:5–10.
137. **Heise C, et al.** 1991. Human immunodeficiency virus infection of enterocytes and mononuclear cells in human jejunal mucosa. *Gastroenterology* 100:1521–1527.
138. **Maresca M, et al.** 2003. The virotoxin model of HIV-1 enteropathy: involvement of GPR15/Bob and galactosylceramide in the cytopathic effects induced by HIV-1 gp120 in the HT-29-D4 intestinal cellline. *J. Biomed. Sci.* 10:156–166.
139. **Brussel A, Sonigo P.** 2003. Analysis of early human immunodeficiency virus type1 DNA synthesis by use of a new sensitive assay for quantifying integrated provirus. *J Virol* 77: 10119–10124.
140. **Landman R, Schiemann R, Thiam S and et al.** 2003. Once- a – day highly active antiretroviral therapy in treatment- naïve HIV-1 infected adults in Senegal. *AIDS* 17: 1017-22.
141. **Abad ML, verdure T, Vela A and et al.** 2004. Construction and characterization of a minimized version of the HIV-1 pNL4-3 plasmid and its application for pdeudotyping HIV-1 vectors. *Molecular Biotechnology* 8:87-95.
142. Chun TW, Curruth I and Finzi and et al. 1997. Quantification of latent tissue reservoirs and total body viral load in HIV-1 infection. *Nature.* 387:183-188.
143. **Akane A. et al.** 1994. Identification of the heme compound copurified with deoxyribonucleic acid (DNA) from bloodstains, a major inhibitor of polymerase chain reaction (PCR) amplification. *J. Forensic Sci.* 39, 362–72.
144. **Al-Soud WA, Rådström P.** 2001. Purification and characterization of PCRinhibitory components in blood cells. *J. Clin. Microbiol.* 39: 485–93.
145. **Al-Soud WA and et al.** 2000. Identification and characterization of immunoglobulin G in blood as a major inhibitor of diagnostic PCR. *J Clin. Microbial.* 38:345-50.
146. **Bessetti J.** 2007. An introduction to PCR inhibitors. *Profiles in DNA.*
147. **Comey CT, et al.** 1994 DNA extraction strategies for amplified fragment length polymorphism analysis. *J. Forensic Sci.* 39, 1254–69.
148. **Khan G, et al.** 1991. Inhibitory effects of urine on the polymerase chain reaction for cytomegalovirus DNA. *J. Clin. Pathol.* 44, 360–5.
149. **Kim CH and et al.** 2001. Optimization of the PCR for detection of *Staphylococcus aureus* nuc gene in bovine milk. *J. Dairy Sci.* 84, 74–83.
150. **Lantz PG and et al.** 1997. Removal of PCR inhibitors from human faecal samples through the use of an aqueous two-phase system for sample preparation prior to PCR. *J. Microbiol. Meth.* 28, 159–67.
151. **Monteiro L and et al.** 1997. Complex polysaccharides as PCR inhibitors in feces: *Helicobacter pylori* model. *J. Clin. Microbiol.* 35, 995–8.
152. **Kreader CA.** 1996. Relief of amplification inhibition in PCR with Bovine Serum Albumin or T4 gene protein. *Applied and environmental microbiology* p. 1102-1106.
153. **Schrader C, Schielke Ellerbroek L and et al.** 2012. PCR inhibitors-occurrence, properties and removal. *Journal of applied microbiology* 113, 1014-1026.
154. **Henrich T and Ghandhi R.** 2013. Early treatment and HIV-1 reservoirs: a stitch in time?. *The journal of infectious diseases* 208:1189-93.
155. **Yukl SA, Shergill AK, Ho T and et al.** 2013. The Distribution of HIV DNA and RNA in cell subset Differs in Gut and Blood of HIV- Positive Patients on ARTL Implications for Viral Persistence. *The Journal of Infectious Diseases.* 208:1212-20.

156. **Baron V, Bouneaud C, Cumano A, et al.** 2003. The repertoires of circulating human CD8(+) central and effector memory T cell subsets are largely distinct. *Immunity* 18:193–204.
157. **Sallusto F, Lenig D, Forster R, Lipp M, Lanzavecchia A.** 1999. Two subsets of memory T lymphocytes with distinct homing potentials and effector functions. *Nature* 401:708–12.
158. **Mannioui A, Bourry O, Sellier P, Delache B, Brochard P, Andrieu T, Vaslin B, Karlsson I, Roques P, Le Grand R.** 2009. Dynamics of viral replication in blood and lymphoid tissues during SIVmac251 infection of macaques. *Retrovirology* 6:106
159. **Josefsson L, Stockenstrom and Faria N and et al.** 2013. The HIV-1 Reservoir in eight patients on long-term suppressive antiretroviral therapy is stable with few genetic changes over time. *PNAS*. 10:1073.
160. **Douek.** 2013. Immune Activation, HIV Persistence, and the Cure. *Topics in Antiviral Medicine*. 21:4
161. **Chomont N and et al.** 2009 HIV reservoir size and persistence are driven by T cell survival and homeostatic proliferation. *Nat Med* 15(8):893–900.
162. **Strain MC, et al.** 2005. Effect of treatment, during primary infection, on establishment and clearance of cellular reservoirs of HIV-1. *J Infect Dis* 191(9):1410–1418.
163. **Cabrera C.** 2008. Raltegravir, an HIV-1 integrase inhibitor for HIV infection. *Curr Opin Invest Dr.* 9: 885-98.
164. **Sharkey M, Triques K, Kuritzkes D, Stevenson M.** 2005. In vivo evidence for instability of episomal human immunodeficiency virus type 1 cDNA. *J Virol.* 79:8662-8673.
165. **Poon B, Chen I.** 2003. Human immunodeficiency virus type 1 (HIV-1) Vpr enhances expression from unintegrated HIV-1 DNA. *J Virol.* 77:3962-3972.
166. **Ibáñez A, Puig T, Elias J and et al.** 1999. Quantification of integrated and total hiv-1 dna after long-term highly active antiretroviral therapy in hiv01 infected patients, *AIDS* 13:10445 1049.
167. **Brussel A, Sonigo P.** 2004 Evidence for gene expression by unintegrated human immunodeficiency virus type 1 DNA species. *J Virol* 78:11263-11271.
168. **Iyer S, Yu D, Biancotto A, Margolis L, Wu Y.** 2009. Measurement of human immunodeficiency virus type 1 preintegration transcription by using Rev-dependent Rev-CEM cells reveals a sizable transcribing DNA population comparable to that from proviral templates. *J Virol* 83:8662-8673.
169. **Keel BF, Giogi EE, Salazar-Gonzalez JF and et al.** 2008. Identification and characterization of transmitted and early founder virus envelopes in primary HIV-1 infection *Proc. Natl. Acad. Sci. USA.* 105:7552-7557.
170. Figure 1 modified from **Frankel, AD, and Young JAT.** 1998. HIV-1: Fifteen proteins and an RNA. *Annual review* 67:1-25.
171. Figure 2 modified from **Shors T.** 2009. *Understanding viruses.* USA: Jones and Bartlett publishers, LLC.
172. Figure 5 modified from **Butler SL, Mark S.T and et al.** 2001. A quantitative assay for HIV DNA integration in vivo. *Nature medicine* 7: 631-634.